LI
LABORATORY INVESTIGATION
THE BASIC AND TRANSLATIONAL PATHOLOGY RESEARCH JOURNAL
VOLUME 100 | SUPPLEMENT 1 | MARCH 2020

ABSTRACTS

DERMATOPATHOLOGY
(459-522)

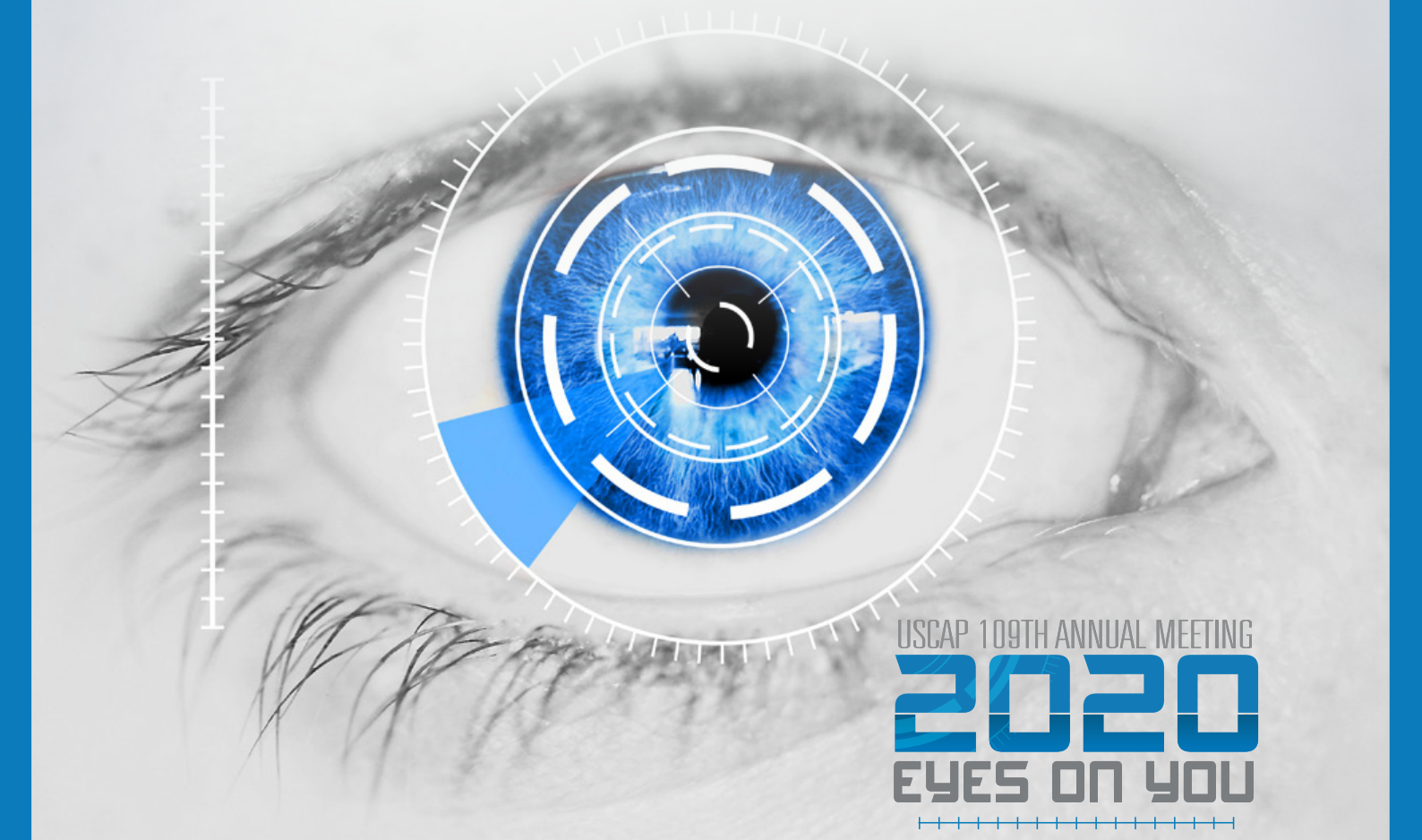

FEBRUARY 29-MARCH 5, 2020

LOS ANGELES CONVENTION CENTER
LOS ANGELES, CALIFORNIA

Published by
SPRINGER NATURE
www.ModernPathology.org

USCAP Creating a Better Pathologist
AN OFFICIAL JOURNAL OF THE UNITED STATES AND CANADIAN ACADEMY OF PATHOLOGY

EDUCATION COMMITTEE

Jason L. Hornick, Chair

Rhonda K. Yantiss, Chair, Abstract Review Board and Assignment Committee

Laura W. Lamps, Chair, CME Subcommittee

Steven D. Billings, Interactive Microscopy Subcommittee

Raja R. Seethala, Short Course Coordinator

Ilan Weinreb, Subcommittee for Unique Live Course Offerings

David B. Kaminsky (Ex-Officio)

Zubair Baloch
Daniel Brat
Ashley M. Cimino-Mathews
James R. Cook
Sarah Dry
William C. Faquin
Yuri Fedoriw
Karen Fritchie
Lakshmi Priya Kunju
Anna Marie Mulligan
Rish K. Pai
David Papke, Pathologist-in-Training
Vinita Parkash
Carlos Parra-Herran
Anil V. Parwani
Rajiv M. Patel
Deepa T. Patil
Lynette M. Sholl
Nicholas A. Zoumberos, Pathologist-in-Training

ABSTRACT REVIEW BOARD

Benjamin Adam
Narasimhan Agaram
Rouba Ali-Fehmi
Ghassan Allo
Isabel Alvarado-Cabrero
Catalina Amador
Roberto Barrios
Rohit Bhargava
Jennifer Boland
Alain Borczuk
Elena Brachtel
Marilyn Bui
Eric Burks
Shelley Caltharp
Barbara Centeno
Joanna Chan
Jennifer Chapman
Hui Chen
Beth Clark
James Conner
Alejandro Contreras
Claudiu Cotta
Jennifer Cotter
Sonika Dahiya
Farbod Darvishian
Jessica Davis
Heather Dawson
Elizabeth Demicco
Katie Dennis
Anand Dighe
Suzanne Dintzis
Michelle Downes
Andrew Evans
Michael Feely
Dennis Firchau
Gregory Fishbein
Andrew Folpe
Larissa Furtado
Billie Fyfe-Kirschner
Giovanna Giannico
Anthony Gill
Paula Ginter
Tamara Giorgadze
Purva Gopal
Anuradha Gopalan
Abha Goyal
Rondell Graham
Alejandro Gru
Nilesh Gupta
Mamta Gupta
Gillian Hale
Suntrea Hammer
Malini Harigopal
Douglas Hartman
John Higgins
Mai Hoang
Mojgan Hosseini
Aaron Huber
Peter Illei
Doina Ivan
Wei Jiang
Vickie Jo
Kirk Jones
Neerja Kambham
Chiah Sui Kao
Dipti Karamchandani
Darcy Kerr
Ashraf Khan
Francesca Khani
Rebecca King
Veronica Klepeis
Gregor Krings
Asangi Kumarapeli
Alvaro Laga
Steven Lagana
Keith Lai
Michael Lee
Cheng-Han Lee
Madelyn Lew
Zaibo Li
Faqian Li
Ying Li
Haiyan Liu
Xiuli Liu
Yen-Chun Liu
Lesley Lomo
Tamara Lotan
Anthony Magliocco
Kruti Maniar
Emily Mason
David McClintock
Bruce McManus
David Meredith
Anne Mills
Neda Moatamed
Sara Monaco
Atis Muehlenbachs
Bita Naini
Dianna Ng
Tony Ng
Michiya Nishino
Scott Owens
Jacqueline Parai
Yan Peng
Manju Prasad
Peter Pytel
Stephen Raab
Joseph Rabban
Stanley Radio
Emad Rakha
Preetha Ramalingam
Priya Rao
Robyn Reed
Michelle Reid
Natasha Rekhtman
Jordan Reynolds
Michael Rivera
Andres Roma
Avi Rosenberg
Esther Rossi
Peter Sadow
Steven Salvatore
Souzan Sanati
Anjali Saqi
Jeanne Shen
Jiaqi Shi
Gabriel Sica
Alexa Siddon
Deepika Sirohi
Kalliopi Siziopikou
Sara Szabo
Julie Teruya-Feldstein
Khin Thway
Rashmi Tondon
Jose Torrealba
Andrew Turk
Evi Vakiani
Christopher VandenBussche
Paul VanderLaan
Olga Weinberg
Sara Wobker
Shaofeng Yan
Anjana Yeldandi
Akihiko Yoshida
Gloria Young
Minghao Zhong
Yaolin Zhou
Hongfa Zhu
Debra Zynger

To cite abstracts in this publication, please use the following format: **Author A, Author B, Author C, et al. Abstract title (abs#). In "File Title."** ***Laboratory Investigation*** **2020; 100 (suppl 1): page#**

459 Nonuremic Calciphylaxis: A Series of 24 Cases from a Single Institution

Emad Ababneh[1], Anthony Fernandez[2], Jennifer Ko[3], Steven Billings[4]
[1]Cleveland Clinic Foundation, Cleveland Heights, OH, [2]Cleveland Clinic Foundation, Cleveland, OH, [3]Highland Hgts, OH, [4]Cleveland Clinic, Lerner College of Medicine, Cleveland, OH

Disclosures: Emad Ababneh: None; Anthony Fernandez: None; Jennifer Ko: None; Steven Billings: None

Background: Calciphylaxis is most commonly seen in end-stage renal disease and hemodialysis (uremic calciphylaxis). Nonuremic calciphylaxis is described, but large studies are lacking.

Design: All calciphylaxis cases from 2010-2019 were identified. Uremic calciphylaxis cases (patients with ESRD, chronic kidney disease with creatinine level ≥ 3 mg/dl, acute kidney injury requiring renal replacement therapy or transplantation) were excluded. Charts and available biopsies were reviewed.

Results: 24/68 (35%) were nonuremic calciphylaxis. Median age was 66 years (range 31-88) with an F: M ratio of 11:1. 19/24 (79%) had BMI >30 (median, 35.75). Patients presented with ulcers (17), retiform purpura (4) or indurated plaques (3) involving the thigh (9), lower leg (7), calf (6), abdomen (2), and axilla (1) Most had multiple medical conditions, including hypertension (19), diabetes mellitus (12), hyperlipidemia (10), autoimmune diseases (8), coronary artery disease (7), deep vein thrombosis (4), and atrial fibrillation (4). 3 had hyperparathyroidism at presentation. All had multiple medications, including diuretics (15), warfarin (11), antiplatelet drugs (10), corticosteroids, statins, opioids (8) and vitamin D supplements (14). Five had corrected serum calcium level > 10 mg/dl (median, 9.51 mg/dl). Seven had elevated parathyroid hormone level (>64 pg/ml, median, 51 pg/ml). 18 biopsies were available. Calcification was apparent on H&E in all cases and confirmed on 10 with von Kossa stains. All had calcification of small-medium caliber vessel walls. The calcification was predominantly stippled in 5, chunky in 2 cases and mixed stippled and chunky in 10. Calcification associated with thrombosis was seen in 11 and vessel wall necrosis in 4. Extravascular calcification was present in 10, involving subcutaneous tissue interstitium (7), perieccrine deposition (4), and dermis (1). Epidermal changes included full-thickness necrosis (3), ulceration (2), and erosion (1) to crust and vesicle formation (2). Dermal changes included reactive angioendotheliomatosis (4), perivascular chronic inflammation (4) and hemorrhage (2). Fat necrosis, present in 14, had septal fibrosis (3) and septal panniculitis (2) in a subset

Conclusions: Nonuremic calciphylaxis is more common than recognized, accounting for >1/3 of our cases and disproportionately affects women. Obesity is the most common predisposing factor, but most patients had multiple comorbidities that could contribute to calciphylaxis.

460 What Influences Mortality in Conjunctival Melanoma? An Updated Analysis of the National Cancer Institute Database

Albert Alhatem[1], Paul Langer[1], Roger Turbin[2], W. Clark Lambert[2]
[1]Rutgers New Jersey Medical School - Rutgers University, Newark, NJ, [2]Rutgers New Jersey Medical School, Newark, NJ

Disclosures: Albert Alhatem: None; Paul Langer: *Consultant*, Matrix Surgical USA; W. Clark Lambert: None

Background: Ocular melanoma (OM), the second most common type of melanoma after cutaneous melanoma, accounts for 3.7% of all melanoma cases. Conjunctival melanoma (CM) accounts for only 5% of all OM patients. We aimed to investigate the changing incidence of CM over the past four decades and factors influencing survival in CM.

Design: The National Cancer Institute Surveillance, Epidemiology and End Results database from 18 registries was queried for all patients with CM from 1973 to 2016. We included only CM specific death cases. Age groups (years) were defined as follows: under 20, 20-44, 45-64, 65-74, and 75+. American Joint Committee on Cancer (AJCC) 7th edition was utilized to assess staging and International Classification of Disease for Oncology (ICD-O-3) codes were used to assess the histologic diagnosis. Age-adjusted incidence rates per 1000,000 population were calculated using the 2000 U.S. census data. Chi-squared test was utilized to identify differences between the variables, Kaplan-Meier analysis was used to estimate the survival and Cox regression models were used to calculate hazard ratios.

Results: A total of 728 patients with CM were identified, including 350 (48 %) females and 665 (91%) whites. The most common cases were in age 45-64 y and the least common were under 20 y. Fourteen histologic subtypes were identified, including Malignant Melanoma-NOS as the most common type and Lentigo Maligna, Mucosal Lentiginous Melanoma, Malignant Melanoma in Congenital Nevus, and Spindle Cell Melanoma, type B as the least common types. The incidence rates per year have increased from 0.0072 in 1973 to 0.12 in 2016. The overall 5-year survival rate was 85% and 10-year survival rate was 77%. Cumulative survival significantly decreased with the following: increased age group, male gender, advanced AJCC T staging, having one primary only, no surgery, and radiotherapy. No statistical differences were identified in survival between white and non-white ethnicity. Multivariate Cox regression model showed that hazard ratios were statistically significant in white race, male gender, AJCC stage T4, no surgery, having either radiotherapy or chemotherapy.

Conclusions: Conjunctival melanoma`s incidence rate has increased in the past four decades. Poor prognostic factors are increased age, male gender, and advanced stages. Similar to cutaneous melanoma, multiple CM primaries have a better prognosis than having only one primary and cancer directed surgery has a better outcome than treatment with radiation or chemo.

461 A Novel Method to Evaluate CAR Immunotherapy for Melanoma Patients Using Precision Medicine

Albert Alhatem[1], Saiaditya Badeti[2], Ke Geng[2], Yan Yang[1], Celso Viana[1], Kien Pham[3], Thu Minh Truong[2], W. Clark Lambert[2], Robert A. Schwartz[2], Ravi Chokshi[4], Dongfang Liu[4], Chen Liu[5]
[1]Rutgers New Jersey Medical School - Rutgers University, Newark, NJ, [2]Rutgers New Jersey Medical School, Newark, NJ, [3]Rutgers - New Jersey Medical School, New Brunswick, NJ, [4]Rutgers - The Cancer Institute of New Jersey, Newark, NJ, [5]Rutgers University NJ and RWJ Medical Schools, Newark, NJ

Disclosures: Albert Alhatem: None; Saiaditya Badeti: None; Ke Geng: None; Yan Yang: None; Celso Viana: None; Kien Pham: None; Thu Minh Truong: None; W. Clark Lambert: None; Robert A. Schwartz: None; Ravi Chokshi: None; Dongfang Liu: None; Chen Liu: None

Background: The rates of invasive melanoma have been rising for the past few decades. The incidences of oncogene mutations and tumor suppressor gene mutations are well described in melanoma. The absence of these mutations precludes certain patients for various types of chemotherapy or immunotherapy. However, not all patients that receive these therapies are guaranteed a good outcome. To our knowledge, no previous study has shown the efficacy of chimeric antigen receptor (CAR) therapies using a specific patient's own cancer cells. Our objective was to investigate anti-neuroectodermal disialoganglioside (GD2) CAR therapy in targeting an invasive rare genotype of melanoma cells using precision medicine.

Design: Culturable tumor cells and patient-derived xenografts (PDX) mice, confirmed by histopathology, were derived from an invasive melanoma tissue donor whose cancer was negative for 50 genes established by next generation sequencing, using the AmpliSeq For Illumina Cancer Hotspot Panel for 207 amplicons, including ABL1, EGFR, GNAQ, KRAS, PTPN11, AKT1, ERBB2, GNAS, MET, RB1, ALK, ERBB4, HNF1A, MLH1, RET, APC, EZH2, HRAS, MPL, SMAD4, ATM, FBXW7, IDH1, NOTCH1, SMARCB1, BRAF, FGFR1, IDH2, NPM1, SMO, CDH1, FGFR2, JAK2, NRAS, SRC, FGFR3, JAK3, PDGFRA, STK11, CSF1R, FLT3, KDR, PIK3CA, TP53, CTNNB1, GNA11, KIT, PTEN, CDKN2A, VHL. PDX-derived cancer cells were cultured and used for immunohistochemistry, flow cytometry, and 4-hour chromium-release killing assays to evaluate anti-GD2 CAR therapy for this patient's tumor.

Results: The patient's cancer cells were characterized and found to be positive for GD-2 and the immune checkpoint ligand; PDL-1. Using the chromium release assay, we determined that NK92MI cells, transduced with a third generation anti-GD2 construct effectively eliminated patient`s tumor cells, even to a greater degree than a similarly structured first generation construct with the same single chain variable fragment (scvF) domain.

Conclusions: Our results provide multiple implications: 1- A novel murine model to study a rare invasive melanoma genotype. 2- An *in vitro* technique to derive cancer cells from solid tumors to evaluate various CAR immunotherapeutic strategies in a patient-directed manner. 3- An excellent collaborative model where clinicians, surgical oncologists, pathologists, and immunologists can combine their efforts to provide optimal immunological and pharmacological care.

462 Correlation between Metastatic Tumor Burden in Sentinel and Non-Sentinel Lymph Nodes and Prognostic Significance of Tumor Burden in Sentinel Nodes in 336 Patients with Cutaneous Melanoma: A Single-Institution Retrospective Study

Phyu Aung[1], Kenjiro Namikawa[1], Denai Milton[1], Priyadharsini Nagarajan[2], Michael Tetzlaff[1], Jonathan Curry[2], Doina Ivan[1], Carlos Torres-Cabala[1], Victor Prieto[1]
[1]The University of Texas MD Anderson Cancer Center, Houston, TX, [2]Houston, TX

Disclosures: Phyu Aung: None; Kenjiro Namikawa: None; Priyadharsini Nagarajan: None; Michael Tetzlaff: *Advisory Board Member*, Myriad; *Advisory Board Member*, Seattle Genetics; *Speaker*, Nanostring; *Advisory Board Member*, Novartis LLC; Jonathan Curry: None; Doina Ivan: None; Carlos Torres-Cabala: None; Victor Prieto: None

Background: In patients with cutaneous melanoma, metastasis in a non-sentinel lymph node (non-SLN) is a strong independent adverse prognostic factor. However, patients with a tumor-involved SLN no longer routinely undergo completion lymph node dissection (CLND). We hypothesized that SLN tumor burden may predict non-SLN tumor burden.

Design: We compared tumor burden parameters between SLN and non-SLN in patients with cutaneous melanoma who underwent SLN biopsy with a positive SLN during 2003-2008 at The University of Texas MD Anderson Cancer Center.

Results: We identified 336 eligible patients with a positive SLN. Of these, 308 (92%) underwent CLND, and 35 (10%) had non-SLN metastasis. The median follow-up time was 6.0 years. For patients with maximum diameter of tumor in the SLN ≤ 2.0 mm, > 2.0-5.0 mm, and > 5.0 mm, non-SLN metastasis was detected in 5 of 200 patients (3%), 10 of 63 patients (16%), and 20 of 57 patients (35%), and the

mean maximum diameters of the non-SLN tumor deposits were 0.09 mm, 1.56 mm, and 2.71 mm, respectively (p<0.0001). The percentage of patients with both subcapsular and intraparenchymal non-SLN tumor was higher for patients with SLN tumor in both locations than for patients with SLN tumor in only one location (p<0.0001). Extranodal extension in a non-SLN was more common in patients with extranodal extension in a SLN (p=0.003).

Conclusions: In patients with cutaneous melanoma who undergo CLND, SLN tumor burden predicts non-SLN tumor burden. SLN tumor burden parameters provide accurate prognostic stratification independent of non-SLN status and should be considered for incorporation into future staging systems and integrated risk models.

463 Systematic Re-Evaluation of Pathologic Lymph Node Examination and Ancillary Studies in Desmoplastic Melanoma

Farah Baban[1], Ruifeng Guo[2], Kabeer Shah[3]
[1]Mayo Clinic Rochester, Rochester, MN, [2]Mayo Clinic, Rochester, MN, [3]St. Mary's Hospital, Madison, WI

Disclosures: Farah Baban: None; Ruifeng Guo: None; Kabeer Shah: None

Background: Desmoplastic melanoma (DM) differs from conventional melanoma (CM) with distinct morphology and clinical behavior. Management of desmoplastic melanoma has been controversial and variable. Only limited studies have been performed and one of the main challenges is in regard to lymph node (LN) examination.

Design: 75 patients with a diagnosis of (DM) and a complete clinical record from our institution were retrospectively evaluated over a 17 year period (1998-2015). All patients had wide local excision and some of them went on with lymph node examination (sentinel and non-sentinel nodes). The clinical and pathological features of the primary tumor and LNs were reviewed systematically and the findings were summarized.

Results: The mean age was 69.5 years (range 33-89 years) with 57 being males and 18 being females. Of the 75 patients, 31 (41.3%) with a pathological stage ranging from T2a to T4b had LN examination. The tumors had strong predilection for head and neck locations (22/31), where most of the examined LNs were from. Among the 31 patients, the primary tumor type included pure DM (24/31, 77.4%) and mixed DM (7/31, 22.6%), with the latter containing variable CM components. 23 patents had a sentinel lymph node (SLN) biopsy and only 1 (4.3%) showed metastatic DM forming a 2mm fibrotic focus. In addition, one case of mixed DM demonstrated micrometastis (0.2mm) by CM component only. 8 (25.8%) patients had a local node dissection without preceding SLN biopsy, triggered by clinical suspicion for regional lymphadenopathy. 3 patients (3/8, 37.5%) were found to contain 4 positive lymph nodes, all with pure DM in the background of dense fibrosis (Figure 1). Grossly, 2 of them were clinically apparent (22mm and 37mm) and 2 with microscopic foci (2mm each). Immunohistochemical stains with S100, Melan A and/or HMB45 were performed on all cases. Melan A and HMB45 were overall noncontributory. S100 highlighted the tumor foci but also showed a high background staining of non-melanoma cells (Figure 2).

Figure 1 - 463

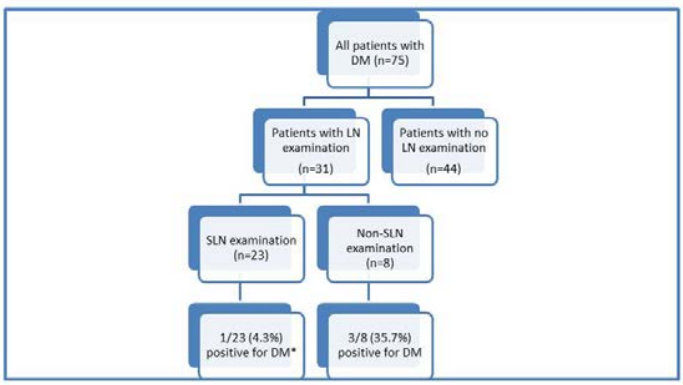

Figure 1. Desmoplastic melanoma and lymph node examination
DM (desmoplastic melanoma), LN (lymph node), SLN (sentinel lymph node)
* one additional patient had positive SNL with conventional melanoma component.

Figure 2 - 463

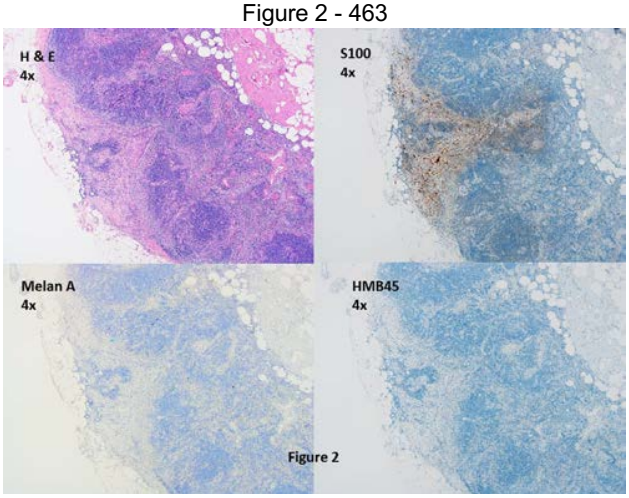

Conclusions: The overall SLN positivity rate for metastatic DM was low. In contrast, non-SLN examination had higher yield when targeted clinical examination was included in the case workup. As for the pathological examination, scrutinization using routine H&E with focus on dense fibrotic regions is of the ultimate importance, which could be assisted by S100 stain in the awareness of background cells. In contrast, Melan A and HMB45 stains play little role in assisting detecting metastatic DM.

464 Malignant Melanoma: Immuno-Oncology Experience in a Tertiary Cancer Center

Andrea Bakker[1], Ksenia Chezar[2], Tina Cheng[3], Edwin Wang[3], Michelle Dean[3], Tilley Derek[4], Zhanpeng Sun[3], Lin Li[3], Aleksi Suo[3], Doha Itani[5], Kim Koczka[3], Carissa Beaulieu[6]

[1]University of Calgary/Alberta Public Laboratories, Calgary, AB, [2]Department of Pathology and Laboratory Medicine, University of Calgary, Calgary Laboratory Services, Calgary, AB, [3]University of Calgary, Calgary, AB, [4]Cancer Control Alberta, Alberta Health Services, Calgary, AB, [5]Calgary Laboratory Services/University of Calgary, Calgary, AB, [6]University of Alberta, Edmonton, AB

Disclosures: Andrea Bakker: None; Ksenia Chezar: None; Tina Cheng: None; Edwin Wang: None; Michelle Dean: None; Tilley Derek: None; Doha Itani: None; Kim Koczka: None

Background: Immuno-Oncology (IO) treatments exploit the interaction of the immune system with malignant melanoma, however; the outcome varies in different patients. Our study aims to evaluate the effect of various IO agents in melanoma patients at our tertiary cancer center in order to understand how certain histologic parameters and sequencing of the IO agents affect clinical course, response and survival.

Design: We compiled a database of all melanoma patients who received systemic IO treatment at our center since 2012 (187 patients). We collected patient demographics, stage at presentation, treatment protocols, clinical response, survival, tumor characteristics (BRAF mutation status, histologic parameters). Data was then analyzed using Log rank survival, Cox regression, and the Holm-Sidak method.

Results: Log rank survival analysis showed improved overall survival measured from time of diagnosis and time of disease recurrence with younger age (<50 vs ≥65, p <0.001 and p =0.04, respectively). Multivariate cox regression analysis showed worse survival of patients with mucosal and acral lentiginous melanomas (HR 4.193 and 3.247, p <0.001 and p= 0.03, respectively). Tumors with BRAF mutations showed improved survival measured from time diagnosis and disease recurrence (p =0.026 and 0.022, respectively). More lines of therapy (≥3 vs <3) were associated with longer survival after disease recurrence (p = 0.025). This included all lines of therapy including IO. M1d disease (CNS involvement) and M1a-c (non-visceral, lung, visceral non-CNS) did not show any significant difference in survival with IO treatment.

	N(187)	%
Sex		
Female	60	32.1
Male	127	67.9
Age		
Median (range)	61	(16-90)
<50	46	24.6
50-64.9	70	37.4
>=65	71	38.0
Primary Site		
Cutaneous	119	63.6
Mucosal	21	11.2
Acral lentiginous	5	2.7
Uveal	8	4.3
Unknown/Other	34	18.2
BRAF Mutation Status		
WIld type	128	71.1
Mutated	52	28.9
Unknown/not performed	7	

Figure 1 - 464

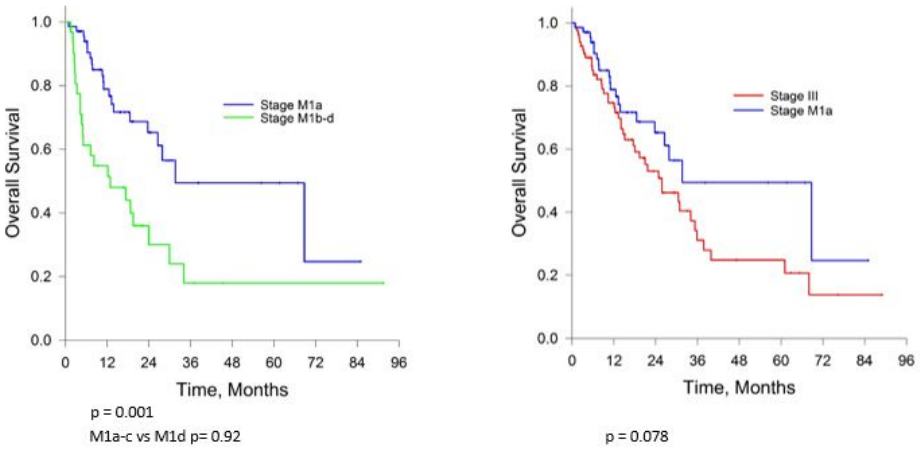

Figure 2 - 464

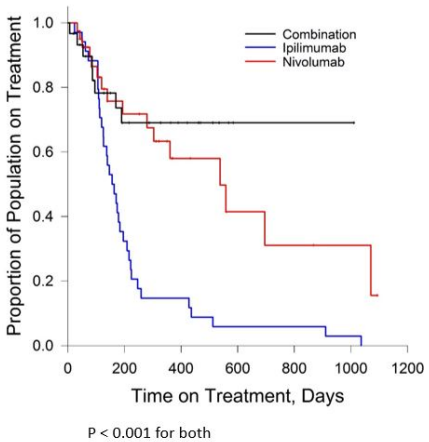

Conclusions: Our study of 187 melanoma patients receiving IO therapy at out tertiary care center demonstrates interesting trends in survival with IO therapy. Further investigation including slide review, histologic parameter confirmation and analysis as correlated to clinical response using the RECIST 1.1 criteria are underway. Using Next Generation Sequencing, we plan to compare tumor and immune cell expression profiles in tissue collected before and after IO therapy. The results will be used to better understand the physiology of immune response in melanoma and to inform treatment decisions.

465 High Resolution Multiplexing of Melanoma Microenvironment in Responders/Non-Responders to Checkpoint Therapy

Francesca Bosisio[1], Asier Antoranz[2], Yannick van Herck[2], Maddalena Bolognesi[3], Seohdna Lynch[4], Arman Rahman[4], William Gallagher[5], Giorgio Cattoretti[3], Joost van den Oord[6], Oliver Bechter[6]
[1]UZ Leuven, Leuven, Vlaams-Brabant, Belgium, [2]KU Leuven, Leuven, Vlaams-Brabant, Belgium, [3]UNIMIB, Milan, MB, Italy, [4]University College of Dublin, Dublin, Dublin, Ireland, [5]University College Dublin, Dublin, Dublin, Ireland, [6]KU Leuven, Leuven, Belgium

Disclosures: Francesca Bosisio: None; Asier Antoranz: None; Yannick van Herck: None; William Gallagher: None; Oliver Bechter: None

Background: An *in situ* "high resolution" investigation of the tumor microenvironment has been urged in recent years by the previously failed attempt to find solid histological biomarkers for immunotherapy response. Our objective is to characterize the melanoma microenvironment with a multi-omics approach to find significative differences between responders and non-responders.

Design: 23 metastases were collected from patients that underwent PD-1 inhibition (10 complete/partial responders, 13 progressive disease) prior the start of the therapy. A Nanostring PanCancer Immune profiling panel was performed on fresh frozen material. On the same patients, a panel of 80 markers was performed according to the MILAN multiplex technique on formalin-fixed, paraffin-embedded material. A bioinformatic pipeline was applied to the first technique to find differences in gene expression between responders and non-responders, and to the second technique to phenotype the inflammatory populations present in the tissue and to investigate the spatial relationships between them.

Results: Several genes implicated in adaptive immunity/T cell activation were found to be differentially regulated in the responders. This was confirmed also by pathway analysis. In tissue sections, part of the proteins on the 80 selected for the panel showed a differential expression in the responders, in particular the immune checkpoint molecule TIM3. The level of CD8+ lymphocytes (cyT) exhaustion was higher in responders before treatment. In an active microenvironment, melanoma cells are in contact not only with active cyT, but also with active T helpers, that tend to fade away with the transition towards exhaustion, while myeloid cells express progressively higher levels of TIM3, assuming an immune suppressive role, and increase their interaction with cyT in all their functional statuses.

Figure 1 - 465

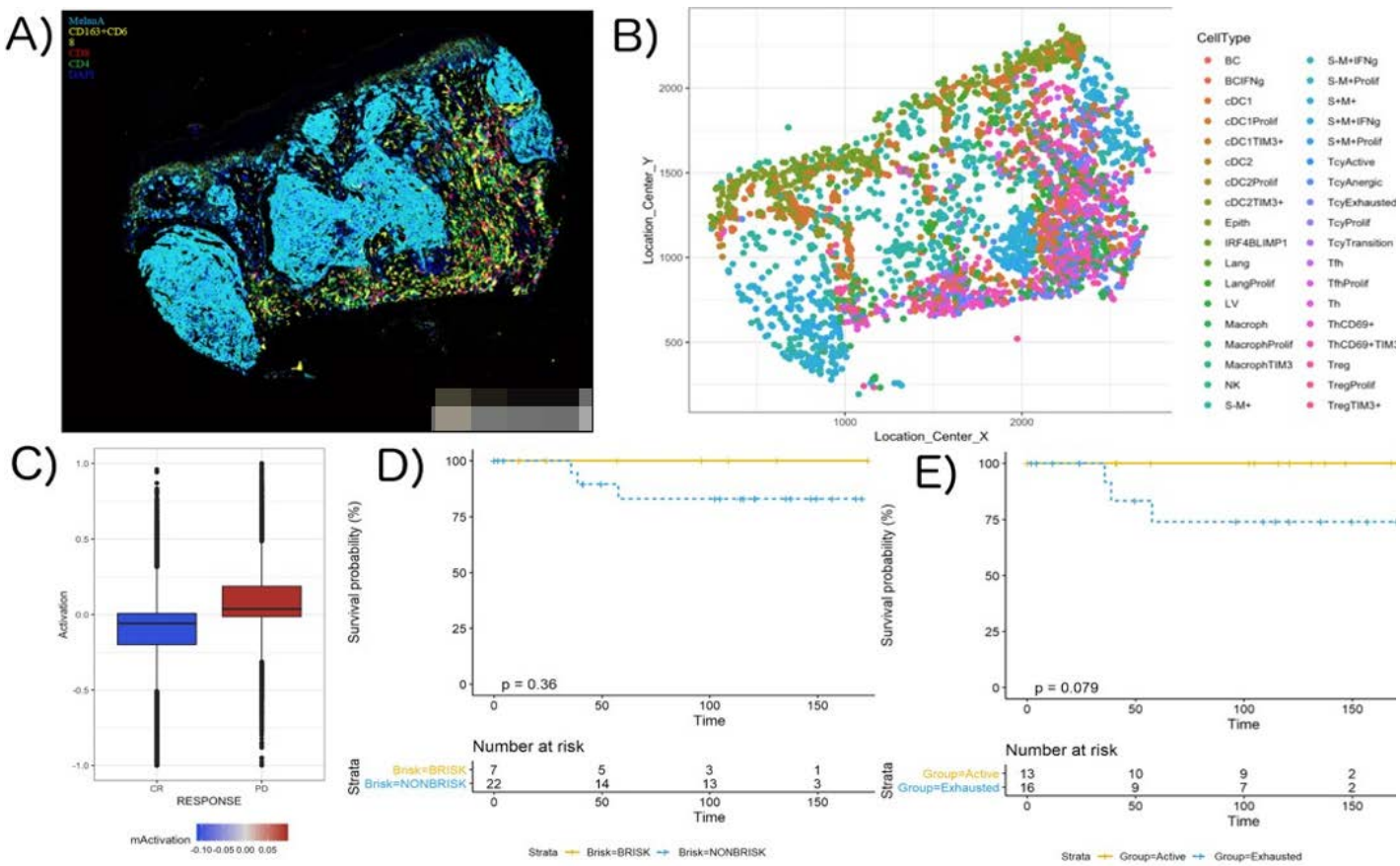

Conclusions: Associating the analysis of the phenotypical and functional heterogeneity of the immune infiltrate to the spatial distribution of each cell type could improve tissue-based biomarkers discovery.

466 Iodine Toxicity After Administration of Iodinated Contrast: New Observations in Iododerma

Scott Bresler[1], Mason Runge[2], Eun-Young Choi[2], May Chan[2], Lori Lowe[2]
[1]University of Michigan Health System, Ann Arbor, MI, [2]University of Michigan, Ann Arbor, MI

Disclosures: Scott Bresler: None; Mason Runge: None; Eun-Young Choi: None; May Chan: None; Lori Lowe: None

Background: Iododerma is a rare halogenoderma that develops following exposure to iodine-containing compounds, including intravenous (IV) iodinated contrast media. Affected patients typically suffer from chronic kidney disease. Although a wide range of cutaneous manifestations have been reported, the most common are papulopustular or vegetative nodules located on the face. The histologic findings in iododerma are classically reported as pseudoepitheliomatous hyperplasia with intraepidermal, follicular, and/or dermal neutrophilic microabscesses. Due to the rarity of this condition, less typical presentations are under-recognized.

Design: The pathology archives of our institution were searched for cases of iododerma diagnosed between 1987 and April 2019. Three cases were confirmed after a retrospective chart review of these patients, who were all evaluated by our inpatient consult dermatology service. Clinical data and histopathologic features are summarized.

Results: Three cases of iododerma following IV iodinated contrast media administration in patients with severe chronic kidney disease are described. All patients had rapid evolution of skin lesions presenting as papules or bullae with variable hemorrhagic crusting (Figure 1). All biopsies demonstrated a neutrophil-rich dermal infiltrate (Figure 2A,B) containing round anucleate structures resembling Cryptococcus (Figure 2B, inset) with or without vasculitis (Figure 2C). One patient had gastrointestinal involvement, with biopsy of a proximal jejunum ulcer showing similar findings. Special stains for microorganisms and tissue cultures were negative in all cases. In all three cases, the presumed nuclear fragments within the haloed spaces stained strongly with PU.1 without appreciable staining for myeloperoxidase, suggesting that the structures are likely degenerating histiocytes. Urine iodine levels were elevated greatly above reference ranges in all cases.

Figure 1 - 466

Figure 2 - 466

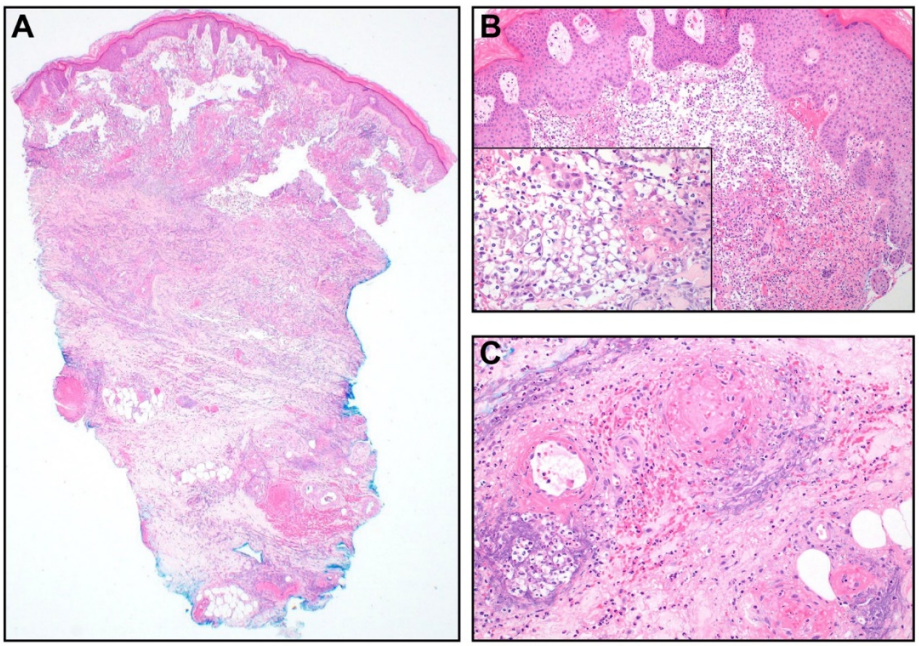

Conclusions: Iododerma may be a sequela of IV iodinated contrast media administration and can manifest as a neutrophilic dermatosis with *Cryptococcus*-like haloed structures with or without concomitant vasculitis**.** Iododerma can progress rapidly and be polymorphous in its clinical presentation and histopathologic features, simulating infection, Sweet syndrome, and/or immune complex vasculitis. Our series expands the histomorphologic spectrum to include cryptococcal-like structures and vasculitis as potential diagnostic clues to this rare condition.

467 Primary Cutaneous Melanoma of the Umbilicus: A Retrospective Study of 18 Patients

Woo Cheal Cho[1], Victor Prieto[1], Stephen Gruschkus[1], Roland Bassett[1], Carlos Torres-Cabala[1], Michael Tetzlaff[1], Jonathan Curry[2], Phyu Aung[1], Doina Ivan[1], Priyadharsini Nagarajan[2]
[1]The University of Texas MD Anderson Cancer Center, Houston, TX, [2]Houston, TX

Disclosures: Woo Cheal Cho: None; Victor Prieto: None; Stephen Gruschkus: None; Roland Bassett: None; Carlos Torres-Cabala: None; Michael Tetzlaff: *Speaker*, Nanostring; *Advisory Board Member*, Novartis LLC; *Advisory Board Member*, Myriad Genetics; *Advisory Board Member*, Seattle Genetics; Jonathan Curry: None; Phyu Aung: None; Doina Ivan: None; Priyadharsini Nagarajan: None

Background: Primary cutaneous melanoma of the umbilicus is exceptionally rare and since umbilicus is embryologically distinct from other body sites, the clinicopathologic parameters of prognostic value in these tumors are currently unclear.

Design: We identified 18 patients (pts) with primary cutaneous melanoma of the umbilicus over a period of 20 years and recorded demographic, clinical, histopathologic features; dates of diagnosis, recurrence, metastasis and death. Kaplan-Meier methods were used to estimate the distribution of disease-specific survival (DSS) and metastasis-free survival (MFS) from the date of diagnosis. Cox proportional hazards regression analysis was used to assess association with covariates of interest. Due to the small number of events, Firth's penalized likelihood was used to estimate hazard ratios and p-values.

Results: Most pts were Caucasians (n=16, 89%), with median age at diagnosis of 46 years (range: 14-76 years) and slight female predominance (44% male). The predominant histologic type was superficial spreading (78%), with a median Breslow thickness of 2.2 mm (range: 0.5 to 18.0 mm) and majority (39%) were non-ulcerated. At presentation, 13 pts had localized disease, while 4 and 1 pts had regional and distant metastasis, respectively. The median times to regional and distant metastases were 1.6 and 16.1 months, respectively. With a median DSS of 74 months, the 1, 3, and 5-year DSS rates were 92%, 64%, and 64%, respectively. Median MFS was not reached. Eight pts developed metastasis, of which 6 had systemic disease. Five pts died, all due to progression of melanoma. Univariate analysis (Table 1) revealed the following features to be correlated with shorter DSS: age at diagnosis (>45 years), histologic type (nodular), Breslow thickness (>2.0 mm), and ulceration. Furthermore, lesion size (>7 mm), histologic type (nodular), Breslow thickness (>2.0 mm), ulceration, dermal mitotic activity, and lymphovascular invasion correlated with shorter MFS. Two tumors were analyzed for hotspot genetic alterations and both were positive for BRAFpV600E mutation.

Table 1. Statistically significant (p<0.05) clinicopathologic features correlating with shorter disease specific and metastasis free survival

	Disease specific survival HR (95% CI); p-value	Metastasis free survival HR (95% CI); p-value
Age at diagnosis (>45 years)	10.8 (1.1, 1435.4); p=0.04	-
Histologic type (nodular)	12.3 (1.6, 136.3); p=0.02	45.3 (3.5, 6344.8); p=0.003
Breslow thickness (>2 mm)	6.0 (1.1, 60.3); p=0.04	9.9 (1.7, 101.5); p=0.009
Lesion size (>7 mm)	-	14.3 (1.4, 1937.0); p=0.02
Mitotic figures (>0/mm^2)	-	14.7 (1.6, 1956.5); p=0.01
Ulceration	6.0 (1.1, 60.3); p=0.04	15.0 (2.6, 153.9); p=0.002
Lymphovascular invasion	-	9.9 (1.7, 101.5); p=0.009

Conclusions: Primary cutaneous melanoma of the umbilicus most frequently affects Caucasian adults and several clinicopathological features predictive of outcome in primary cutaneous melanomas such as histologic type, Breslow thickness, ulceration, mitotic rate and lymphovascular invasion also predict DSS in these tumors. In addition, lesion size also correlated with MFS in our cohort.

468 Use of Non-Coding Promoter Mutations to Distinguish Melanomas from Nevi

Andrew Colebatch[1], Robert Rawson[1], Peter Ferguson[2], Louise Jackett[3], James Wilmott[4], Richard Scolyer[5]
[1]Royal Prince Alfred Hospital, Camperdown, NSW, Australia, [2]Royal Prince Alfred Hospital, Sydney, NSW, Australia, [3]Austin Hospital, Mt Stuart, VIC, Australia, [4]The University of Sydney, Camperdown, NSW, Australia, [5]Royal Prince Alfred Hospital, Wollstonecraft, NSW, Australia

Disclosures: Andrew Colebatch: None; Louise Jackett: None

Background: While the distinction between benign and malignant melanocytic neoplasms is often straightforward, lesions with overlapping features that are diagnostically challenging are not uncommon. Molecular diagnostic adjuncts to improve classification of these borderline lesions are therefore urgently needed.

The cutaneous melanoma genome shows large numbers of ultraviolet radiation induced somatic mutations. A proportion of these mutations occur within specific binding sites for ETS transcription factors, located within active core promoters of numerous genes. These are distinct from noncoding promoter mutations in the core promoter of *TERT*, present in approximately 80% of cutaneous melanoma cases, which lead to the creation of novel ETS binding sites.

Given recent work demonstrating that cutaneous melanomas have higher mutation loads compared to benign and intermediate precursors, we hypothesised that non-coding promoter mutation loads will distinguish nevi from melanomas. This study sought to identify differences in non-coding mutations between nevi and melanoma (including in melanomas associated with a precursor nevus).

Design: We collected 30 cases: 18 melanomas (including 10 with an adjacent precursor nevus) and 12 nevi. DNA was extracted and sequenced using a custom amplicon based panel. In the 10 melanoma cases with an adjacent precursor nevus, representative areas of nevus and melanoma were dissected and both regions were sequenced and compared. In addition droplet digital PCR was performed for *BRAF, NRAS* and *TERT* promoter mutations.

Results: Analysis of 21 of the cases (9 melanomas, including one with an adjacent precursor nevus, and 12 nevi) showed that 7 melanomas harbored at least two promoter mutations, whereas one nevus case had two promoter mutations, and two cases had one promoter mutation each. *TERT* promoter mutations were confined to melanomas (6/9). Specifically, in the one case of a melanoma with an adjacent precursor nevus sequenced to date, the nevus component carried fewer promoter mutations than the melanoma.

Conclusions: From preliminary data, we confirm that nevi carry fewer noncoding promoter mutations than melanomas. A molecular assay evaluating promoter mutations may assist in the diagnosis of challenging borderline melanocytic neoplasms.

469 Mismatch Repair Deficiency and PD-L1 Expression in Sebaceous Carcinomas and Basal Cell Carcinomas with Sebaceous Features.

Bre Ana David[1], Shyam Raghavan[2], Anne Mills[3]
[1]UVA Medical Center, Charlottesville, VA, [2]Stanford University, Stanford, CA, [3]University of Virginia, Charlottesville, VA

Disclosures: Bre Ana David: None; Shyam Raghavan: None; Anne Mills: None

Background: Muir-Torre Syndrome (MTS) is a rare autosomal dominant cancer syndrome that is attributable to heritable defects in the MMR genes *MLH1*, *MSH2*, *PMS2,* and *MSH6*. Affected individuals are at increased risk for both internal malignancies and skin lesions including keratoacanthomas and sebaceous neoplasms. We know that mismatch repair (MMR)-deficient endometrial and colorectal cancers show higher expression of Programmed Death Ligand-1 (PD-L1) and improved response rates to anti-PD-1/PD-L1 immunotherapies when compared to their MMR-intact counterparts. It is unknown, however, whether the same is true in sebaceous malignancies. We evaluated PD-1/PD-L1 expression in MMR-intact and deficient tumors with sebaceous differentiation, including sebaceous carcinomas (SC) and basal cell carcinomas with sebaceous differentiation (BCC-S), to assess the potential utility of targeted immunotherapy in these patients.

Design: The departmental files were reviewed for all cases of MMR-d SC and BCC-S. All other cases of SC and BCC-S diagnosed in the last 12 years were also pulled and were stained for the 4 MMR proteins (MLH1, PMS2, MSH2, and MSH6). PD-L1 immunohistochemistry was performed on all cases and was assessed for staining in the tumor cells (tumor proportion score, TPS) and associated immune cells (combined positive score, CPS).

Results: A total of 15 cases were reviewed (SC=11, BCC-S=4), 7 (47%) of which were MMR-deficient (2 previously identified, 5 identified on study staining). (**Table**) Of the MMR-deficient cases, 1 MSH2/6-deficient SC had known MTS while the others (4 SC and 2 BCC-S; 2 MLH1/PMS2-deficient, 4 MSH2/6-deficent) were considered possible MTS. Overall, PD-L1 staining in tumor cells and/or immune cells (CPS≥1) was seen in the majority (80%) of cases, while 33% had staining specifically in tumor cells. A positive PD-L1 TPS and CPS were both more common in MMR-deficient vs. MMR-intact cases (57% vs. 12.5% and 100% vs. 62.5%, respectively) however these differences were not statistically significant due to limited power.

	PD-L1 TPS+ (≥1%)	PD-L1 CPS+ (≥1)
Total (n=15)	33% (5/15)	80% (12/15)
MMR-d (n=7)	57% (4/7)	100% (7/7)
MMR-i (n=8)	12.5% (1/8)	62.5% (5/8)

Conclusions: Although more common among MMR-deficient tumors, tumoral and tumor-associated immune cell expression of PD-L1 can be seen in both MMR-deficient and MMR-intact skin malignancies with sebaceous differentiation. This suggests that immunotherapy may be a therapeutic options for some patients with these tumors, with potential increased efficacy in the setting of MMR deficiency.

470 Chronic Pruritus of Unknown Origin is Associated with Histologic Evidence of Th2 Cell Polarization

Carina Dehner[1], Lu Chen[2], Ilana Rosman[3], Brian Kim[3]
[1]Washington University School of Medicine, St. Louis, MO, [2]NYU Langone, Newtown Square, PA, [3]Washington University School of Medicine in St. Louis, St. Louis, MO

Disclosures: Carina Dehner: None; Lu Chen: None; Ilana Rosman: *Consultant*, Appollo Optics; Brian Kim: *Employee*, Nuogen Pharma, Inc.

Background: Chronic pruritus of unknown origin (CPUO) is described as chronic itch lasting longer than 6 weeks in the absence of a defined skin rash any known causative disease process. Prior reports have indicated that CPUO patients exhibit features of Th2 cell-associated responses in the blood. However, whether Th2 cells are enriched in the skin of CPUO patients has never been tested. We sought to take a histopathologic approach to determine the association of CPUO and Th2 cell polarization in the skin.

Design: Skin biopsies from 23 patients diagnosed with CPUO and 9 control patients without evidence of cutaneous histopathological abnormalities were obtained and underwent a detailed clinical chart review including confirmation of chronic itch symptoms as assessed by the numerical rating scale (NRS) itch score. H&E sections were assessed and additional dual-staining for CD3/T-bet and CD3/GATA-3 was performed to quantify relative numbers of Th1 and Th2 cell subsets, respectively.

Results: Analysis of H&E stained sections showed sparse to moderate perivascular inflammation predominated by lymphocytes and occasional eosinophils in a subset of cases. Dual-staining of corresponding sections showed an increase in $CD3^+$ cells in CPUO skin compared to controls. CPUO patients showed significantly more $CD3^+$ cells co-expressing GATA-3, a Th2 cell-associated transcription factor, than T-bet, the Th1 cell-associated transcription factor, compared to healthy individuals. Meanwhile, healthy individuals presented with a balanced T-bet/GATA-3 ratio of co-expression in their skin.

Conclusions: The current study demonstrates for the first time enrichment of Th2 cells in CPUO skin as assessed by T cell/GATA-3 co-staining. These findings lend further support for the emerging clinical paradigm in which CPUO is increasingly considered a Type 2/Th2 cell-associated disease. We thus speculate that type 2 cytokine blockade-based therapies may represent effective treatments for CPUO.

471 Intravascular Lobular Capillary Hemangioma (Pyogenic Granuloma): A Study of 40 Cases

Josephine Dermawan[1], Jennifer Ko[2], Steven Billings[3]
[1]Cleveland Clinic, Cleveland, OH, [2]Highland Hgts, OH, [3]Cleveland Clinic, Lerner College of Medicine, Cleveland, OH

Disclosures: Josephine Dermawan: None; Jennifer Ko: None; Steven Billings: None

Background: Intravascular lobular capillary hemangioma (ILCH) or pyogenic granuloma (PG) is a relative rare entity with very few reports in the literature, and is clinically and histopathologically under recognized.

Design: We retrospectively reviewed all ILCH cases confirmed pathologically between 2006 and 2019. Immunostains for SMA and WT1 were performed on all cases. Clinicopathologic information were collected.

Results: 40 cases (21 in house; 19 consultations) were identified (22F;18M) with a median age of 53 (range 13-85). Among the 21 in-house cases with clinical information, all were well-circumscribed, mobile, subcutaneous, and stable to slow-growing raised/cystic skin lesions ranging from 3 mm to 4 cm. Of all cases, most were located on the upper extremities [18, 45%: 12 on palmar/digits], followed by head/neck (16, 40%), trunk (5, 12.5%), and feet (1, 2.5%). 6 were tender on palpation. Clinically, vascular lesions were suspected in only 6 (29%) cases. Of the 16 consult cases with provided preliminary histologic diagnoses, 8 included ILCH, and the remaining differential diagnoses included Masson tumor (3), glomus tumor (3), vascular tumors of intermediate malignant potential (3), angiosarcoma (1), melanocytic lesion (1), and basal cell carcinoma (1). The common histologic features were an intravascular, lobular/nodular proliferation of well-circumscribed, closely packed capillaries lined by bland endothelial cells. The surrounding vascular wall was well-visualized in < 50% of the cases. The majority (75%) was not associated with significant inflammation. Notably, one-third of the cases were mitotically active (up to 20 MF/10 HPF) and showed mild to moderate cytological atypia. Hobnail features were present in 40% of cases. All cases tested were diffusely and strongly positive for vascular markers (ERG, CD31, or CD34), and WT-1. SMA stains highlighted pericytes in all cases. Of the 20 cases with clinical follow-up (median follow-up: 40 months), none had recurred.

Conclusions: ILCH most commonly involve the upper extremities and a vascular tumor is suspected clinically in the minority. Mitotic activity and cytologic atypia, when present, can cause confusion with more aggressive vascular tumors. Recognition of this entity is essential as it is a benign lesion with no risk of recurrence following limited local excision.

472 Prognostic Role of Tumoral PDL1 Expression, and CD8+ and FoxP3+ Lymphocytes in Merkel Cell Carcinomas

Piotr Donizy[1], Cheng-Lin Wu[2], Janusz Kopczynski[3], Malgorzata Pieniazek[4], David Miller[5], Mai Hoang[6]
[1]Wroclaw Medical University, Wroclaw, Poland, [2]National Cheng Kung University Hospital, College of Medicine, National Cheng Kung University, Tainan, Taiwan, [3]Department of Surgical Pathology, Holy Cross Cancer Centre, Kielce, Kielce, Poland, [4]Department of Clinical Oncology, Tadeusz Koszarowski Regional Oncology Centre, Opole, Poland, [5]Massachusetts General Hospital, Harvard Medical School, Boston, MA, [6]Massachusetts General Hospital, Brookline, MA

Disclosures: Piotr Donizy: None; Cheng-Lin Wu: None; Janusz Kopczynski: None; Malgorzata Pieniazek: None; David Miller: *Consultant*, Merck; *Consultant*, Pfizer; *Consultant*, Regeneron; Mai Hoang: None

Background: The prognostic role of FoxP3+ lymphocytes in Merkel cell carcinomas (MCCs) has not been studied.

Design: PDL1, CD8 and FoxP3 immunostains were performed on tissue microarrays constructed from paraffin-embedded tissues of 132 MCCs. PDL1 expression >1% was considered positive. The absolute cell counts of tumoral CD8+ and FoxP3+ lymphocytes were assessed in 3 consecutive images captured at 40× magnification of the hotspot. The scores were dichotomized into high and low using the median as the cutoff value. We correlated PDL1 expression, and CD8+ and FoxP3+ immune infiltrates with clinicopathologic variables, Merkel cell polyomavirus (MCPyV) status, and patient outcomes.

Results: Tumoral PDL1 expression (>1%) was seen in 64/132 cases (48%). By Fisher's exact tests, tumoral PDL1 expression >1% significantly correlated with tumor size >30 mm (p=0.04), tumor thickness >10 mm (p=0.0048), lack of tumor progression (p=0.05), survival status (p=0.0003), and positive MCPyV status (p=0.018). High tumoral CD8+ cell count significantly correlated with absence of ulceration (p=0.0092) and positive MCPyV status (p=0.018). High tumoral FoxP3+ cell count correlated with survival status (p=0.024). By linear regression analyses, correlations between tumoral PDL1 expression with the density of tumoral CD8+ (p<0.0001) and tumoral FoxP3+ lymphocytes (p<0.0001), and tumoral CD8+ lymphocytes with tumoral FoxP3+ lymphocytes (p<0.0001) were observed.

By univariate analyses, tumoral PDL1 expression >1%, combined tumoral PDL1 >1% and high tumoral CD8+ infiltrate as well as combined tumoral PDL1 >1% and high tumoral FoxP3+ infiltrate correlated with improved Merkel cell carcinoma-specific survival (MSS) (p=0.038, 0.038, 0.022, respectively) and progression-free survival (PFS) (p=0.047, 0.037, 0.0083, respectively). Expression of MCPyV T-antigen correlated with improved overall survival (OS) (p=0.016). Ulceration correlated with worse OS (p=0.0051) and MSS (p=0.0041). By multivariate analyses, tumoral PDL1 expression >1% remained a predictor of better OS (p=0.039). Ulceration remained an independent predictor of worse OS (p=0.049) and MSS (p=0.0094).

Conclusions: Tumoral PDL1 expression and increased density of tumoral CD8+ lymphocytes and FoxP3+ lymphocytes may positively impact on survival in a subset of MCCs. Tumoral PDL1 expression correlated with tumoral CD8+ and FoxP3+ lymphocytes, supportive of an adaptive immune response. There is a correlation between immune response and MCPyV positivity.

473 Diverging Role of Immune Checkpoints in Cutaneous versus Uveal Melanomas: Hierarchical Clustering from TCGA Cases Highlights Different Clinical Behavior and Histological Variations

Philippe Echelard[1], Simon Roy[2], Leonardo Lando[3], Anne Xuan-Lan Nguyen[4], Vincent Quoc-Huy Trinh[5]
[1]Université de Sherbrooke, Sherbrooke, QC, [2]University of Montréal, Montréal, QC, [3]Federal University of Goias, Goiania, GO, Brazil, [4]McGill University, Montreal, QC, [5]Vanderbilt University Medical Center, Nashville, TN

Disclosures: Philippe Echelard: None; Simon Roy: None; Leonardo Lando: None; Anne Xuan-Lan Nguyen: None; Vincent Quoc-Huy Trinh: None

Background: Although cutaneous melanoma (CM) and uveal melanoma (UM) both originate from melanocytes, their oncogenic and clinical profiles share few similitudes. For example, immune checkpoint (IC) inhibition therapy shows promise in CM while being of little use in UM. In this study we explored The Cancer Genome Atlas (TCGA) dataset in order to compare CM and UM histological, molecular and clinical data along with their IC genes expression profile.

Design: Primary CM and UM were obtained from the TCGA. 6 CM did not have RNAseq data available and were excluded. We selected 72 IC related genes from a review of Pubmed-cited publications, and then extracted normalized gene expression data from cbioportal.org. ConsensusClusterPlus in R x64 3.5.1 was used to determine the optimal number of clusters per cancer type, based on cumulative distribution function (CDF) testing. Clinical and pathological data were reviewed in order to aggregate datapoints optimally. Diagnostic slides were downloaded with GDC Data Transfer Tool and reviewed in Aperio by 1 pathologist and 2 residents. Progression-free survival according to clusters were assessed using Kaplan-Meier curves and log-rank testing. Statistics were performed in SPSS v23.0.

Results: 103 primary CM and 80 UM were retained. ConsensusClusterPlus set K=4 as the optimal number of clusters for each subtype of melanoma after CDF. The CM clusters were only significantly associated with TNM nodal status (p=0.016) and BRAF (p=0.014) mutations. Alternatively, the UM clusters were significantly associated to known histological and molecular prognostic factors such as the formation of

vascular loops (p=0.043), the histologic variant (p=0.00045), the presence of BAP1 (p=0.000026) and SF3B1 (p=0.001) mutations and chromosomal alterations such as chromosome 3 loss (p= 0.006) and chromosome 8 gain (p=0.000355). At histological review, lymphocyte infiltration showed no association in CM (P=0.574) but was very significantly associated to UM (P=0.000444). Disease free survival was significantly associated to the immune checkpoint clusters in UM (log-rank P=0.000062), while showing no trends in cutaneous melanoma (P=0.165).

Table 1. Baseline clinical and pathological characteristics of 4 clusters of uveal and cutaneous melanoma cases from TCGA.

	Uveal Melanoma					Cutaneous Melanoma				
Parameters	**K1 (n=9)**	**K2 (n=17)**	**K3 (n=22)**	**K4 (n=31)**	**p***	**K1 (n=37)**	**K2 (n=48)**	**K3 (n=12)**	**K4 (n=6)**	**p***
Clinical Stage	0%	0%	0%	0%	0.319	3%	0%	0%	17%	0.423
I	33%	47%	41%	61%		71%	67%	67%	50%	
II	56%	41%	59%	35%		24%	28%	33%	33%	
III	11%	12%	0%	3%		3%	4%	0%	0%	
IV										
T stage	0%	0%	0%	0%	0.480	0%	4%	0%	0%	0.724
TX	0%	0%	0%	0%		3%	0%	0%	0%	
T1	11%	12%	9%	29%		5%	2%	8%	17%	
T2	33%	47%	41%	39%		14%	6%	8%	17%	
T3	56%	47%	50%	32%		78%	88%	83%	67%	
T4										
N stage	11%	11%	5%	0%	0.288	0%	2%	0%	0%	**0.015**
NX	89%	89%	96%	100%		19%	4%	25%	50%	
N0	0%	0%	0%	0%		68%	71%	50%	17%	
N1	/	/	/	/		3%	15%	0%	33%	
N2	/	/	/	/		11%	8%	25%	0%	
N3										
M stage	22%	22%	41%	32%	0.570	3%	2%	0%	0%	0.971
MX	67%	67%	59%	65%		95%	94%	100%	100%	
M0	11%	11%	0%	3%		3%	4%	0%	0%	
M1										
Mitoses per mm² (±SD)	2.8 (1.8)	2.2 (1.8)	1.7 (1.2)	1.9 (1.6)	0.315	0.8 (2.4)	6.7 (6.2)	5.1 (4.6)	4.1 (5.1)	0.787
Lymphoid infiltrate	56%	11%	59%	48%	**0.000444**	72%	55%	56%	33%	0.574
Low	33%	44%	32%	52%		12%	28%	11%	33%	
Intermediate	11%	44%	9%	0%		16%	17%	33%	33%	
High										
Vascular loops, presence	67%	61%	27%	32%	**0.043**	53%	63%	30%	17%	0.067
Pigmentation	33%	17%	23%	65%	**0.007**	64%	44%	46%	83%	0.417
Low (0-5%)	44%	39%	50%	13%		28%	44%	46%	17%	
Intermediate (6-50%)	22%	44%	27%	23%		8%	13%	9%	0%	
High (51-100%)										
Histologic variant	11%	11%	50%	52%	**0.00045**	-	-	-	-	-
Spindle	89%	33%	27%	29%		-	-	-	-	-
Mixed	0%	56%	23%	19%		-	-	-	-	-
Epithelioid										
Breslow (±SD)	-	-	-	-	-	10.0 (7.7)	15.8 (18.4)	13.6 (19.2)	12.0 (13.4)	0.379
Ulceration, presence	-	-	-	-	-	84%	88%	78%	80%	0.833
Prognostic mutations	89%	44.%	36%	7%	**0.000026**	-	-	-	-	-
BAP1	0%	6%	18%	16%	0.376	-	-	-	-	-
EIF1AX	0%	0%	18%	45%	**0.001**	-	-	-	-	-
SF3B1										
Chromosomal alterations	0%	0%	14%	19%	0.133	-	-	-	-	-
1 loss	56%	67%	32%	19%	**0.006**	-	-	-	-	-
3 loss	0%	28%	36%	32%	0.217	-	-	-	-	-
6 gain	56%	72%	46%	13%	**0.000355**	-	-	-	-	-
8 gain										
Mutations	-	-	-	-	-	62%	27%	42%	50%	**0.014**
BRAF mutated	-	-	-	-	-	3%	13%	17%	17%	0.322
NRAS mutated	-	-	-	-	-	5%	10%	0%	33%	0.094
NF1 mutated	-	-	-	-	-	0%	10%	8%	0%	0.200
KIT mutated	-	-	-	-	-	5%	2%	0%	17%	0.289
CDKN2A mutated	-	-	-	-	-	0%	8%	0%	0%	0.190
TERT amplified										
Mean fraction of genome altered (±SD)	0.196 (0.042)	0.179 (0.123)	0.188 (0.162)	0.123 (0.094)	0.153	0.37 (0.21)	0.29 (0.17)	0.33 (0.28)	0.24 (0.09)	0.248
Mean mutations in genome (±SD)	14.1 (5.0)	14.3 (3.3)	34.3 (81)	15.2 (4.3)	0.354	267.6 (301.0)	534.8 (1091.5)	148.8 (131.2)	575.6 (536.9)	0.400

Figure 1 - 473

Figure 1. Preliminary clusters of cutaneous melanoma (left) and uveal melanoma (right) cases from TCGA formed along their immune checkpoint genes expression profile using Morpheus from the Broad Institute.

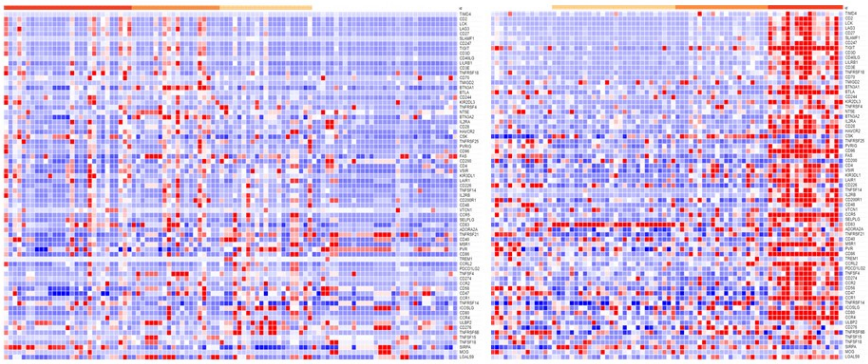

Figure 2 - 473

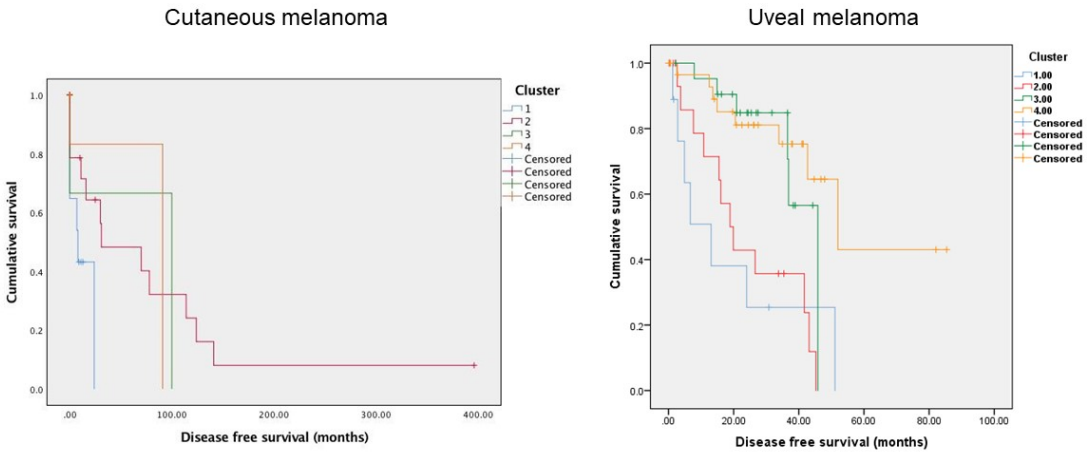

Figure 2. Disease-free survival of cutaneous (log-rank P=0.165) and uveal melanoma (log-rank P=0.000062) according to the immune checkpoint genes expression clusters.

Conclusions: Widely divergent roles of immune checkpoint gene expression clusters are noted between cutaneous and uveal melanomas. If validated, and further explored, this might explain why immunotherapy response in both cancers diverge in success.

474 Bridging Pigmentation between Cutaneous and Uveal Melanoma: Histo-Genomic Commonalities and Differences between Clinical, Genomic and Pathological Parameters from The Cancer Genome Atlas (TCGA)

Philippe Echelard[1], Simon Roy[2], Leonardo Lando[3], Anne Xuan-Lan Nguyen[4], Vincent Quoc-Huy Trinh[5]
[1]Université de Sherbrooke, Sherbrooke, QC, [2]University of Montréal, Montréal, QC, [3]Federal University of Goias, Goiania, GO, Brazil, [4]McGill University, Montreal, QC, [5]Vanderbilt University Medical Center, Nashville, TN

Disclosures: Philippe Echelard: None; Simon Roy: None; Leonardo Lando: None; Anne Xuan-Lan Nguyen: None; Vincent Quoc-Huy Trinh: None

Background: The importance of pigmentation in cutaneous melanoma (CM) is poorly understood yet a higher intensity of pigmentation seems to entail a worse prognosis in uveal melanoma (UM). In this study, we used the TCGA CM and UM datasets in order to analyze the similarity and differences of the signification of tumor pigmentation in both types of cancer.

Design: Primary CM and UM cases, including their clinical, pathological, mutational and transcriptomic data were extracted from the TCGA using cBioportal, TCGABiolinks 3.7, GDC Legacy Archive and GDC Transfer Tool v1.3.0. Digital diagnostic and frozen section slides were reviewed by at least 2 observers in Aperio Imagescope v12 and pigmentation was stratified into 3 pigment groups (pigment poor: 0-5%, pigment intermediate: 6-50% and pigment rich: 51-100%). Pigmentation-associated genes (Pubmed-cited reviews, 2010-2018) in CM and in UM were selected. Differential gene expressions (DGE) were tested in EdgeR in R, with a false discovery rate (FDR)<0.05. Overall survival was assessed using Kaplan-Meier curves and log-rank testing. Statistics were conducted using SPSS software v25.

Results: 109 primary CM and 80 UM are available from the TCGA. 2 cases of CM were excluded as their diagnostic slides were not available. Both CM and UM showed a significant association between pigmentation grade and TNM T stage (respectively p**<**0.0001 and p=0.01). CM's significant association with T stage was also reflected with the AJCC clinical stage (p**<**0.0001). Prognostic mutations varied across groups in UM (BAP1 (p=0.024) and EIF1AX (p=0.045), as did loss of chromosome 3 (p=0.023) and gain of chromosome 8 (p=0.017). The mean mutational burden in the pigment poor UM group was significantly higher (p=0.003). Log-rank analysis of survival curves for pigmentation groups in UM showed poorer prognosis with increasing pigmentation (P=0.003), which was not seen in the pigmentation groups of CM (P=0.479). In DGE analysis, 229 genes were differentially expressed in CM and 1737 in UM. Nineteen percent of genes were commonly differentially expressed in both CM and UM.

Table 1. Baseline clinical and pathological characteristics of uveal and cutaneous melanoma cases from TCGA separated along their pigmentation profile.

	Uveal Melanoma				**Cutaneous Melanoma**			
Parameters	**Pigment poor (n=31)**	**Pigment intermediate (n=26)**	**Pigment rich (n=23)**	**p***	**Pigment poor (n=56)**	**Pigment intermediate (n=39)**	**Pigment rich (n=12)**	**p***
Clinical Stage **I** **II** **III** **IV**	0% 52% 45% 3%	0% 36% 56% 8%	0% 61% 35% 4%	0.494	0% 6% 7% 87%	0% 5% 8% 88%	9% 0% 55% 36%	**<0.0001**
T stage **TX** **T1** **T2** **T3** **T4**	0% 0% 26% 39% 36%	0% 0% 19% 19% 62%	0% 0% 4% 65% 30%	**0.01**	4% 0% 5% 7% 84%	0% 0% 5% 8% 87%	8% 8% 0% 50% 33%	**<0.0001**
N stage **NX** **N0** **N1** **N2** **N3**	7% 94% 0% - -	8% 92% 0% - -	0% 100% 0% - -	0.418	4% 18% 57% 9% 13%	0% 13% 46% 13% 5%	0% 8% 58% 17% 17%	0.813
M stage **MX** **M0** **M1**	48% 48% 3%	23% 69% 8%	17% 78% 4%	0,112	5% 89% 5%	3% 97% 0%	0% 100% 0%	0.414
Mitotic activity (SD)	12.5 (10.0)	12.8 (9.5)	11.5 (9.5)	0.891	1.8 (4.7)	0.7 (2.1)	0.2 (0.5)	0.207
Lymphoid infiltrate **Low** **Intermediate** **High**	42% 52% 7%	42% 35% 23%	48% 39% 13%	0.403	72% 17% 11%	44% 30% 26%	71% 0% 29%	0.133
Vascular loops	14 (45)	10 (39)	9 (39)	0.851	29 (52.7%)	20 (55.6%)	3 (27.3%)	0.241
Histologic variant **Spindle** **Mixed** **Epithelioid**	36% 42% 23%	50% 35% 15%	26% 30% 44%	0.174	- - -	- - -	- - -	- - -
Breslow (SD)	-	-	-	-	11.8 (14.2)	10.2 (11.3)	3.9 (3.9)	0.143
Ulceration	-	-	-	-	88%	84%	78%	0.697
Pronostic mutations **BAP1** **EIF1AX**	16% 23% 26%	50% 12% 27%	35% 0% 13%	**0.024** **0.045** 0.435	- - -	- - -	- - -	- - -

SF3B1								
Chromosomal alterations	13%	8%	13%	0.783	-	-	-	-
1 los	29%	27%	61%	**0.023**	-	-	-	-
3 loss	36%	15%	35%	0.186	-	-	-	-
6 gain	23%	43%	61%	**0.017**	-	-	-	-
8 gain								
Mutations	-	-	-	-	45%	43%	25%	0.558
BRAF mutated	-	-	-	-	14%	8%	0%	0.287
NRAS mutated	-	-	-	-	9%	5%	25%	0.084
NF1 mutated	-	-	-	-	5%	%	8%	0.873
KIT mutated	-	-	-	-	5%	5%	0%	0.737
CDKN2A mutated	-	-	-	-	4%	5%	0%	0.728
TERT amplified								
Mean fraction of genome altered (SD)	0.1 (0.1)	0.2 (0.1)	0.2 (0.1)	0.491	0.34 (0.21)	0.29 (0.20)	0.25 (0.14)	0.278
Mean mutations in genome (SD)	27.4 (68.9)	15.8 (5.2)	15.2 (4.6)	**0.003**	483.1 (1002.1)	213.8 (248.0)	439.9 (380.9)	0.345

Figure 1 - 474

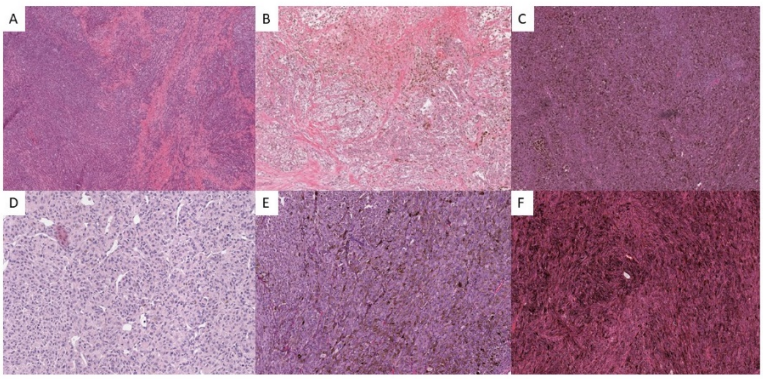

Figure 1. Different degrees of pigmentation in cutaneous (A/B/C) and uveal melanoma (D/E/F). Pigment levels are qualified as poor (A/D), intermediate (B/E) and rich (C/F).

F

Figure 2 - 474

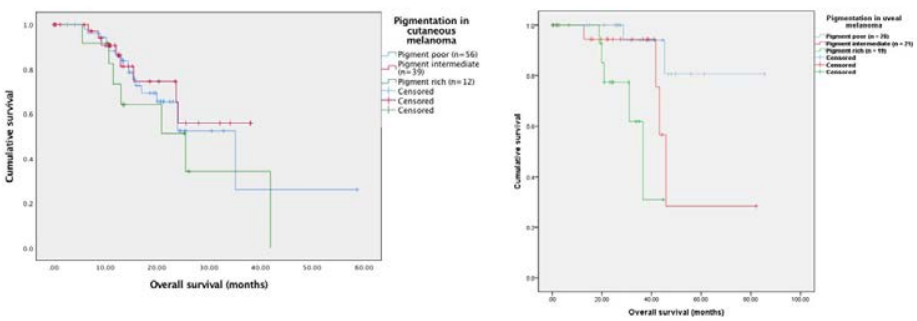

Figure 2. Overall-survival in cutaneous melanoma (left) and uveal melanoma (right) according to degree of pigmentation (log-rank P= 0.479 for cutaneous melanoma and log-rank P=0.003 for uveal melanoma)

Conclusions: Pigmentation in UM is associated with worse overall survival while its effect in CM is uncertain. Several clinical, pathological and molecular differences exist between these melanoma types. Comparing CM and UM may clarify the role of the tumor microenvironment in the pathogenesis of melanoma.

475 Adipophilin Expression in Cutaneous Malignant Melanoma is Associated with High Proliferation and Poor Clinical Prognosis

Masakazu Fujimoto[1], Ibu Matsuzaki[2], Kazuchika Nishitsuji[3], Fumiyoshi Kojima[2], Shin-ichi Murata[2]
[1]Department of Diagnostic Pathology, Kyoto University Hospital, Kyoto, Japan, [2]Wakayama Medical University, Wakayama, Japan, [3]Department of Biochemistry, Wakayama Medical University, Wakayama, Japan

Disclosures: Masakazu Fujimoto: None; Fumiyoshi Kojima: None

Background: Adipophilin (ADP) is a prominent protein component of lipid droplets (LDs). It has been acknowledged more than half a century that certain types of cancer cells contain LDs in their cytoplasm. However, pathological significance of adipophilin or LDs in cancers remains unclear. In the present study, we evaluated an association between ADP and other pathological characteristics in cutaneous malignant melanomas to further clarify the role of ADP in melanoma cells.

Design: Whole paraffin sections of 90 cases of primary skin melanomas were immunostained for ADP, after which the correlation between ADP immunohistochemistry (IHC) and patient survival data was analyzed. We further addressed the association between the ADP IHC score and in situ hybridization (ISH) score of ADP mRNA, and the Ki67 labeling index (Ki67-LI) by using tissue microarrays consisting of 74 primary cutaneous malignant melanomas, 19 metastasizing melanomas, and 29 melanocytic nevi. Finally, relationship between the ADP expression and proliferation in cutaneous melanoma cell lines was analyzed.

Results: We found that high ADP expression was associated with poor metastasis free survival, disease specific survival, and overall survival rates of skin melanoma patients ($p < 0.05$). By linear regression analysis, the ADP IHC corelated with increasing ADP mRNA-ISH H-scores and Ki67-LI in the melanocytic lesions ($p < 0.01$). The ADP IHC and ADP-ISH H-scores and Ki67-LI were greater in pT3-4 than in pT1-2 melanomas. In cell-based assays, cells with increased ADP expressions showed higher proliferation rates.

Conclusions: Taken together, ADP expression in malignant melanoma was significantly associated with cellular proliferation and poor clinical prognosis. Our results thus further disclose a significant association between ADP and melanoma progression, and we propose that ADP would serve as a novel marker of aggressive skin melanoma with lipogenic phenotype.

476 Transcriptomic and Immunohistochemical Study of Platelet Activating Factor Receptor (PAF-R) in Lesional Skin (wheals) of Chronic Spontaneous Urticaria (LS-CSU)

Monica Gonzalez Farre[1], Evelyn Andrades López[2], Miquel Clarós[2], Lara Nonell[2], Eulàlia Puigdecanet[2], Laia Curto Barredo[2], Ghita Tagmouti[1], Ramón Gimeno[2], Natalia Papaleo[1], Aurelio Ariza[3], Ramón M Pujol[4], Belen Lloveras[1], Ana Arnau[5], Carlos Barranco[1]
[1]Hospital del Mar, Barcelona, Spain, [2]IMIM-Hospital del Mar, Barcelona, Spain, [3]Universitat Autònoma de Barcelona, Barcelona, Spain, [4]Hospital del Mar-Parc de Salut Mar, Barcelona, Spain, [5]Hospital del Mar-Parc de Salut Mar, San Cugat del Valles, Barcelona, Spain

Disclosures: Monica Gonzalez Farre: None; Evelyn Andrades López: None; Miquel Clarós: None; Lara Nonell: None; Eulàlia Puigdecanet: None; Laia Curto Barredo: None; Ghita Tagmouti: None; Ramón Gimeno: None; Natalia Papaleo: None; Aurelio Ariza: None; Ramón M Pujol: None; Belen Lloveras: None; Ana Arnau: None; Carlos Barranco: None

Background: Histamine and platelet activating factor (PAF) are involved in wheal pathogenesis in urticaria. Intradermal PAF injection results in a wheal and flare type response unassociated with histamine release (Krause 2013). However, PAF is a labile molecule undetectable even by microdyalisis in PAF-induced wheals. In contrast, PAF-R gene overexpression in CSU lesional skin (LS-CSU) versus CSU nonlesional skin (NLS-CSU) and healthy controls' skin (HCS) has been described (Giménez-Arnau 2017). Transcriptomic and immunohistochemal expression of PAF-R in LS-CSU, NLS-CSU, and HCS is herein investigated.

Design: LS-CSU and NLS-CSU samples from 13 CSU patients with an Urticaria Activity Score 7 (UAS7) >16 and HCS samples from 5 individuals were studied by quantitative polymerase chain reaction (qPCR). Additionally, LS-CSU and NLS-CSU biopsies from 33 CSU patients and HCS biopsies from 13 individuals were evaluated by hematoxylin-eosin (H-E) staining and c-kit and PAF-R immunohistochemistry (IHC). Five independent observers evaluated PAF-R IHC results in epidermal and dermal structures in LS-CSU, NLS-CSU, and HCS samples.

Results: PAF-R overexpression in LS-CSU vs HCS ($p=0.014$) and in NLS-CSU vs HCS ($p=0.051$) was shown with the aid of ExpressionSuitev1.0.3. H-E and c-kit staining served to guarantee CSU and HCS samples' homogeneity. PAF-R cytoplasmic immunostaining was demonstrated in colonic epithelial cells and psoriasis epidermal keratinocytes, used as positive controls. Patchy PAF-R immunoreactivity, absent in HCS, was present in keratinocytes of all epidermal layers in LS-CSU and, with less intensity, in NLS-CSU.

PAF-R/CD43 IHC identified most PAF-R-expressing wheal inflammatory cells as lymphocytes. PAF-R immunopositivity was also present in LS-CSU (and less so in NLS-CSU) endothelial cells. No PAF-R expression differences among LS-CSU, NLS-CSU, and HCS were detected in sebaceous glands, eccrine glands, nerves, hair follicles or erector pili muscles.

Conclusions: PAF-R overexpression in epidermal keratinocytes, endothelial cells, nerves and lymphocytic infiltrates in CSU wheals suggests that PAF is a relevant mediator in CSU pathogenesis. PAF acts downstream of mast cell activation and, as other mast cell-released mediators involved in wheal pathogenesis, could be useful as a target for therapy.

477 Genetic Gender Differences in Cutaneous Melanoma and Potential Roles in Clinical Presentations and Outcomes

Saleh Heneidi[1], Dorian Willhite[2], Ashis Mondal[3], Ravindra Kolhe[4]
[1]Augusta University, Augusta, GA, [2]Augusta University-Medical College of Georgia, Augusta, GA, [3]GEM Labs, LLC, Augusta, GA, [4]Medical College of Georgia-Augusta University, Augusta, GA

Disclosures: Saleh Heneidi: None; Dorian Willhite: None; Ravindra Kolhe: *Speaker*, Qiagen, Illumina, Thermofischer

Background: Men diagnosed with melanoma are known to have a worse prognosis than women, however, contributing factors and underlining pathophysiologic mechanisms are yet to be elucidated.

Design: We sought to determine possible sex-linked differences between melanomas presenting in men and women. Exploring The Cancer Genome Atlas (TCGA) data, as well as cBioPortal, we were able review data from cutaneous melanomas of men (n=511) and women (n=335). Available data was first analyzed to confirm women had better overall survival than men at 120 months (n=461). Tumor mutation burden, tumor location, depth of invasion, and differential expression of genes between genders was explored and found to be significantly different between genders.

Results: Looking at data on overall survival, 42% of women died by 120 months (73/173), whereas 54% of men died by the same endpoint (157/291). Significant gender differences were observed in mutation count, with men displaying a higher tumor mutation burden (p=5.784e-4), as well as significantly different gender differences in tumor location (p= 8.474e-3), with 18.8% of men having melanoma of the head or neck vs. 5% of women. Unexpectedly, when comparing depth of invasion at time of diagnosis, as determined by Breslow depth score, women actually had a significantly higher depth of invasion than men. When exploring genes associated with low depth of invasion, the most significant was *PCLO* (7q21.11, p=0.0074). Genes associated with high depth include *SLCO1B3*, *TTN*, *MUC16* and *USH2A*. Exploring gender differences in genes expressed revealed several clusters of genes with gender specific amplifications and deep deletions, including amplifications of 1q22 and 12p12 in 6 men and 1 women, amplifications of 12p13 in 5 women and 0 men, and deep deletions of 11q23.3 in 13 men and 0 women. Of note, the region of deletion at 11q23.3 is flanked by the *SIK3* gene, that has had a reported role in imprinting. Looking at our own data (n=100), we observed a similar deep deletion in 3 cases.

Conclusions: Comparing the melanoma clinical outcomes and genetics revealed novel differential expression of numerous genes with potential differences that may play a role in observed differences in survivability, tumor location, depth of invasion, and mutation burden. Additionally, a potential role of gene imprinting may play a role in up to 5% of cancers observed in men, and is an area that would benefit from further exploration.

478 Tumor Microenvironment Characteristics in Early and Advanced TERT Promoter Hotspot Mutant Melanomas

Issa Hindi[1], Douglas Donnelly[2], Stephen Kelly[3], Russell Berman[4], Eleazar Vega-Saenz de Miera[3], Anna Pavlick[2], Iman Osman[3], George Jour[5]
[1]NYU Langone Medical Center, New York, NY, [2]New York University Langone Medical Center, New York, NY, [3]New York University Medical Center, New York, NY, [4]New York University School of Medicine, New York, NY, [5]NYU Langone Health, New York, NY

Disclosures: Issa Hindi: None; Douglas Donnelly: None; Stephen Kelly: None; Russell Berman: None; Eleazar Vega-Saenz de Miera: None; Anna Pavlick: None; Iman Osman: None; George Jour: None

Background: *TERT* promoter mutations in various reports have been associated with poor patient survival in early stage melanomas emphasizing it as a separate subset of melanoma. Thus far, no studies investigated whether the immune composition of the tumor microenvironment (TME) in *TERT* (HS) mutant melanomas differs from *TERT* WT melanomas. Furthermore, the mechanism underlying the worse outcome in early stage TPHS melanomas remains unclear. Herein, we aim to characterize the tumor microenvironment (TME) of *TERT* promoter hotspot (TPHS) mutant melanomas & compare them to *TERT* WT melanomas in a cohort of early and advanced stage melanomas. We also aim to elucidate the clinical significance of the TME composition.

Design: We analyzed tissue from a cohort of 93 melanoma patients. DNA and RNA were extracted from primary and metastatic tumor tissue, resected prior to treatment with immune checkpoint inhibitors. The extracted DNA was genotyped using a customized next generation sequencing high throughput panel that targets 580 cancer-related genes to determine TPHS mutation status. Gene expression analysis was performed on the RNA from 52 patients using a customized 770-gene expression panel combining markers 48 biologically significant signatures with the N-counter system. Differential gene expression (DGE) and Gene set enrichment analysis (GSEA) were performed using R package [(p<0.01; FDR<0.01; FDR<0.30 for GSEA] using *TERT* WT as a reference.

Results: Table 1 illustrates the clinicopathological characteristics of the cohort. TPHS mutant melanoma was associated with downregulation of melanoma-associated antigens (MAGES) and endothelial cells/angiogenesis signature (p<0.01). Notably, *MAGEA4*, *MAGEA1, CTAG1B, PALMD* & *KDR* were among the most downregulated genes in the (lg2fc= -3.2; -2.2; -2.66, -1.23; -0.66, respectively). GSEA showed a significant enrichment for NOD-like receptor (NLR) signaling pathway including *NFKB1, TNF* & *NLR3P* in TPHS mutant melanoma (Figure 1). Within TPHS mutant melanoma, high endothelial cells/angiogenesis signature (score >3.85/median) was more prevalent in stage (I/II) melanomas (p=0.025). No significant association between *TERT* mutational status, outcome nor histologic subtype were noted.

Table 1: Clinical, pathologic and genomic characteristics of different genotypes of malignant melanoma

		***TERT* promoter Wild-Type**	***TERT* promoter Mutant**
N	**Total = 93**	27 (29%)	66 (71%)
Gender	**Male**	16 (59%)	44 (67%)
	Female	11(41%)	22 (33%)
Follow-up, median (months)		47	49
Stage at Initial Diagnosis	**I**	3 (11%)	13 (20%)
	II	8 (30%)	13 (20%)
	III	13 (48%)	28 (42%)
	IV	3 (11%)	12 (18%)
Tumor Mutational Burden (TMB), median (Mutation/Mb)		145	207
Histologic Classification	**Nodular**	6 (22%)	26 (39%)
	Superficial Spreading	3 (11%)	7 (11%)
	Desmoplastic	1 (4%)	2 (3%)
	Acral Lentiginous	6 (22%)	0 (0%)
	Mucosal	2 (8%)	0 (0%)
	Other/unspecified	9 (33%)	31 (47%)

Figure 1 - 478

Figure 1: **(A)** GSEA showing upregulation of "NOD=like receptor signaling pathway" signatures in TPHS mutant vs. TPHS wild-type. ES, enrichment score; NES, normalized ES; NOM p-val, normalized p-value. **(B)** Horizontal position shows the magnitude of a gene or signature's association with a clinical variable; vertical position shows -log10(p-value), which increases with statistical significance. Melanoma-associated antigens (MAGES) and endothelial cells/angiogenesis signatures and the 50 most significant genes are highlighted. Horizontal lines show False Discovery Rate (FDR) cutoffs.

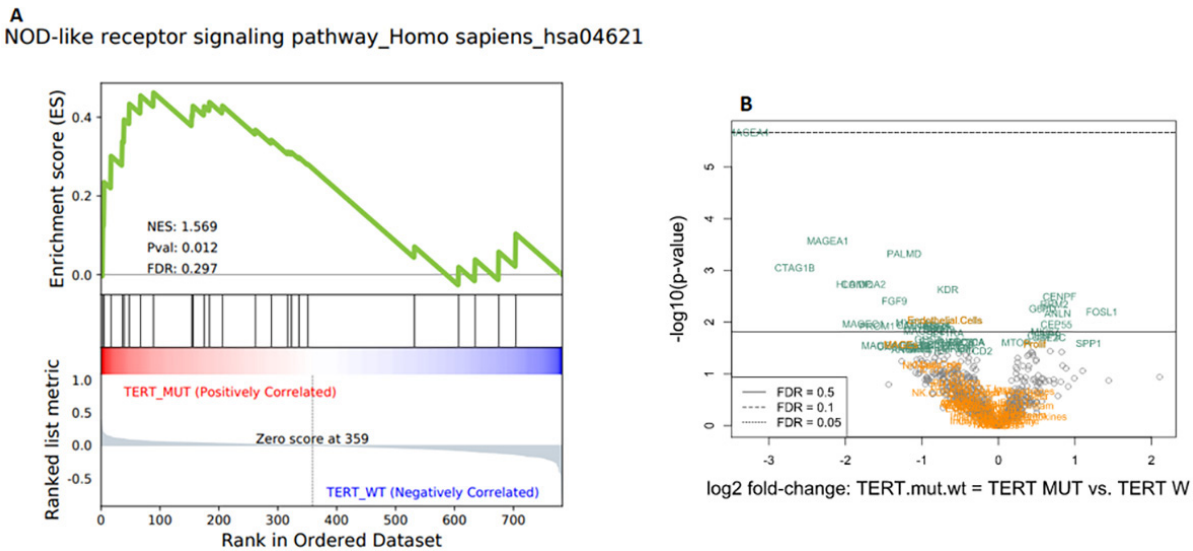

Conclusions: Our findings show that TPHS mutant melanoma and TERT WT have distinct TME composition. The higher endothelial/angiogenesis signature seen in early stage TPHS mutant melanoma compared to stage III/IV TPHS mutant melanomas could contribute to the poor outcome reported in the former group.

479 Genomic Profiling of Metastatic Uveal Melanoma Revealed Frequent Co-Existing Mutations of BAP1 and SF3B1 with GNAQ/GNA11 and Potential Correlation with Prognosis

Alexandra Isaacson[1], Aaron Bossler[2], Deqin Ma[3]
[1]Coralville, IA, [2]University of Iowa, Iowa City, IA, [3]University of Iowa Hospitals and Clinics, Iowa City, IA

Disclosures: Alexandra Isaacson: None; Aaron Bossler: None; Deqin Ma: None

Background: Uveal melanoma (UM) is the most common primary malignancy of the eye with metastasis in up to 50% of all patients despite successful treatment of the primary tumor. Over 90% of UMs metastasize to the liver and metastasis is uniformly fatal. *GNAQ* and *GNA11* activating mutations are the drivers for UM tumorigenesis and loss of *BAP1* tumor suppressor activity is associated with metastasis. Although targeted therapy is effective for cutaneous melanoma, there is no effective treatment for metastatic UM and immunotherapy has little impact. We evaluated 19 UMs (17 metastatic, 2 primary) using a custom-designed, targeted next generation sequencing (NGS) assay in searching for potential therapeutic targets and correlated the findings with clinical information.

Design: Twenty-five genes (*AKT1 BAP1 BRAF CDKN2A CTNNB1 EIF1AX ERBB4 FGFR1 FGFR2 FGFR3 GNA11 GNAQ HRAS KIT MET NRAS PDGFRA PIK3CA PTEN RAF1 RB1 SF3B1 STK19 TP53 TRRAP*) were included. 235 patients' melanomas from different sites were tested, 19 of them were UMs including 16 liver metastases (met), 1 tracheal met, and 2 primaries. Total nucleic acid was extracted from microdissected, formalin-fixed, paraffin-embedded tissue to generate NGS libraries and sequencing was performed on Illumina MiSeq.

Results: *GNA11* (11) and *GNAQ* (7) mutations were found in 18/19 (95%) cases and 17 mutation-positive ones had co-existing *BAP1* (13) or *SF3B1* (4) mutation. All *BAP1* or *SF3B1* positive cases had *GNA11/Q* mutations. One liver met only had a *GNA11* variant and 1 had no mutation. *BAP1* variants included 10 truncating, 2 splicing, and 1 missense; and *SF3B1* mutations were all at codon 625. Patients with co-existing *GNAQ/11-SF3B1* mutations had a longer average time to first met than those with *GNAQ/11-BAP1* mutations (130 vs 35 months [mo]) but a shorter survival time after first met (13 vs 22 mo). Three patients with *BAP1* mutations received trametinib after liver met; 2 were still alive after 15 and 23 mo, and 1 was deceased at 32 mo. *BAP1* mutations were found in 10/216 non-UMs (4.6%) and *SF3B1* in 1; none had co-existing *GNAQ/11* mutations. Table 1.

Table 1. Molecular Findings in Uveal Melanoma with Clinical Information

Case	Age	M / F	TNM at Dx	Primary	Metastasis	Variant 1	Variant 2	Time to Met	Treatment	Outcome (time after metastasis)
1	46	F	Unknown	Ciliochoroidal	Liver spine soft tissue breast	*GNA11 c.626A>T*: p.Q209L	*BAP1 c.14G>A*:p.W5Ter	23 mo	Pembro, XRT, Astellas trial	Alive (17 mo)
2	69	M	pT4bNx Mx	Ciliochoroidal	Liver	*GNA11 c.626A>T:* p.Q209L	*BAP1 c.272G>C:* p.C91S	18 mo	Pembro + indoximod, ipilimumab, Temodar, XRT	Deceased (20 mo)
3	48	M	Unknown	Choroidal	Liver	*GNAQ c.626A>T*: p.Q209L	*BAP1 c.2057-4G>T*	49 mo	Pembro, resection, XRT, Astellas trial, Temodar, trametinib	Alive (15 mo)
4	79	F	pT3dNx Mx	Choroidal	Liver skin	*GNAQ c.626A>T*: p.Q209L	*BAP1 c.580+2T>C*	10 mo	IMC-GP100 trial, pembro, XRT	Deceased (14 mo)
5	32	F	Unknown	Ciliochoroidal	Liver	*GNA11 c.626A>T*: p.Q209L	*BAP1 c.588G>A:* p.W196Ter	40 mo	Pembro, XRT	Deceased (7 mo)

6	46	M	Unknown	Ciliochoroidal	Liver	*GNAQ c.626A>C*: p.Q209P	*BAP1 c.1202delA*: p.Y401LfsTer29	17 mo	Pembro, XRT, trametinib	Alive (23 mo)
7	68	M	Unknown	Choroidal	Liver spine humerus bladder	*GNAQ c.626A>C*: p.Q209P	*BAP1 c.261_302del42*: p.I87_L101delinM	57 mo	Pembro, XRT	Lost to follow-up, presumed deceased (4 mo)
8	68	F	Unknown	Choroidal	Liver	*GNA11 c.626A>T*: p.Q209L	*BAP1 c.1192_1200 delinsA*: p.E398IfsTer2	34 mo	IMC-GP100 trial, pembro	Deceased (13 mo)
9	50	F	Unknown	Choroidal	Trachea scalp brain lung	*GNAQ c.626A>C*: p.Q209P	*BAP1 c.630dupC:* p.Met211HisfsTer32	105 mo	Pembro, XRT	Alive (24 mo)
10	46	M	pT3cNxMx	Ciliochoroidal	Liver	*GNA11 c.626A>T*: p.Q209L	*BAP1 c.266_281del*: p.N89MfsTer4	18 mo	Pembro, XRT, Temodar, trametinib	Deceased (32 mo)
11	68	F	pT3dNxMx	Ciliochoroidal	Liver lung	*GNA11 c.626A>T*: p.Q209L	*BAP1 c.695_700del*: p.A232_Val233del	29 mo	Pembro	Deceased (13 mo)
12	43	F	pT3bNxMx	Ciliochoroidal	Liver, adrenal pancreas skin	*GNAQ c.548G>A*: p.R183Q	*BAP1 c.178 C>T*: p.R60Ter	15 mo	Resection, pembro, XRT	Alive (79 mo)
13	54	M	pT4aNxMx	Ciliochoroidal	Liver lung	*GNAQ c.626A>C*: p.Q209P	*SF3B1 c.1873C>T*: pR625Cys	55 mo	Pembro	Alive (14 mo)
14	39	M	Unknown	Choroidal	Liver brain	*GNA11 c.626A>T*: p.Q209L	*SF3B1 c.1873 c>T*: p. Q625C	228 mo	XRT	Deceased (3 mo)
15	54	F	Unknown	Choroidal	Liver	*GNA11 c.626A>T*: p.Q209L	*SF3B1 c.1873 c>T*: p. R625C	238 mo	Pembro	Deceased (3 mo)
16	55	F	pT4bNxMx	Ciliochoroidal	Liver	*GNA11 c.626A>T*: p.Q209L	*SF3B1 c.1874 G>T*: p. R625L	0 mo	Pembro, XRT, Astellas trial	Alive (31 mo)
17	67	F	pT4aNxMx	Choroidal	N/A	*GNA11 c.626A>C:* p.Q209P	*BAP1 c.299_309del11*: p.L100Qfs*22	N/A	None	Alive (N/A)
18	56	F	pT4dNxMx	Ciliochoroidal	Liver spine	*GNA11 c.626A>T*: p.Q209L	N/A	9 mo	None	Deceased (1 mo)
19	76	M	pT2aNxMx	Choroidal	Liver	N/A	N/A	73 mo	None	Alive (4 mo)

Dx, diagnosis; M/F, male/female; Met, metastasis; Mo, month; Pembro, pembrolizumab; XRT, radiation therapy.

Conclusions: *BAP1* and *SF3B1* mutations were frequent in metastatic UMs. Co-existing *BAP1*/*SF3B1* and *GNAQ/11* mutations seem to be unique to UM. In melanoma, *SF3B1* mutations were reported to be UM-specific and associated with rare or no metastasis. 23.5% (n=17) of metastatic UMs had mutated *SF3B1* suggesting its role should be further evaluated. The correlation of *BAP1/SF3B1* mutation with survival also warrants investigation.

480 Clinical and Pathological Study of Hidradenocarcinoma, Atypical Hidradenoma and Benign Hidradenoma with Pilot Molecular Studies in Selected Cases

Hong Jiang[1], Ruifeng Guo[1], Kabeer Shah[2]
[1]Mayo Clinic, Rochester, MN, [2]St. Mary's Hospital, Madison, WI

Disclosures: Hong Jiang: None; Ruifeng Guo: None; Kabeer Shah: None

Background: Hidradenoma is a cutaneous adnexal tumor of sweat gland origin, characterized by its diverse but overlapping histomorphologic features. Although hidradenoma has an excellent prognosis, its malignant counterpart, hidradenocarcinoma (HAC), has debatable clinical behavior based on limited studies, ranging from high metastasis rate to low frequency of local recurrence and regional spread. Recognition of pathologically atypical hidradenoma adds to the prognostic uncertainty for this spectrum of diseases.

Design: Cases of hidradenoma (10), atypical hidradenoma (7) and HAC (11) with complete follow-up (24-168 months) were studied. The main diagnostic features include necrosis, mitotic rate, infiltrative growth pattern, and extent of cytological atypia. Each diagnosis was rendered by at least two experienced dermatopathologists upon independent review. All cases had DNA extracted, submitted for single nucleotide polymorphism (SNP) microarray analysis at the time of abstract submission.

Results: Histologically, HAC group had at least 2/4 of following features: necrosis, increased mitotic figures (>10/10HPF) infiltrative growth and evident malignant cytology, while atypical hidradenoma group only showed equivocal features, with mitotic rates invariably lower(2-10/10HPF). Benign hidradenomas did not show any above features. Clinically, all cases underwent complete excision. None of the benign hidradenoma or atypical hidradenoma patients had recurrence or metastasis. Among the 11 HAC patients, 2 had local recurrences and required additional excisions. One of them presented with multifocal disease and a large positive regional lymph node (6.7 cm) in onset, which also showed the highest extent of histological atypia in addition to microsatellites and lymphatic invasion. The other 9 patients had no recurrence or metastasis after complete excision. In our pilot cases with SNP microarray analysis, one case of HAC showed multiple chromosomal gains and losses, while the hidradenoma (n=1) and atypical hidradenoma (n=1) cases showed normal profiles. The rest of the cases are being analyzed.

Figure 1 - 480

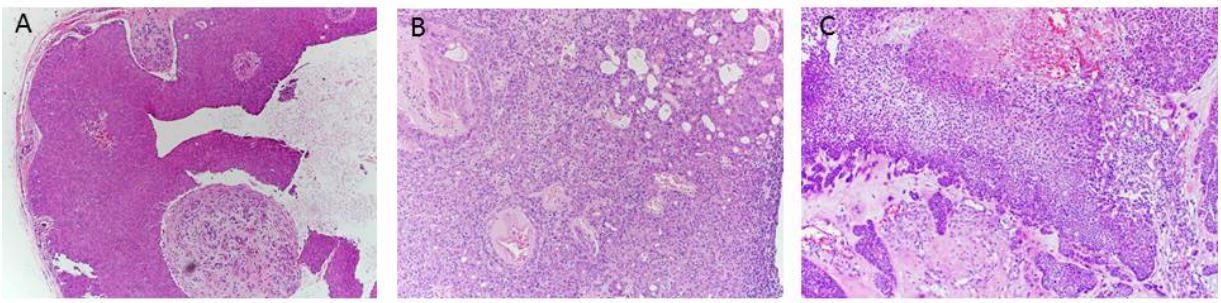

Fig 1. Histologic features of hidradenoma (A), atypical hidradenoma (B) and hidradenocarcinoma (C). (10x10)

Conclusions: Our study supports that most HACs behave more in keeping with a local cutaneous malignancy. However, rare cases of aggressive clinical behavior do occur, Atypical hidradenoma, in spite of its histological ambiguity, behaves in an indolent manner similar to hidradenoma. Lastly, molecular profiling may shed light on further diagnostic and prognostic stratification for these rare tumors.

481 Differential Network Analysis of Melanoma Transcriptomes Identifies Metastasis-Associated Coexpression Modules

Igor Katsyv[1], George Niedt[2]
[1]Columbia University/New York Presbyterian Hospital, New York, NY, [2]Columbia University, New York, NY

Disclosures: Igor Katsyv: None; George Niedt: None

Background: Over the past decade, there has been an explosion in "omics" profiling of cancers and other diseases. A remaining challenge is integration of this data to reconstruct disease-driving molecular interactions. Many studies have examined the molecular underpinnings of melanomas, however changes in the gene interaction structure that occur during melanoma progression remain poorly understood. Here, we use differential network analysis to dissect the network architectural differences between primary and metastatic melanomas.

Design: TCGA RNA-seq data was downloaded from the Broad Institute GDAC Firehose and processed using the *edgeR* R package, yielding a final dataset of 471 samples (103 primary, 368 metastatic) and 14,126 genes. Weighted Gene Coexpression Network Analysis (WGCNA) was applied to identify modules of coexpressed genes. Subsequently, gains or losses of intra-modular connectivity were quantified using Module Differential Connectivity (MDC) in the *DGCA* R package. Differentially-expressed genes were called using the *edgeR* and *limma* R packages. Functional annotation was performed using genesets from the Molecular Signatures Database (MSigDB).

Results: WGCNA identified 82 coexpression modules ranging in size from 26 to 1908 genes. Sixteen modules showed significant gains or losses of connectivity (GoC and LoC, respectively) in metastatic compared to primary melanomas (FDR < 5%). The top two differentially-connected modules show LoC of genes involved in estrogen signaling and cell adhesion ($p < 0.01$). GoC modules were enriched for genes involved in extracellular matrix remodeling, epithelial-to-mesenchymal transition, and immune response ($p < 0.01$). Within primary tumors, expression of the two estrogen signaling-associated LoC modules was anticorrelated with Breslow thickness ($r = -0.21$ and -0.15, $p = 4.5e-02$ and $1.45e-01$). Differentially-connected modules were significantly enriched for differentially-expressed genes between primary and metastatic melanomas ($p < 0.01$).

Figure 1 - 481

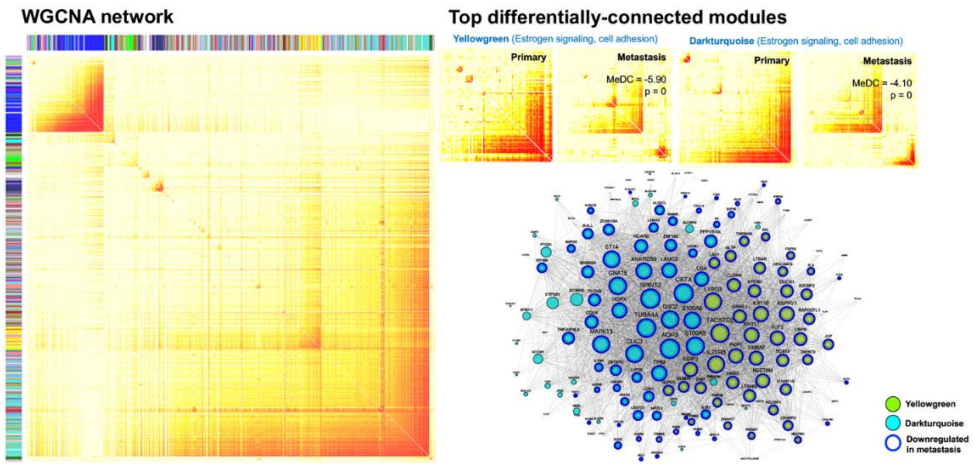

Conclusions: We show increased connectivity of modules involved in tumor invasiveness and extracellular matrix remodeling and reduced connectivity of modules involved in estrogen signaling. The latter finding supports clinically-observed gender differences in melanoma outcomes. We are the first, to our knowledge, to show network-level differences in estrogen signaling between primary and metastatic melanomas. Further work is required to interrogate the role of estrogen signaling genes in melanoma progression.

482 Factors Associated with Patient Outcomes After Diagnosis with Invasive Melanoma; An 8-Year Retrospective Study of AJCC Staging and Clinical Parameters

Elizabeth Keiser[1], Shira Ronen[1], Rami Al-Rohil[2], George Jour[3], Priyadharsini Nagarajan[4], Michael Tetzlaff[1], Jonathan Curry[4], Doina Ivan[1], Carlos Torres-Cabala[1], Victor Prieto[1], Phyu Aung[1]
[1]The University of Texas MD Anderson Cancer Center, Houston, TX, [2]Duke University, Durham, NC, [3]NYU Langone Health, New York, NY, [4]Houston, TX

Disclosures: Elizabeth Keiser: None; Shira Ronen: None; Rami Al-Rohil: None; George Jour: None; Priyadharsini Nagarajan: None; Michael Tetzlaff: *Speaker*, Nanostring; *Advisory Board Member*, Novartis LLC; *Advisory Board Member*, Myriad Genetics; *Advisory Board Member*, Seattle Genetics; Jonathan Curry: None; Doina Ivan: None; Carlos Torres-Cabala: None; Victor Prieto: None; Phyu Aung: None

Background: When given a diagnosis of invasive melanoma, patients invariably ask their prognosis. Much of what is available to patients is based purely on stage. We seek to examine additional pathologic and clinical factors possibly associated with patient outcomes after diagnosis of invasive melanoma.

Design: This study retrospectively examined patients with invasive melanoma derived from a one year period of referrals to a tertiary academic care center for confirmation of pathology and clinical assessment (N=856). We utilized multivariate logistic regression to evaluate possible factors associated with disease progression over an 8-year follow-up period. Proposed factors included age at time of confirmed diagnosis, anatomic site, histologic type, Clark level, Breslow depth, radial and vertical growth phases, mitoses, ulceration, regression, lymphovascular invasion, perineural invasion, microsatellitosis, regression, concurrent nevus, and AJCC stage. Outcomes were defined as clinically or pathologically confirmed regional or distant sites of disease, recurrence or growth of residual disease, and death. Treatment was defined as whether the patient received chemotherapy, radiation, and/or immunotherapy treatment.

Results: Of the 856 patients referred with suspected primary invasive melanoma, 811 (95%) patients were confirmed to have primary invasive melanoma (57% male, average age at diagnosis 57 years old). Of these, 708 cases contained complete pathologic and clinical data for assessment. After diagnosis, 222 (27%) patients received treatment, 279 (34%) progressed, and 166 (20%) died within the eight-year period. Factors statistically associated with disease progression included microsatellitosis (OR=20.2, 95% CI 1.9-214) and AJCC stage (OR 1.37, 95% CI 1.1-1.7). Factors associated with death included disease progression (OR 7.5, 95% CI 3.9-14.3), age at confirmed diagnosis (OR 1.05, 95% CI 1.0-1.1), ulceration (OR 2.3, 95% CI 1.2-4.4), and treatment (OR 2.2, 95% CI 1.2-4.1). Of those without disease progression, 49 (6%) patients died within the same timeframe due to other causes.

Table 1 Factors associated with outcomes of "progression" and "death" over an eight year period.

	Progression (N=708)	**Death (N=708)**
	Odds ratio (95% CI)	*Odds ratio (95% CI)*
Progression	-	7.45 (3.88-14.3)*
Gender (male)	0.78 (0.43-1.40)	1.21 (0.76-1.92)
Age at diagnosis (years)	1.00 (1.00-1.00)	1.05 (1.04-1.07)*
Anatomic site**	1.23 (0.86-1.77)	0.85 (0.65-1.12)
Invasive melanoma type+	0.94 (0.87-1.03)	0.97 (0.91-1.04)
Breslow thickness (mm)	0.90 (0.77-1.06)	1.00 (0.88-1.12)
Radial growth phase	1.88 (0.93-3.82)	1.08 (0.65-1.80)
Vertical growth phase	2.10 (0.80-5.51)	0.76 (0.36-1.59)
Ulceration	1.39 (0.59-3.28)	2.30 (1.21-4.36)*
Lymphovascular invasion	0.77 (0.26-2.26)	1.45 (0.71-2.93)
Perineural invasion	0.70 (0.14-3.42)	0.65 (0.26-1.61)
Mitoses (number)	0.98 (0.95-1.02)	0.99 (0.96-1.01)
Microsatellitosis	20.2 (1.91-214)*	1.40 (0.42-1.37)
Regression	1.53 (0.77-3.03)	0.76 (0.42-1.37)
Nevus	1.17 (0.58-2.36)	1.13 (0.62-2.05)
Change in stage on review	1.68 (0.96-2.94)	0.92 (0.60-1.41)
AJCC stage	1.37 (1.08-1.74)*	1.14 (0.95-1.37)
Treatment	305.5 (111-836)*	2.18 (1.15-4.10)*

**Anatomic site: H&N, trunk, extremities, lymph node
+Superficial spreading, nodular, lentigo maligna, acral, mucosal, NOS

Conclusions: Approximately one third of patients referred to an academic tertiary care center with confirmed primary invasive melanoma progressed, and of these, almost two-thirds passed away within eight years. While recent therapies have improved patient outcomes, much research is still needed to prevent and treat invasive melanoma.

483 Squamoid Eccrine Ductal Carcinoma: Elucidating Clinicopathologic Features of Prognostic Significance

Elizabeth Keiser[1], Shira Ronen[1], Doina Ivan[1], Carlos Torres-Cabala[1], Michael Tetzlaff[1], Jonathan Curry[2], Phyu Aung[1], Victor Prieto[1], Priyadharsini Nagarajan[2]
[1]The University of Texas MD Anderson Cancer Center, Houston, TX, [2]Houston, TX

Disclosures: Elizabeth Keiser: None; Shira Ronen: None; Doina Ivan: None; Carlos Torres-Cabala: None; Michael Tetzlaff: *Speaker*, Nanostring; *Advisory Board Member*, Novartis LLC; *Advisory Board Member*, Myriad Genetics; *Advisory Board Member*, Seattle Genetics; Jonathan Curry: None; Phyu Aung: None; Victor Prieto: None; Priyadharsini Nagarajan: None

Background: Squamoid eccrine ductal carcinoma (SEDC) is a rare cutaneous adnexal neoplasm that clinically and histopathologically overlaps significantly with cutaneous invasive squamous cell carcinoma (SCC) and microcystic adnexal carcinoma (MAC). Similar to SCC

and MAC, SEDC most commonly affects the head and neck (scalp) of older adults. However, SEDC is characterized by aggressive clinical behavior, including frequent lymphovascular/ perineural invasion, recurrence and metastasis. Owing to the rarity of these tumors, relevant prognostic clinicopathologic parameters remain elusive.

Design: In this retrospective study, we identified patients with SEDC from our archives over a period of 9 years and recorded demographic, clinical, histopathologic features (tumor size and thickness, anatomic level, percent of tumor with ductal differentiation, margin status, and presence of overlying squamous cell carcinoma in situ, perineural [PNI], lymphovascular invasion [LVI], and poorly differentiated or sarcomatoid components), dates of diagnosis, recurrence, metastasis and death.

Results: Fourteen patients with confirmed cases of SEDC were available for clinicopathologic review. Most patients were Caucasians with male predominance (93%) and median age at diagnosis of 73.4 years. Most primary tumors were located in the head and neck region (n=11), with a median tumor thickness of 7.0 mm. PNI and LVI were noted in 50% and 7% of cases, respectively. The extent of ductal differentiation varied among cases, ranging from 5 to 95% of the tumor islands, with an average of 50% (SD-36%) of islands involved.

Patients were treated with surgical excision in all cases. Additional therapies included immunotherapy in 1 and adjuvant radiotherapy in 3 patients. Five patients experienced local recurrence of their tumor at the primary site, with average time to local recurrence of 3 years after surgical excision; presence of LVI significantly correlated with recurrence (p=0.04). Six patients (43%) developed regional lymph node metastases (average time to metastasis 1.8 years). Four patients died (average time to death 4.3 years), of which three were due to SEDC.

Conclusions: Consistent with prior reports, SEDC most commonly affects head and neck region of elderly Caucasian men and is associated with high rates of recurrence, metastasis and death. In our cohort, LVI correlated with local recurrence in SEDC.

484 Immunohistochemistry of P16 in Nevi of Pregnancy and Nevoid Melanomas: A Clinical Follow-up

Stephen Koh[1], Sean Lau[2], David Cassarino[3]
[1]Kaiser Permanente Medical Center, Anaheim, CA, [2]Kaiser Permanente (SCPMG), South Pasadena, CA, [3]Los Angeles, CA

Disclosures: Stephen Koh: None; Sean Lau: None; David Cassarino: None

Background: Hormonal changes in pregnancy alter melanocytes. Some nevi were noted to have increased mitotic figures, increased Ki-67 proliferation index, and cytomorphologic changes known as superficial micronodules of pregnancy; alarming pathologists for malignancy. Previous report revealed the application of p16 immunohistochemistry (IHC) to distinguish nevi from pregnant patients from nevoid melanomas. Here we present a followup study of the patients from the previous report.

Design: Fourteen patients with 16 nevomelanocytic lesions obtained from pregnant or postpartum patients along with 20 patients with nevoid melanomas were followed. Prior p16 IHC results were reviewed. Length of followup, surgical excision, recurrence/melanoma progression, living or deceased status, and chemotherapy (for nevoid melanoma) were evaluated.

Results: All patients were followed except for one melanoma patient lost to followup. Average follow up time was 43 months (nevi patients) and 51 months (melanoma patients). Except for the patient lost to followup, 7 out of 16 nevi (43%) were excised and all melanomas (100%) were excised. As previously reported, 81% of nevi from pregnant patients showed >5% p16 IHC positivity. In contrast, 65% of nevoid melanoma had <5% p16 positivity. Among the nevi group, all patients were alive and there was no evidence of recurrence or melanoma progression. In the melanoma group, two recurred/metastasized, two were deceased, and one patient initially received chemotherapy.

Conclusions: Previous report revealed differences in p16 IHC expression in nevi from pregnant patients versus nevoid melanomas. Followup of those patients also revealed some differences in clinical outcome. Those within the nevi group had no disease progression vs few of those in the melanoma group showed disease progression. The results presented here may support a correlation between high p16 IHC expression in nevi of pregnant patients with a benign clinical course.

485 The Subtlety of Granulomatous Mycosis Fungoides: A Retrospective Case-Series Study and Proposal of Novel Multimodal Diagnostic Approach for Clinicians and Dermatopathologists

Volha Lenskaya[1], Ellen de Moll[1], Shivangi Bhatt[2], Shafinaz Hussein[3], Garrett Desman[1], Robert Phelps[1]
[1]Icahn School of Medicine at Mount Sinai, New York, NY, [2]University of Delaware, Newark, DE, [3]Mount Sinai Hospital, New York, NY

Disclosures: Volha Lenskaya: None; Ellen de Moll: None; Shivangi Bhatt: None; Shafinaz Hussein: None; Garrett Desman: None; Robert Phelps: None

Background: Granulomatous mycosis fungoides (GMF) is a very rare subtype of mycosis fungoides that remains a significant diagnostic challenge for clinicians and pathologists due to diverse overlapping clinical presentation and heterogeneous morphologic findings of the skin biopsy. This can lead to delay in diagnosis and patient treatment. We aimed to summarize clinical, histopathological,

immunophenotypical and molecular data in order to emphasize the subtle presentations of GMF and to propose a standardized approach for making a diagnosis of GMF.

Design: A single-center retrospective case-series study was performed using pathology database and keywords “granulomatous” + “mycosis fungoides”. All cases of granulomatous slack skin were excluded. Six cases with well-documented disease history and laboratory data were identified. All skin biopsies were stained with H&E, CD2, CD3, CD4, CD5, CD7, CD8. Five biopsies were submitted for T cell receptor (TCR) gamma and/or beta gene rearrangement studies. Peripheral blood samples from 2 cases were submitted for TCR gene rearrangement studies. Flow cytometry studies were performed.

Results: Six unique patients with 7 biopsies of GMF were identified with the following demographics: male-to-female ratio 1:2, white ethnicity-to-other ratio 2:1 and median age of 67. In all patients, skin manifestations were localized to sun-protected areas and had variable clinical phenotype. Histological findings showed superficial/dermal T cell infiltrate with scant (n=2), focal (n=3) and absent (n=2) epidermotropism. All skin biopsies showed atypical predominantly CD4+ T cell infiltrate with granuloma formation or histiocytes with giant cells. In 85.7% of biopsies (n=6) the CD4:CD8 ratio was >4 and 66.6% (n=4) of biopsies showed ≥ 50% loss of CD7 expression. TCR gene rearrangement studies was positive in 85.7% (n=5) of cases and negative in 16.7% (n=1). Peripheral blood TCR gene rearrangement studies did not identify clonal population.

Table 1. Diagnostic criteria / scoring system for GMF. In order to make the diagnosis of GMF, both major criteria must be fulfilled and using the algorithm patient must reach at least total score of 4 points.

Criteria		Score
1. **Clinical Criterion:**		Major+2 minor =2 points Major+1 minor =1 point
• **Major:**		
• Persistent/progressive red or hyper pigmented patches/plaques;	☐	
• **Minor:**		
• Non-sun exposed location;	☐	
• Granuloma annulare-like lesion;	☐	
2. **Histopathological Criterion:**		Major+2 minor=2 points Major+1 minor=1 point
• **Major:**		
• Atypical lymphoid infiltrate with granulomatous reaction/histiocytes with multinucleated giant cells;	☐	
• **Minor:**		
• Any degree of nuclear atypia/convoluted nuclei;	☐	
• Epidermotropism sparse/present;	☐	
3. **Immunopathologic Criterion:**		1 point for one or more criteria
• More than 50% loss of CD7; • CD4:CD8 ratio > 4;	☐	
4. **Molecular Studies Criterion:**		1 point
• TCR gamma and/or TCR beta rearrangement result;	☐	
5. **Repeat biopsy from different anatomic location:**		1 point
• Presence of both major histopathological criterions +/- molecular studies criterion	☐	

Conclusions: Epidermotropism is a key histopathological finding in mycosis fungoides while our case series show that GMF has very subtle or absent epidermotropism with variable degree of granulomatous reaction. These atypical features can lead to misdiagnosis. The diagnosis of GMF requires a multimodal approach and our scoring criteria provide a framework for a challenging diagnostic entity. TCR gene rearrangement studies are ancillary and help support a diagnosis however a negative result does not preclude a neoplasm.

486 Primary Cutaneous Synovial Sarcoma: Clinical and Histopathological Characteristics in a Series of Cases with Molecular Confirmation

Philippa Li[1], William Laskin[2], Wei-Lien Billy Wang[3], Gauri Panse[1]
[1]Yale University, New Haven, CT, [2]Milford, CT, [3]The University of Texas MD Anderson Cancer Center, Houston, TX

Disclosures: Philippa Li: None; William Laskin: None; Wei-Lien Billy Wang: None; Gauri Panse: None

Background: Synovial sarcoma is a translocation-associated sarcoma characterized by varying degrees of epithelioid differentiation, and most commonly occur in deep soft tissues, especially of the proximal extremities or limb girdles. Synovial sarcomas limited to superficial soft tissues (dermis/subcutis) are extremely rare and could potentially be misdiagnosed as other keratin-positive cutaneous malignancies.

Design: Primary cutaneous synovial sarcomas from two tertiary academic institutions were retrospectively examined. All available slides were reviewed and clinical, histological and immunohistochemical characteristics were recorded. Tumors confined to dermis/subcutis (based on imaging studies and/or gross and microscopic examination) were included in the study.

Results: Five cases met the criteria. All of the cutaneous synovial sarcomas originated from females, with the average age at time of diagnosis as 31 years (range 14-42 years). The average size was 1.8 cm (range 0.9-3.3 cm). Tumors involved extremities (n=4) and trunk (n=1). Three tumors were biphasic and showed an epithelial/glandular and spindle cell component, while two tumors were monophasic and demonstrated spindle cells arranged in sheets or fascicles with hyperchromatic nuclei and high nuclear to cytoplasmic ratio. Calcifications were seen in one case. Mitotic rate ranged between 5-28 per 10 high power fields. All cases showed keratin expression (pankeratins, Cam 5.2, or AE1/AE3) with EMA and BCL-2 positivity. Tumor cells were negative for S-100 (n=4), SOX-10 (n=1) and CD34 (n=5). SYT translocations were identified (by fluorescence in situ hybridization or polymerase chain reaction) in all five cases. All cases were treated with complete excision. Follow up was available on three cases (range 2-9 years) and showed no recurrence or metastases.

Conclusions: Primary cutaneous synovial sarcomas are a rare but important entity in the differential diagnosis of keratin-positive skin tumors such as adnexal or spindle cell squamous cell carcinoma. Recognition that synovial sarcoma may present in dermis/subcutaneous tissues, and evaluation for SYT translocation would avoid misclassification as other keratin-positive cutaneous neoplasms.

487 Utility of RNA in Situ Hybridization in the Identification of Primary Cutaneous B Cell Lymphomas and Pseudolymphomas

Pamela Madu[1], Imran Siddiqi[1], Gene Kim[2]
[1]University of Southern California Keck School of Medicine, Los Angeles, CA, [2]Keck Hospital of USC and LAC-USC Medical Center, Los Angeles, CA

Disclosures: Pamela Madu: None; Imran Siddiqi: None; Gene Kim: None

Background: Primary cutaneous B-cell lymphomas (e.g. follicle center type and marginal zone lymphomas) can be diagnostically challenging due to the lack of reliable immunophenotypic markers and histopathologic overlap with reactive processes (e.g. pseudolymphomas). In addition, biopsy material is often limited for a wide panel of immunohistochemical stains combined with molecular clonality studies, the latter which are frequently confounded by false positives or false negatives. RNA in situ hybridization (RNAScope) for kappa (K) and lambda (L) light chain transcripts (RNAScope K/L) offers a highly sensitive means of detecting light chain expression on B-cells in tissue sections and has recently been shown to be a valuable diagnostic modality in systemic small B-cell lymphomas. We sought to determine whether incorporation of RNAScope K/L into an abbreviated immunohistochemical panel can assist in the timely and accurate diagnosis of cutaneous B-cell proliferations.

Design: We designed and validated a diagnostic testing algorithm that incorporates CD3 and CD20 directly reflexed to RNAScope K/L for identification of clonal B-cell proliferations, followed by a smaller set of stains for lymphoma subclassification. This algorithm was tested on 10 primary cutaneous follicular center lymphomas (PCFCL), 10 primary cutaneous mantle cell lymphomas (MCL), and 10 reactive lymphoproliferations and compared to molecular B-cell gene rearrangement results.

Results: In nine out ten cases of pseudolymphoma, the initial screening reflex of CD3, CD20, RNAscope Kappa and lambda was able to exclude the possibility of lymphoma without additional testing. In the remaining case, because of the equivocal results RNAscope Kappa and lambda, additional immunohistochemical stains were necessary to render the final diagnosis.

Conclusions: We show that the algorithm has the potential to streamline the diagnostic process and compares favorably with gene rearrangement studies. In addition, we discuss the advantages and limitations of this approach.

488 Differentially Expressed Genes in Bullous Pemphigoid Immune-Related Adverse Event (BP-irAE) from Immune Checkpoint Inhibitor Therapy: Implications in the Immunopathogenic Mechanisms Driving BP-irAE Compared to De Novo BP Control

Mario Marques-Piubelli[1], Michael Tetzlaff[1], Aaron Muhlbauer[2], Jing Wang[1], Kelly Nelson[1], Priyadharsini Nagarajan[3], Phyu Aung[1], Carlos Torres-Cabala[1], Omar Pacha[1], Victor Prieto[1], Sandesh Subramanya[1], Ignacio Wistuba[1], Jonathan Curry[3]
[1]The University of Texas MD Anderson Cancer Center, Houston, TX, [2]Loyola University Medical Center, Chicago, IL, [3]Houston, TX

Disclosures: Mario Marques-Piubelli: None; Michael Tetzlaff: *Speaker*, Nanostring; *Advisory Board Member*, Novartis; *Advisory Board Member*, Myriad Genetics; *Advisory Board Member*, Seattle Genetics; Aaron Muhlbauer: None; Jing Wang: None; Kelly Nelson: None; Priyadharsini Nagarajan: None; Phyu Aung: None; Carlos Torres-Cabala: None; Omar Pacha: None; Victor Prieto: None; Sandesh Subramanya: None; Ignacio Wistuba: None; Jonathan Curry: None

Background: Immune-related adverse events (irAEs) are a commonly encountered consequence of immune checkpoint inhibitor (ICI) therapy that can impact ~75% of treated patients. Bullous pemphigoid (BP) is a serious, but rare complication of ICI therapy and the most frequently encountered autoimmune bullous skin toxicity. Despite BP-irAE and *de novo* BP exhibiting identical clinical, histologic, and immunologic features, our knowledge of the immune mechanisms driving BP-irAE is limited and an obstacle for developing effective therapy. We examined the gene expression profile of BP-irAE and *de novo* BP to identify cellular mediators of the immune response that drive BP-irAE.

Design: Sixteen patients with clinical, histologic, and immunologic criteria for the diagnosis of BP (8 *de novo* BP control and 8 BP-irAE) were included in the study (Figure 1). Formalin-fixed paraffin-embedded tissue of bullous lesions from both groups were subjected to gene expression profiling with the NanoString nCounter PanCancer Immune Profiling Panel. The expression of immune response genes involved in the innate, humoral, and adaptive immunity and genes were assessed. Log_2 fold differences in mRNA transcript levels of 770 genes were examined and compared between the groups using two-sample t-tests.

Results: The mean age of the *de novo* BP control group was 76 years (range: 57 to 91) while the BP-irAE group was 72 years (range: 56 to 82). Both groups had a male predominance (M:F ratio: *de novo* BP control, 5:3; BP-irAE, 6:2). The clinical characteristics of all patients are summarized in Table 1.

BP-irAE group had a significant log_2 fold difference ($p < 0.05$) in 119 differentially expressed genes (DEGs) (Figure 2), of which 30 mRNA transcripts were up-regulated and 89 were down-regulated when compared to *de novo* BP control group. Dendritic cell marker CD209, CCL18 chemokine, C1R, and C1S complement, and toll-like receptor (TLR)-4 were among the highest DEGs in the BP-irAE group. Genes related to Th17 activation and Il-23 signaling pathways had a positive *z* score only in the *de novo* BP control group and a negative *z* score in BP-irAE group.

Table 1. Clinicopathological features of Bullous Pemphigoid (BP)

Case	Age	Sex	Ethnicity	Previous disease	Primary Cancer	Treatment of primary cancer	Time appears the lesions	Localization	Treatment
1	77	F	Caucasian	HTN	NSCLC	Nivolumab	1 week	Arms and Legs	Prednisone and Clobetasol
2	80	M	Caucasian	HTN, stroke, and Gout	Melanoma	Pembrolizumab	44 weeks	Arms and Legs	Prednisone and Doxycyline
3	73	M	Caucasian	Asthma, Eczema, HTN, and Hypothyroidism	Urothelial CA	Nivolumab	28 weeks	Arms and Legs	Triamcinolone
4	56	M	Asian	COPD and CHF	NSCLC	Pembrolizumab	16 weeks	Back	Prednisone and Clobetasol
5	63	M	Caucasian	BPH	H&N SCC	Nivolumab	8 weeks	Head and Neck	Prednisone
6	74	F	Caucasian	HTN	Urothelial CA	Nivolumab and Ipilimumab	12 weeks	Arms, Legs, and trunk	Methylprednisolone
7	68	M	Caucasian	Psoriasis, CAD, HTN, DM, Asthma, and Hypothyroidism	Melanoma	Pembrolizumab	20 weeks	Arms, Legs, and trunk	Prednisone
8	82	M	Caucasian	Atrial fibrillation and Hypothyroidism	Melanoma and met SCC	Pembrolizumab	64 weeks	Head and Neck, Trunk, Arms and Legs	Prednisone
9	68	F	Black	HTN and DM	N/A	N/A	N/A	Right mastoid	Doxycycline, Niacinamide and Steroid Rinses
10	91	F	Caucasian	HTN	N/A	N/A	N/A	Left upper arm	Prednisone and Clobetasol
11	86	F	Black	CHF and DM	N/A	N/A	N/A	Left Arm	Prednisone and Minocycline
12	77	M	Caucasian	N/A	N/A	N/A	N/A	Right chest	Doxycycline, Niacinamide, and Triamcinolone
13	85	M	Caucasian	CHF and DM	N/A	N/A	N/A	Right volar wrist	Doxycycline, Niacinamide, and Triamcinolone
14	84	M	Caucasian	HTN and DM	N/A	N/A	N/A	Left chest	Doxycycline, Niacinamide, and Clobetasol
15	60	M	Caucasian	TIA	N/A	N/A	N/A	Left shin	Methylprednisolone
16	57	M	Caucasian	HTN, DM, and Psoriasis	N/A	N/A	N/A	Scrotum	Doxycycline and Niacinamide

BP: bullous pemphigoid; BPH: benign prostatic hyperplasia; CAD: coronary arterial disease; CHF: congestive heart failure; COPD: chronic obstructive pulmonary disease; DM: diabetes mellitus; HTN: hypertension; N/A: not available; TIA: transient ischemic attack

Figure 1 - 488

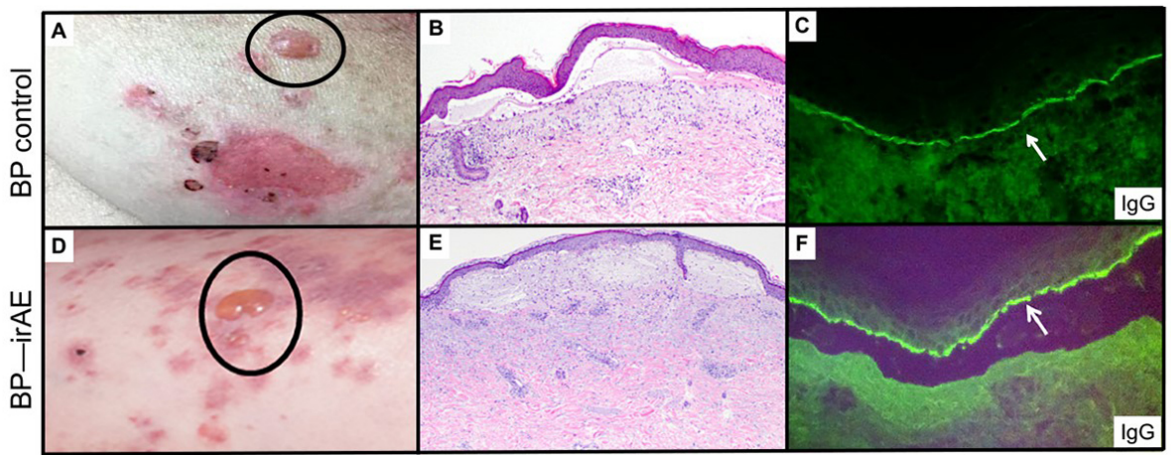

Figure 2 - 488

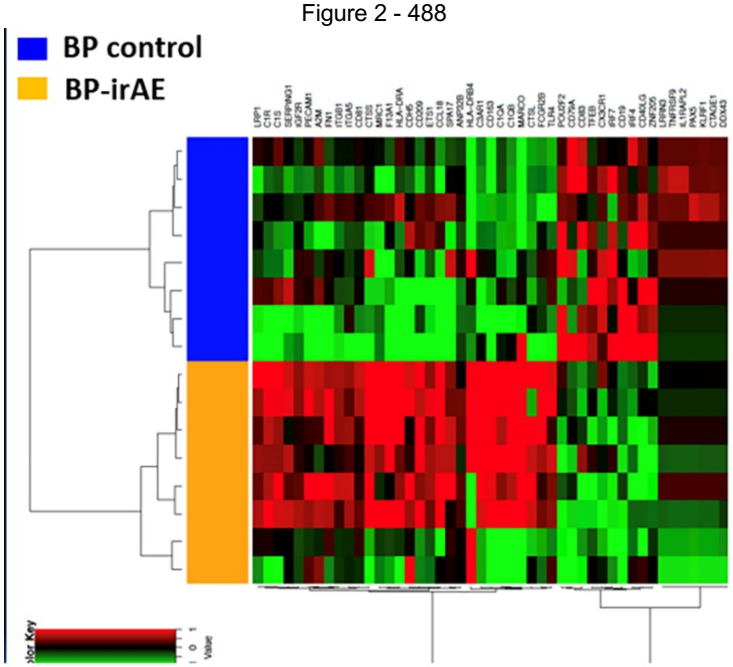

Conclusions: BP-irAE have a unique gene expression profile compared to *de novo* BP control. BP-irAE immune response may involve loss of self-tolerance, autoantibody production against BP antigens, and blister formation via activation of critical mediators of the innate and humoral immune response and classical complement pathway distinct from *de novo* BP.

489 Investigating the Effect of Infiltration with Different Macrophage Phenotypes on Gene Expression in Melanoma

Mark Mc Cabe[1], Liam Friel Tremble[2], Cynthia Heffron[3]
[1]Cork University Hospital, Dundalk, Louth, Ireland, [2]University College Cork, Clonsilla, Dublin, Ireland, [3]Cork University Hospital, Cork, Ireland

Disclosures: Mark Mc Cabe: None; Liam Friel Tremble: None; Cynthia Heffron: None

Background: The density and phenotype of tumour-associated macrophages have been linked with prognosis in a range of solid tumours. While there is strong preclinical evidence that tumour-associated macrophages promote aspects of tumour progression, it can be difficult to infer clinical activity from surface markers and ex vivo behaviour.

Design: 59 formalin-fixed paraffin embedded primary melanomas were analysed by immunohistochemical analysis of CD68, CD163, iNOS and arginase expression. RNA sequencing was performed on serial sections of 20 of the stained tumours to determine the influence of macrophage infiltration on gene expression.

Results: CD68+ cells were found to be a functionally active subset of macrophages that are associated with increased iNOS and arginase staining and altered gene expression within the tumour. In comparison, while there is a greater accumulation of CD163+ macrophages in larger tumours, and increased infiltration correlates to reduced overall survival, these cells are comparatively inactive, with no effect on the level of iNOS or arginase staining, and no effect on gene expression within the tumour.

Conclusions: Thus, melanomas contain distinct macrophage populations with diverse phenotypes. Despite stronger prognostic links, the predominant population of macrophages are less functionally active, and exert less of an effect on gene expression within the tumour.

490 Comparative Study of Acral Lentiginous Melanoma in Patients from USA and Japan

Haider Mejbel[1], Taisuke Mori[2], Carlos Torres-Cabala[3], Denai Milton[3], Yusuke Muto[4], Kenta Nakama[4], Naoya Yamazaki[4], Priyadharsini Nagarajan[5], Michael Tetzlaff[3], Doina Ivan[3], Jonathan Curry[5], Wen-Jen Hwu[3], Victor Prieto[3], Kenjiro Namikawa[3], Phyu Aung[3]

[1]East Tennessee State University, Johnson City, TN, [2]Department of Pathology and Clinical Laboratories, National Cancer Center Hospital, Tokyo, Chuo City, Japan, [3]The University of Texas MD Anderson Cancer Center, Houston, TX, [4]Department of Dermatologic Oncology, National Cancer Center Hospital, Chuo City, Tokyo, Japan, [5]Houston, TX

Disclosures: Haider Mejbel: None; Carlos Torres-Cabala: None; Yusuke Muto: None; Kenta Nakama: None; Naoya Yamazaki: None; Priyadharsini Nagarajan: None; Michael Tetzlaff: *Speaker*, Nanostring; *Advisory Board Member*, Novartis; *Advisory Board Member*, Myriad Genetics; *Advisory Board Member*, Seattle Genetics; Doina Ivan: None; Jonathan Curry: None; Kenjiro Namikawa: None; Phyu Aung: None

Background: Acral lentiginous melanoma (ALM) is a rare and aggressive subtype of melanoma. To determine whether disease prognosis is influenced by geographic areas and ethnic groups, we investigated large series of ALM cases from USA and Japan.

Design: We retrospectively reviewed the demographics and clinicopathologic features of 290 ALM patients [196 (68%) from US and 94 (32%) from Japan] and determine the associations with the clinical outcomes: overall (OS) and disease-specific survival (DSS).

Results: The US group was predominantly composed of Caucasians, younger in age, the foot was the predominate tumor site, have higher rates of higher Clark levels, intermediate (1.01 mm-4.00 mm) thickness, non-brisk tumor infiltrating lymphocytes (TIL), epithelioid cytomorphology, positive peripheral tissue margins, and more advanced clinical stage. In comparison, the Japan group was entirely composed of Asians and associated with higher rates of subungual melanomas, lower Clark levels, thin ($\leq$1.00 mm) melanomas, brisk TIL, and nevoid cytomorphology. The 5- and 10-year OS and DSS rates for the entire cohort were 59% and 30% and 64% and 36%, respectively. With long-term follow-up time (median=40.8 months in US and 32.1 months in Japan), higher Clark levels, greater Breslow thickness, increased number of mitosis, ulceration, lymphovascular invasion, increased number of positive lymph nodes, systemic therapy, and higher disease stage were significantly associated with worse OS and DSS. In addition, perineural invasion was significantly associated with worse DSS. In multivariable analysis, increased number of positive lymph nodes and the systemic therapy were associated with higher risks of death [hazard ratio (HR [95% CI])=1.13 [1.04, 1.22] and 1.74 [1.01, 3.03], respectively, for OS and 1.12 [1.02, 1.23] and 1.89 [1.01, 3.52], respectively for DSS]. In contrast to OS, DSS in Japanese patients showed a significantly lower risk of melanoma-specific death with HR [95% CI]=0.54 [0.30, 0.96] and 0.47 [0.23, 0.95] assessed by univariate and multivariable analyses, respectively.

Table 1. Summary of Patient, Clinical and Histopathological Measures – All Patients and by Country

			Country		
Measure	**Level**	**All (N=290)**	**US (N=196)**	**Japan (N=94)**	**p-value**
Gender, n (%)	Male	152 (52)	99 (51)	53 (56)	0.38
	Female	138 (48)	97 (49)	41 (44)	
Age at diagnosis	Median	64.8	61.6	70.1	< 0.001
	Range	(4.4 - 94.1)	(4.4 - 94.1)	(37.1 - 88.7)	
Race/Ethnicity, n (%)	Caucasian	153 (53)	153 (78)	0	< 0.001
	Hispanic	29 (10)	29 (15)	0	
	Other	108 (37)	14 (7)	94 (100)	
Stage, n (%)	0	20 (7)	5 (3)	15 (17)	< 0.001
	1	64 (23)	44 (23)	20 (23)	
	2	67 (24)	43 (22)	24 (28)	
	3	129 (46)	102 (52)	27 (31)	
	4	1 (<1)	1 (1)	0	
	Missing	9	1	8	
Site, n (%)	Foot/toe/heel	216 (74)	163 (83)	53 (56)	< 0.001
	Hand/finger/wrist	16 (6)	13 (7)	3 (3)	
	Nailbed	58 (20)	20 (10)	38 (40)	
LN at diagnosis, n (%)	Regional	177 (61)	117 (60)	60 (64)	0.61
	Sentinel	112 (39)	78 (40)	34 (36)	
	Missing	1	1	0	
Total number of LN at diagnosis	Median	0.0	1.0	0.0	0.003
	Range	(0.0 - 15.0)	(0.0 - 15.0)	(0.0 - 14.0)	
Clark level, n (%)	I	19 (7)	1 (1)	18 (19)	< 0.001
	II	27 (10)	14 (7)	13 (14)	
	III	17 (6)	11 (6)	6 (6)	
	IV	157 (56)	126 (67)	31 (33)	
	V	62 (22)	37 (20)	25 (27)	
	Missing	8	7	1	
Breslow thickness, n (%)	≤ 1 mm	64 (23)	29 (15)	35 (38)	< 0.001
	1.01-2 mm	54 (19)	43 (23)	11 (12)	
	2.01-4 mm	56 (20)	45 (24)	11 (12)	
	> 4 mm	107 (38)	71 (38)	36 (39)	
	Missing	9	8	1	
Mitotic figures, n (%)	< 1/mm^2	61 (22)	33 (18)	28 (30)	0.19
	1-4/mm^2	117 (42)	83 (45)	34 (37)	
	5-9/mm^2	51 (18)	37 (20)	14 (15)	
	10-20/mm^2	37 (13)	24 (13)	13 (14)	
	> 20/mm^2	13 (5)	9 (5)	4 (4)	
	Missing	11	10	1	
Ulceration, n (%)	Present	127 (46)	92 (49)	35 (38)	0.08
	Not identified	151 (54)	94 (51)	57 (62)	
	Missing	12	10	2	
Regression, n (%)	Present	26 (9)	19 (10)	7 (8)	0.52
	Not identified	253 (91)	167 (90)	86 (92)	
	Missing	11	10	1	
Vascular invasion, n (%)	Present	48 (17)	34 (18)	14 (15)	0.51
	Not identified	229 (83)	150 (82)	79 (85)	
	Missing	13	12	1	
Perineural invasion, n (%)	Present	49 (18)	47 (25)	2 (2)	< 0.001
	Not identified	231 (83)	140 (75)	91 (98)	
	Missing	10	9	1	

Microscopic satellitosis, n (%)	Present	12 (4)	9 (5)	3 (3)	0.76
	Not identified	268 (96)	178 (95)	90 (97)	
	Missing	10	9	1	
TIL, n (%)	Non-brisk	236 (86)	180 (99)	56 (60)	< 0.001
	Brisk	38 (14)	1 (1)	37 (40)	
	Missing	16	15	1	
Associated nevus, n (%)	Present	14 (5)	7 (4)	7 (8)	0.24
	Not identified	265 (95)	180 (96)	85 (92)	
	Missing	11	9	2	
Predominant cytology, n (%)	Epithelioid	146 (52)	128 (68)	18 (19)	< 0.001
	Nevoid	43 (15)	22 (12)	21 (23)	
	Small cell	41 (15)	0	41 (44)	
	Spindle	51 (18)	38 (20)	13 (14)	
Peripheral tissue edge, n (%)	Yes	116 (42)	116 (64)	0	< 0.001
	In-situ at edge	25 (9)	24 (13)	1 (1)	
	Not identified	132 (48)	40 (22)	92 (99)	
	Missing	17	16	1	
Treatment, n (%)	Yes	141 (49)	98 (51)	43 (46)	0.45
	No	146 (51)	95 (49)	51 (54)	
	Missing	3	3	0	
Vital status, n (%)	Alive w/ NED	137 (47)	78 (40)	59 (63)	< 0.001
	Alive w/ disease	44 (15)	28 (14)	16 (17)	
	Died	103 (36)	84 (43)	19 (20)	
	Lost to f/up	5 (2)	5 (3)	0	
	Missing	1	1	0	
Follow-up time in months *(all patients)*	Number of patients	289	195	94	0.017
	Median	36.6	40.8	32.1	
	Range	(0.8 - 317.0)	(2.4 - 317.0)	(0.8 - 106.8)	
Follow-up time in months *(survivors)*	Number of patients	181	106	75	0.010
	Median	40.9	46.3	33.7	
	Range	(0.8 - 317.0)	(2.5 - 317.0)	(0.8 - 93.9)	

Conclusions: Our data reveal that there are significant demographic and clinicopathologic differences between the US and Japan ALM groups. In addition, clinical outcome is primarily affected by tumor histologic features and disease stage while geographic factor impacted DSS and not OS.

491 A Genomic Survey of Sarcomas on Sun-Exposed Skin Reveals Distinctive Drivers and Potentially Targetable Mutations

Timothy Miller[1], Paul Harms[1], Bryan Johnson[2], Dan Rhodes[2], Scott Tomlins[1], Nicholas Zoumberos[1], May Chan[1], Aleodor Andea[1], Rajiv Patel[3]
[1]University of Michigan, Ann Arbor, MI, [2]Strata Oncology, Ann Arbor, MI, [3]Michigan Medicine, University of Michigan, Ann Arbor, MI

Disclosures: Timothy Miller: None; Paul Harms: None; Bryan Johnson: None; Dan Rhodes: *Employee*, Strata Oncology; *Stock Ownership*, Strata Oncology; Scott Tomlins: *Employee*, Strata Oncology; *Stock Ownership*, Strata Oncology; Nicholas Zoumberos: None; May Chan: None; Aleodor Andea: None; Rajiv Patel: None

Background: Malignant spindle cell proliferations of chronically sun-exposed skin vary considerably in prognosis and management, but can display overlapping microscopic and immunophenotypic features. Improved understanding of molecular alterations in these tumors may provide diagnostic and therapeutic insights.

Design: We characterized 81 cutaneous sarcomatoid malignancies, including primary angiosarcoma (PAS)(n=7), atypical fibroxanthoma (AFX)(n=21), pleomorphic dermal sarcoma (PDS)(n=18), leiomyosarcoma (LMS)(n=5), desmoplastic/spindled melanoma (DMM)(n=5), and sarcomatoid squamous cell carcinoma (S-SCC)(n=25), by next generation sequencing (NGS) using the StrataNGS panel for copy number variations (CNVs), mutations, and/or fusions in over 50 cancer-related genes.

Results: We detected oncogenic mutations and/or CNVs in cancer-relevant genes in all groups of tumors. No oncogenic fusions were detected. *TP53* mutations were highly recurrent, with the exception of PAS. Consistent with previous reports, recurrent *MYC* amplifications were present in PAS; we also detected recurrent *CCND1* gains in this group. *RB1* mutations were relatively restricted to LMS. As previously described, *PIK3CA* mutations predominantly occurred in AFX, whereas *RAS* family gene activation was more frequent in S-SCC and PDS. *CDKN2A* mutations were recurrent in AFX and S-SCC, and absent in PDS. In contrast, *CDKN2A* deletions were more frequent in PDS compared to AFX and S-SCC. DMM harbored diverse driver events including *CDK4* amplification and *PIK3CA* mutation. Among cases with clinical follow-up, *BRCA1/2* mutations were specific to S-SCC and PDS tumors with disease progression. In a subset of tumors, we also detected potentially actionable driver events novel to these tumor types, including activating mutations in *IDH2* (PDS), *MAP2K1* (PAS, PDS), *MTOR* (PAS), and *JAK1* (S-SCC); and copy gains in *FGFR1* (PAS, S-SCC), *KIT* (AFX), *MET* (PDS), and *PDGFRA* (PDS).

Conclusions: Here, we confirm and expand the spectrum of known genomic aberrations in cutaneous sarcomatoid malignancies. We find that certain events (e.g. *MYC* amplification, *RB1* mutation, *CDKN2A* mutation/deletion) are relatively specific to particular tumor types within this differential diagnosis, and hence might be diagnostically informative in challenging cases. Specific mutations such as *BRCA1/2* might be prognostically informative. In addition, we expand the repertoire of known targetable driver events in these tumors, suggesting utility for NGS-guided therapy in aggressive cases.

492 Proteomics-Based Typing Identified 11 Different Amyloid Types in Cutaneous Amyloidosis

Prasuna Muppa[1], Julie Vrana[2], Thomas Flotte[2], Carilyn Wieland[2], Paul Kurtin[2], Karen Rech[2], Jason Theis[2], Surendra Dasari[2], Ellen Mcphail[2]
[1]Rochester, MN, [2]Mayo Clinic, Rochester, MN

Disclosures: Prasuna Muppa: None; Julie Vrana: None; Thomas Flotte: None; Carilyn Wieland: None; Paul Kurtin: None; Karen Rech: None; Jason Theis: None; Surendra Dasari: None; Ellen Mcphail: None

Background: Amyloidosis is characterized by extracellular deposition of insoluble misfolded proteins that form beta-pleated sheets. Cutaneous amyloidosis can be either localized (primary cutaneous amyloidosis) or systemic (secondary amyloidosis). At present 36 human amyloid proteins have been described and accurate determination of amyloid type is essential for optimal patient management. As immunohistochemistry is potentially unreliable for amyloid typing due to lack of antigen-antibody specificity, we utilized the current clinical standard of mass spectrometry-based proteomics for typing cutaneous amyloid deposits to understand the proteomic and demographic spectrum of disease in cutaneous amyloidosis.

Design: We queried our liquid chromatography and tandem mass spectrometry (LC-MS/MS) amyloid typing database (2009 – 2018) for skin tissue specimens. This database consists of internal and external specimens for which Congo red-stained amyloid deposits were laser microdissected and subjected to shotgun proteomics using a clinically validated proteomics method.

Results: We identified 754 cutaneous amyloid cases (16% internal cases and 84% external consults). There were 367 females and 378 males (9 unknown); median age of 68. Table 1 summarizes the frequency and demographic information of the 11 types of amyloidosis in our cohort. AL, which may be localized or systemic, was the most common type (67% of total cases). Insulin amyloidosis (AIns: 13%) and KRT5-14 amyloidosis (11%) were common localized forms. TTR mutations were identified by proteomic analysis in 9 (11%) of ATTR cases [V122I (n=7), P24S (n=1) and T60A (n=1)]. By differential laser microdissection, we identified 10 cases that contained two different amyloid types. In these cases, KRT5-14 amyloid was present in the papillary dermis and AL amyloid was detected in deep dermal and perivascular regions.

Type	Number (%) Cases	Age	Gender (F/M/U)
AL	505 (66.98%)	68	265/236/4
AIns	102 (13.53%)	66	39/63/0
KRT5-14*	84 (11.14%)	68	47/36/1
ATTR	40 (5.31%)	79	5/34/1
AH	8 (1.06%)	65	3/5/0
Ab2MG	5 (0.66%)	70	3/1/1
AA	4 (0.53%)	64	2/1/1
AEnf	2 (0.27%)	58	0/1/1
AGel	2 (0.27%)	64	1/1/0
AApoAI	1 (0.13%)	72	1/0/0
AApoAIV	1 (0.13%)	71	1/0/0

Table 1: Frequency of amyloid types in assayed cutaneous amyloid cohort. #F stands for female, M stands for male and U stands for unknown. *KRT5-14 denotes amyloid type characterized by overexpression of high molecular weight keratins 5 and 14.

Conclusions: Cutaneous amyloidosis encompasses at least 11 different amyloid types that may be localized (AIns, KRT5-14, AEnf), systemic (ATTR, Ab2MG, AA, AGel, AApoA1, AApoAIV) or both (AL, AH). Accurate determination of amyloid type is essential for patient management. Mass spectrometry, which unambiguously detects all amyloid types in a single assay, is the optimal technique for this application.

493 A Subset of Superficial Angiomyxomas Demonstrate Loss of PRKAR1A Expression: A Clinicopathologic Analysis of 25 Cases

Neil Neumann[1], Philip LeBoit[1], Jarish Cohen[1]
[1]*University of California San Francisco, San Francisco, CA*

Disclosures: Neil Neumann: None; Philip LeBoit: None; Jarish Cohen: None

Background: Superficial angiomyxomas are benign tumors that can arise *de novo* and in the setting of the Carney complex, an autosomal dominant disease with several cutaneous manifestations including lentigines, pigmented epithelioid melanocytomas, and myxomas. Histopathologically, superficial angiomyxomas are characterized by a multinodular, sparsely cellular proliferation of stellate and spindled cells embedded within abundant myxoid stroma containing small vessels. Although most cases do not pose a diagnostic challenge, a subset can demonstrate histopathologic overlap with other cutaneous myxoid tumors and traditional immunohistochemical markers are largely non-specific. Since myxomas are one of the defining tumors of the Carney complex, the majority of which are driven by *PRKAR1A* genetic alterations, we investigated whether cutaneous angiomyxomas demonstrate loss of PRKAR1A expression by immunohistochemistry.

Design: 25 cases of cutaneous angiomyxoma were retrieved from the dermatopathology diagnostic and consultation files from 2015 to 2019. PRKAR1A immunohistochemistry was performed in all cases.

Results: The cases demonstrated a male predilection (16 male; 9 female) and tumors tended to arise in adults (Table 1, mean = 52.6 years, range: 13-87 years). The tumors arose on the extremities (44%), head and neck (32%), and trunk (24%). Architecturally, the lesions were dome-shaped (56%), polypoid (32%), or subcutaneous nodules (20%) (Figure 1A). A neutrophilic infiltrate was present in 20% of cases. Loss of PRKAR1A expression was seen in 32% of cases (Figure 1D). Nucleomegaly of tumor cells was observed in 100% of cases that exhibited PRKAR1A loss and in 35% of PRKAR1A-retained cases (Figure 1B-C). Multinucleation was present in 88% of PRKAR1A-negative cases and in 35% of the PRKAR1A-retained cases.

Table 1. Cutaneous Angiomyxoma Clinicopathologic Characteristics

	Positive PRKAR1A IHC	Negative PRKAR1A IHC	
# Cases	17	8	
Mean Age (yr)	54.5	48.6	
Sex	47.1% M (8/17); 52.9% F (9/17)	100% M (8/8); 0% F (0/8)	
Tumor Architecture (nodular-domed)	78.6% (11/14)	37.5% (3/8)	
Neutrophils Present	5.9% (1/17)	50% (4/8)	
Nuclear Enlargement	35.2% (6/17)	100% (8/8)	
Multinucleation	35.2% (6/17)	87.5% (7/8)	

Figure 1 - 493

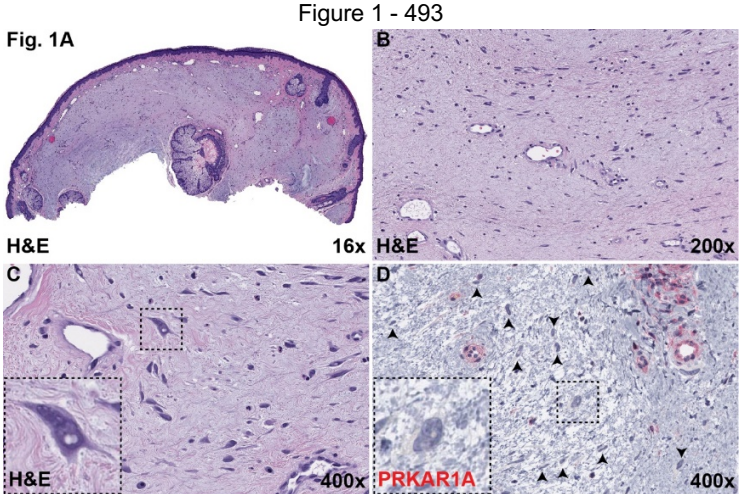

Conclusions: Nucleomegaly and multinucleation of stellate and spindled cells correlated with loss of PRKAR1A expression in the tumors examined in this series. Therefore, in tumors showing these histopathologic features, PRKAR1A immunohistochemistry can be used as a supportive adjunctive test. Given that negative staining for PRKAR1A in superficial angiomyxomas might represent a manifestation of the Carney complex, germline testing and clinical examination for other cutaneous stigmata (lentigines, darkly pigmented papules/nodules) may be warranted.

494 The Irish Curse? Low Incidence of BRAF and NRAS Mutations in a Population with a High Incidence of Melanoma

Grace Neville[1], Barbara Marzario[2], David Shilling[2], Collette Hand[2], Cynthia Heffron[3]
[1]Brigham and Women's Hospital, Harvard Medical School, Boston, MA, [2]University College Cork, Cork, Ireland, [3]Cork University Hospital, Cork, Ireland

Disclosures: Grace Neville: None; Barbara Marzario: None; David Shilling: None; Collette Hand: None; Cynthia Heffron: None

Background: Melanoma is currently the 5th most commonly diagnosed cancer in Ireland and by 2040 it is projected that melanoma incidence in the country will increase by up to 327% in men and 175% in females. The significant success of BRAF and MEK inhibitor therapy in patients with BRAF V600 mutated melanoma is well documented. It has recently been reported that the rate of BRAF mutation in Irish cohorts was only 24%, which is significantly lower than international figures. However, this was an observational finding in a cohort of patients who underwent testing for therapeutic decision making in advanced disease. We aimed to assess the mutational status of a cohort of primary cutaneous melanomas diagnosed in the Irish population and to correlate these findings with clinical follow up data.

Design: With IRB approval; all 132 cases of primary cutaneous melanoma that were diagnosed in a single tertiary referral institution in the year 2012 were reviewed. After microdissection of melanoma; 92 cases progressed to DNA extraction from formalin-fixed paraffin-embedded (FFPE) blocks using the High Pure FFPET DNA Isolation kit (Roche). Regions containing common mutations in the BRAF and NRAS genes were investigated by PCR amplification followed by Sanger sequencing. For validation, results were cross referenced in cases where clinical testing had also occurred. Demographic details, tumor characteristics and 5-year outcome data were also obtained.

Results: The sequencing success rates for BRAF V600 and NRAS Q61 were 93.4% (85/91) and 87% (80/92) respectively. NRAS and BRAF mutations were mutually exclusive in all cases where both were successfully sequenced (n=78). BRAF V600 testing showed wild type (wt) status in 77 (90.6%) cases and 8 (9.4%) cases with a V600E mutation. NRAS Q61testing showed wt status in 75 (93.8%) cases and 5 (6.3%) cases with a mutation (80%, n=4 of which had a Q61R mutation and 20% n=1 of which had a Q61K mutation).No statistically significant differences were noted between the groups for age, gender, depth of invasion, nodal status or recurrence status (p=>0.05).

Table 1: Correlation with NRAS and BRAF status with clinical and pathological outcomes:

	NRAS wild type	NRAS mutant	BRAF wild type	BRAF mutant
Age (years)	60.5	63.7	62.6	**50.5**
Gender (%male)	53.4%	60.0%	49.3%	50.0%
Nodal Status (% nodal disease at diagnosis)	1.4%	**20.0%**	6.7%	-
Depth of invasion (mm)	2.56	2.05	1.96	2.66
Recurrence %	13.9%	60.0%	13.5%	25.0%
Melanoma Subtype	Nodular: 5.4% SS: 64.9% AL: 5.4% LM: 18.9% Other: 5.4%	SS: 80% Nodular: 20%	Nodular: 6.7% SS: 60% AL: 8% LM: 20% Other: 5.3%	SS: 100%
SS: superficial spreading, AL: Acral Lentiginous, LM: Lentigo maligna melanoma				

Conclusions: These findings suggest that the Irish population has a markedly lower incidence of BRAF and NRAS mutations in melanoma than that reported in other cohorts and will therefore benefit less from the success of BRAF and MEK inhibitor therapy. As has previously been published, the NRAS mutated cases trended towards a higher incidence of nodal disease at primary excision and the BRAF mutated cases were younger.

495 Malignant Melanoma in Lagos Nigeria: A 10 Year Retrospective Study

Omobolade Obadofin[1], Kabir Badmos[2], Olubukola Aseru[3], Adekunbiola Banjo[4]
[1]Federal Medical Center Ebute-Metta, Surulere, Lagos, Nigeria, [2]Mushin, Lagos, Nigeria, [3]Federal Medical Center Ebute-Metta, Lagos, Nigeria, [4]Lagos University Teaching Hospital, Lagos, Nigeria

Disclosures: Omobolade Obadofin: None; Adekunbiola Banjo: None

Background: Malignant melanoma (MM) is the most lethal of all cutaneous malignancies, accounting for about 79% of skin cancer related deaths. In blacks, it is associated with greater morbidity and mortality compared to Caucasians. Breslow thickness and ulceration status are two of the most important histopathologic prognostic factors in MM. No study on MM in Nigeria has however examined these factors.

Design: Formalin-fixed paraffin-embedded (FFPE) tissue blocks and corresponding haematoxylin and eosin (H&E) stained slides of all confirmed cases of MM from January 2005 to December 2014 in the Anatomic and Molecular Pathology Department of Lagos University Teaching Hospital (LUTH) were retrieved. The cutaneous MM cases were classified into histologic variants according to the 2006 WHO criteria and the Clark's stage, Breslow thickness and ulceration statuses of the tumours were determined. The Clark's level and Breslow thickness were correlated with the ulceration statuses of the tumours.

Results: Fifty-two MM cases were histologically diagnosed in LUTH during the study period which represented 1.0% of total solid malignancies. Forty three of these occurred in the skin accounting for 19.7% of all skin malignancies and making MM the 3rd commonest skin malignancy after squamous cell carcinoma (SCC) and kaposi sarcoma (KS). The age range was from 24 to 85 years and the peak age of incidence was the 5th decade. Male to female ratio was 1: 1.5. Fifty eight percent (58%) of the 52 MM cases occurred in the foot. Cutaneous MM constituted 82.7% of the cases, while mucosal, metastatic and ocular melanoma constituted 7.7%, 5.8%, and 3.8% respectively.

Histologically, the cutaneous cases were Nodular, Acral lentiginous and Desmoplastic MM accounting for 84%, 14% and 2% respectively. Eighty eight percent (88%) of cutaneous MM cases were in Clark's stage IV and V while 84% had Breslow thickness ≥4mm. Ulceration was present in 67% of the cases. The Clark's level and Breslow thickness were correlated with the ulceration status of the tumour. There is significant correlation between the Brelow thickness and ulceration with p-value < 0.05 while there is no significant association between the Clark's level and ulceration (p-value > 0.05).

CLARK'S LEVEL	NO OF CASES	PERCENTAGES (%)
III	5	12
IV	25	58
V	13	30
TOTAL	43	100
BRESLOW THICKNESS	NO OF CASES	PERCENTAGES (%)
<4mm	7	16
4mm - <10mm	28	65
10mm - <20mm	7	16
>20mm	1	3
TOTAL	43	100

Figure 1 - 495

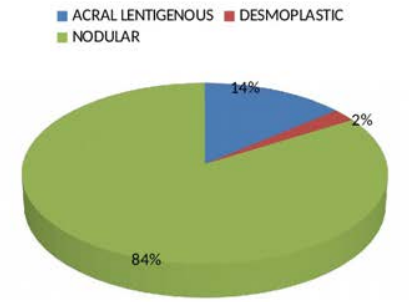

Conclusions: MM constituted a significant proportion of skin malignancy in LUTH and majority of the cases present at an advanced stage. Breslow thickness and ulceration statuses of the tumour are important histopathologic parameters that should be reported in all MM biopsies.

496 Loss of p16 Expression is Frequent in Dermatofibrosarcoma Protuberans with Fibrosarcomatous Transformation and Metastatic Disease

Gauri Panse[1], David Wang[2], Carina Dehner[3], Elizabeth Demicco[4], John Chrisinger[3], Alexander Lazar[5], Wei-Lien Billy Wang[5]
[1]Yale University, New Haven, CT, [2]Hummelstown, PA, [3]Washington University School of Medicine, St. Louis, MO, [4]Mount Sinai Hospital, Toronto, ON, [5]The University of Texas MD Anderson Cancer Center, Houston, TX

Disclosures: Gauri Panse: None; David Wang: None; Carina Dehner: None; Elizabeth Demicco: None; John Chrisinger: None; Alexander Lazar: None; Wei-Lien Billy Wang: None

Background: Dermatofibrosarcoma protuberans (DFSP) is a cutaneous fibroblastic tumor of intermediate malignant potential (WHO Classification). A subset of DFSP undergo fibrosarcomatous transformation (FS-DFSP), with increased metastatic risk. Homozygous *CDKN2A* deletion with loss of p16 protein expression has been reported in FS-DFSP. We examined the prevalence and significance of p16 expression by immunohistochemistry in a large, multi-institutional cohort of DFSP, including cases with fibrosarcomatous transformation and metastases.

Design: Unstained slides prepared from a clinically annotated tissue microarray and whole slide sections comprising a total of 83 DFSP cases were reviewed. These included 56 conventional DFSP (47 primary & 9 recurrent tumors), 18 FS-DFSP (16 primary & 2 recurrent tumors), and 9 metastatic FS-DFSP cases. Immunohistochemical studies were performed using an anti-p16 (clone E6H4, prediluted, Roche Laboratories). Loss of p16 expression was defined as complete loss of staining within the tumor cells in the presence of positive internal control. Chi square or Fisher's exact test were used to calculate *P* values as appropriate using Graphpad Prism software.

Results: Loss of p16 expression was more frequent in FS-DFSP (9/18 cases, 50%) as compared to conventional DFSP (5/56 cases, 9%), p=0.001. Thirteen of 18 FS-DFSP cases showed foci of conventional DFSP; of these, 12/13 cases had similar p16 labeling in both conventional DFSP and fibrosarcomatous areas, while one case showed retained p16 in conventional DFSP with p16 loss in areas of fibrosarcomatous transformation. Of the 5 conventional DFSP with p16 loss, three cases showed multiple local recurrences, with subsequent fibrosarcomatous transformation in one case. Eight of 9 cases of metastatic DFSP showed loss of p16 expression. All patients

with metastatic disease had a history of FS-DFSP; and interestingly, the metastatic specimens showed histopathologic features of conventional DFSP (n=2), FS-DFSP (n=6) or undifferentiated pleomorphic sarcoma-like change (n=1).

Table 1: Loss of p16 in dermatofibrosarcoma protuberans

	Conventional without metastasis (n=56)	FS-DFSP without metastasis (n=18)	FS-DFSP with metastasis (n=6)
Primary	3/47	7/16	NA
Recurrent	2/9	2/2	NA
Metastatic	--	--	8/9
Total	5/56	9/18	8/9

Conclusions: Loss of p16 staining is more frequent in FS-DFSP when compared to conventional DFSP without fibrosarcomatous transformation, and was seen in 8/9 metastatic DFSP in our series, suggesting p16 loss to be a marker of more aggressive behavior in these tumors. Further investigation in a cohort with long term follow up is needed.

497 Aberrant DNA Methylation Predicts Melanoma-Specific Survival in Patients with Acral Melanoma

Dinesh Pradhan[1], Denai Milton[2], Varshini Vasudevaraja[3], Michael Tetzlaff[2], Priyadharsini Nagarajan[4], Jonathan Curry[4], Doina Ivan[2], Lihong Long[2], Yingwen Ding[5], Ravesanker Ezhilarasan[5], Erik Sulman[5], Wen-Jen Hwu[2], Victor Prieto[2], Carlos Torres-Cabala[2], Phyu Aung[2]

[1]The University of Texas MD Anderson Cancer Center, Jacksonville, FL, [2]The University of Texas MD Anderson Cancer Center, Houston, TX, [3]New York University, New York, NY, [4]Houston, TX, [5]NYU Langone School of Medicine, New York, NY

Disclosures: Dinesh Pradhan: None; Varshini Vasudevaraja: None; Michael Tetzlaff: *Advisory Board Member*, Seattle Genetics; *Advisory Board Member*, Novartis LLC; *Speaker*, Nanostring; *Advisory Board Member*, Myriad genetics; Priyadharsini Nagarajan: None; Jonathan Curry: None; Doina Ivan: None; Ravesanker Ezhilarasan: None; Victor Prieto: None; Carlos Torres-Cabala: None; Phyu Aung: None

Background: Acral melanoma (AM) is a rare, aggressive type of cutaneous melanoma (CM) with a distinct genetic profile for which comprehensive genome-wide methylation analysis (GWMA) is lacking. We aimed to identify a methylome signature distinguishing primary acral lentiginous melanoma (PALM) from primary non-lentiginous AM involving the acral sites (NALM), metastatic ALM (MALM), primary non-acral CM (PCM), and acral nevus (AN) as well as delineate additional prognostic and predictive biomarkers and/or novel therapeutic targets for AM since the response of ALM to immune checkpoint blockade therapy and targeted therapy remains unpredictable.

Design: A total of 22 PALM, 9 NALM, 10 MALM, 9 PCM, and 3 AN cases were subjected to GWMA using the Illumina Infinium Methylation EPIC array interrogating 866,562 CpG sites, and their methylomes were compared.

Results: A prominent finding was that the methylation profiles of PALM and Nalm were distinct, although both are considered canonical AMs. Four of the genes most differentially methylated between PALM and NALM or PALM and MALM were *HHEX*, *DIPK2A* (formerly *C3orf58*), *NELFB* (formerly *COBRA1)*, and *TEF*. However, when primary AMs (PALM+NALM) were compared with MALM, *IFITM1* and *SIK3* were the most differentially methylated, highlighting their pivotal role in the metastatic potential of AMs. Patients with NALM had significantly worse disease-specific (DSS) and overall survival than patients with PALM. Aberrant methylation was significantly associated with aggressive clinicopathologic parameters, including greater Breslow thickness, ulceration, increased mitotic rate, and lymph node metastasis, and with worse DSS.

Conclusions: Our study emphasizes the importance of distinguishing between PALM and NALM. We also identified novel epigenetic prognostic biomarkers that may serve to risk-stratify patients with AM and may be leveraged for development of targeted therapies.

498 Clinicopathologic Analysis of CD8+ Primary Cutaneous Anaplastic Large Cell Lymphoma

Dinesh Pradhan[1], Manas Baisakh[2], Subhasini Naik[3], Sambit Mohanty[4]

[1]The University of Texas MD Anderson Cancer Center, Jacksonville, FL, [2]Apollo Hospitals, Bhubaneswar, India, [3]Prolife Diagnostics and Apollo Hospitals, Bhubaneswar, India, [4]AMRI Hospital, Bhubaneswar, India

Disclosures: Dinesh Pradhan: None; Manas Baisakh: None; Subhasini Naik: None; Sambit Mohanty: None

Background: Primary cutaneous anaplastic large cell lymphoma (PCALCL) is extremely rare. Most of the PCALCL cases show expression of CD4 (CD4+/CD8-). Only a few cases of CD8 positive (CD4-/CD8+) PCALCL have been reported in the literature. These cases pose a diagnostic challenge and very little are known about their clinicopathologic characteristics and clinical outcome.

Design: In this retrospective study, seven cases of CD8+ PCALCL on biopsies were retrieved from the databases of three hospitals and the demography, clinical history, management, imaging and histopathologic findings and immunohistochemical profile were recorded.

Results: The median age of the patients was 44 years (range: 18-80) and all of them were Asian. The male:female ratio was 4:3. Most of the lesions involved trunk followed by extremities. Most cases presented with a solitary (86%) ulcerated (57%) nodule (71%). There was no evidence of any nodal or systemic disease. All cases with follow up (4/7) were alive and doing well. Sections showed diffuse dermal infiltration by sheets of atypical lymphoid cells extending to the subcutis. The tumor cells had abundant eosinophilic cytoplasm and marked nuclear pleomorphism with prominent nucleoli. Numerous atypical mitotic figures and focal areas of coagulative tumor cell necrosis were observed. Epidermotropism, pseudoepitheliomatous hyperplasia, angiocentricity and eccrine gland infiltration was identified in 42% cases each, while myxoid changes were identified in 29% cases. All cases were diffusely CD8 and CD30 positive and CD4 negative in the lesional CD3 positive large T-cells. CD2, CD5 and CD7 were significantly diminished in 29%, 71% and 57%, respectively. ALK1 was negative in all cases. Two cases in which EMA was performed were negative. The majority of the cells expressed cytotoxic molecules such as TIA1 and granzyme B in all the 4 cases in which it was performed. T-cell gene rearrangement studies were performed in 2 cases in which the lymphoid infiltrate demonstrated clonal T-cell population.

Conclusions: In this retrospective analysis, we found that CD8-positive PCALCL predominantly affects middle-aged men and displays indolent behavior like the usual CD4+ PCALCL. Interestingly, 42% of patients in our cohort were female and 29% were younger than 30 years.

499 TERT Amplification is Involved in Acral Lentiginous Melanoma Progression to Metastasis

Nisha Ramani[1], Jun Gu[1], Phyu Aung[1], Steven Sfamenos[1], Chiara Sdringola-Maranga[1], Priyadharsini Nagarajan[2], Michael Tetzlaff[1], Jonathan Curry[2], Doina Ivan[1], Adi Diab[1], Wen-Jen Hwu[1], Victor Prieto[1], Carlos Torres-Cabala[1]
[1]The University of Texas MD Anderson Cancer Center, Houston, TX, [2]Houston, TX

Disclosures: Nisha Ramani: None; Jun Gu: None; Phyu Aung: None; Steven Sfamenos: None; Chiara Sdringola-Maranga: None; Priyadharsini Nagarajan: None; Michael Tetzlaff: *Speaker*, Nanostring; *Advisory Board Member*, Novartis; *Advisory Board Member*, Myriad Genetics; *Advisory Board Member*, Seattle genetics; Jonathan Curry: None; Doina Ivan: None; Carlos Torres-Cabala: None

Background: Acral lentiginous melanoma (ALM) is a rare type that occurs in non-sun exposed areas of hands and feet and appears to have poor prognosis. Little is known about the role of *TERT* amplification in disease progression to metastasis in ALM. We studied *TERT* gene amplification and molecules involved in Wnt pathway in both primary and metastatic ALM. These findings were also correlated with the clinical outcomes.

Design: *TERT* amplification by FISH and immunohistochemical expression of β-catenin and LEF-1 were investigated in 79 cases (34 primary ALM, 20 metastatic ALM, 10 primary non-ALM, and 15 acral nevi). Gene amplifications were considered positive when the ratio between *TERT* gene copy number and control was greater than 1.11. β-catenin and LEF-1, intensity (0, 1+, 2+, and 3+) and number of positive cells (%) were recorded and H score was calculated.

Results: Median age (years) and M:F ratio for our melanoma groups were: primary ALM (71, 1.4:1), metastatic ALM (71, 1.2:1), and primary non-ALM (70, 1.5:1). The most common location of primary ALM was foot/toe (81.5%). *TERT* amplification was detected in 6 of 28 (21.4%) primary ALM, 2 of 8 (25%) primary non-ALM, and 8 of 18 (44.4%) metastatic ALM, the latter showing significantly higher frequency compared to primary melanomas (p=0.043). Cytoplasmic and not nuclear expression of β-catenin was variably detected in all of the cases. Metastatic ALM revealed lower expression of β-catenin than primary ALM (p=0.017). No differences in H-scores of LEF1 were detected among the groups; however, acral nevi showed decreased labeling with descent, in contrast to melanoma. No correlation between any of the biomarkers and clinical outcomes was found.

Figure 1 - 499

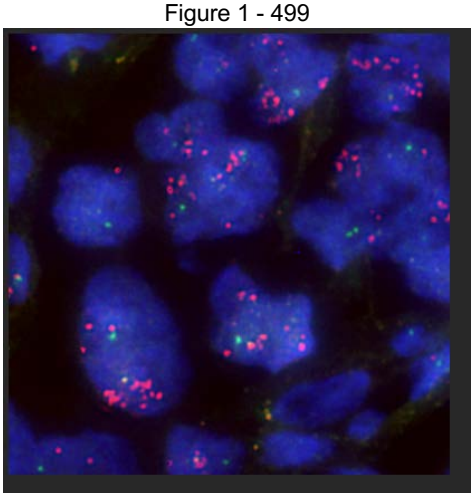

Conclusions: *TERT* amplification was frequently found in primary ALM and increased in metastatic tumors, suggesting a role in tumor progression to metastasis. This appears to be unique for ALM, since changes in *TERT* promoter mutation status, and not amplification, are detected in metastasis of other types of melanoma. Activation of Wnt pathway in ALM may involve non-canonical Wnt cascades, based on the lack of nuclear β-catenin (and decreased cytoplasmic expression) seen in metastatic ALM. *TERT* amplification by FISH and LEF1 immunohistochemistry may help in the differential diagnosis between primary ALM and acral nevus. *TERT* amplification and non-canonical Wnt pathways may be targets for therapy in metastatic ALM.

500 Merkel Cell Polyomavirus is Implicated in a Subset of Cases of Merkel Cell Carcinomas from the Indian Subcontinent

Bharat Rekhi[1], Reety Arora[2], Pratik Chandrani[3], Sudhir Krishna[2], Amit Dutt[4]
[1]Tata Memorial Hospital, Mumbai, IND, India, [2]National Centre for Biological Sciences, Tata Institute of Fundamental Research, Bengaluru, Karnataka, India, Bengaluru, Karnataka, India, [3]Integrated Genomics Laboratory, Advanced Centre for Treatment, Research and Education In Cancer, Tata Memorial Centre, Navi Mumbai, Maharashtra, India, [4]ACTREC- Tata Memorial Centre, Navi Mumbai, Maharashtra, India

Disclosures: Bharat Rekhi: None; Amit Dutt: None

Background: Merkel cell carcinoma(MCC) is a rare, lethal cancer, histopathologically composed of cells showing similarity with mechanoreceptor Merkel cells. MCCs manifest in two distinct forms. While a virus, namely Merkel cell polyomavirus(MCV) causes one form of the disease; the other is driven by Ultraviolet (UV)-linked mutations. Except for a report from a single country, there has been no other documentation on the association of MCV with cases of MCC from our continent.

Design: Paraffin-embedded tissue sections of 18 cases of MCC and 14 other cutaneous cancers were tested for immunohistochemical(IHC) expression of Merkel cell polyomavirus(MCV) T antigen, using two sensitive antibodies(CM2B4 and Ab3), targeting the viral large T antigen protein. Furthermore, 12 cases of MCC were tested by real-time PCR, using primers targeting the N terminus of T antigen.

Results: Eighteen cases of MCC occurred in 11 men and 7 women, with age ranging from 34-74 years(average=58), in lower extremities(9, 50%), head and neck region(4, 22.2%), upper extremities(4, 22.2%) and chest wall(1.5.5%), with tumor size(n=4) varying from 2.5-16 cm. Immunohistochemically, 15/15 cases(100%) of MCC displayed 'dot-like' to cytoplasmic immunopositivity for CK20; 5/5 cases(100%) were positive for CD56, 15/16(93.7%) were positive for chromogranin, 12/13(92.3%) were positive for synaptophysin and 7/18 cases(38.8%) showed positive IHC expression for MCV T antigen (diffuse in 5 and focal in 2 cases; using CM2B4 in 5 and Ab3 in 7 cases)[Fig.1]. On testing samples from 12 cases of MCC(with an optimal DNA quality) for MCV, by real-time PCR, 8 showed viral copy numbers ranging from 2.8-9.7. Three out of 12 cases(25%) showed positive results for MCV, by both, immunohistochemistry and real-time PCR. Among other tumors, 5/5 cases of basal cell carcinoma, 5/5 melanomas and 3/4 cases of squamous cell carcinoma showed complete negative immunostaining for both the MCV antibodies.

Figure 1 - 500

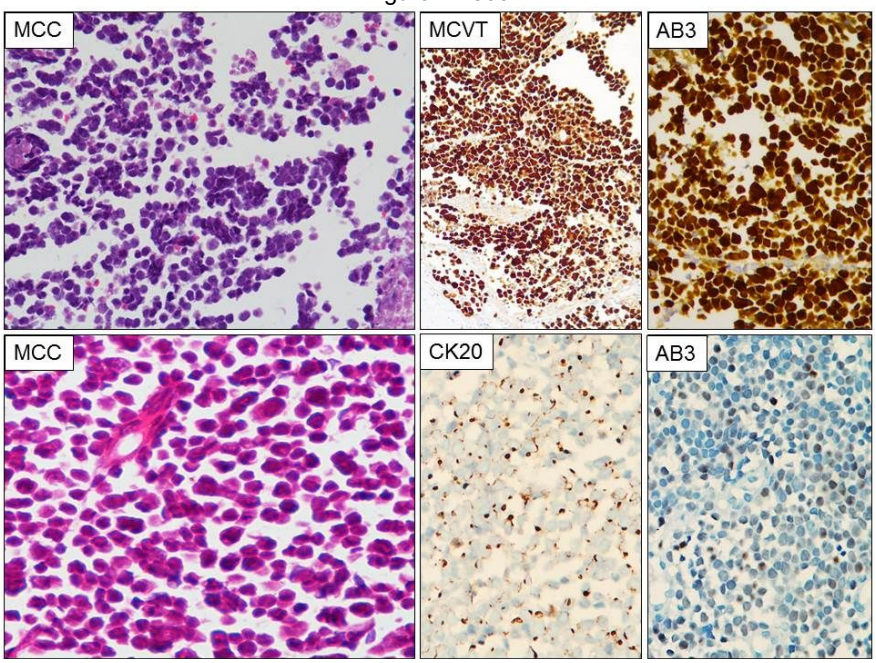

Conclusions: This constitutes the first report from India and probably the second from our continent showing the implication of MCV in MCCs. Moreover, this is one of the larger series of MCCs, tested for MCV, by both immunohistochemistry and real-time PCR, from this part of the world, indicating that Merkel cell polyomavirus is definitely implicated in a subset of MCC cases from this region, where relatively more number of such cases are likely to be caused by UV-linked damage. While both the antibodies were fairly specific (92.8%), AB3 was relatively more sensitive.

501 Immunofluorescence and Electronic Microscopy in Diagnosis and Classification of Inherited Epidermolysis Bullosa: A Single-Center Retrospective Comparative Study of 79 Genetically Confirmed Cases

Sabrina Rossi[1], Renata Boldrini[2], Daniele Castiglia[3], Elisa Pisaneschi[4], Andrea Diociaiuti[4], Alessandra Stracuzzi[4], Giovanna Zambruno[4], Elisa Pisaneschi[2], Rita Alaggio[4], May El Hachem[4]
[1]Rome, Italy, [2]Bambino Gesù Children's Hospital, Roma, Italy, [3]Istituto Dermopatico dell'Immacolata-IRCCS, Rome, Italy, [4]Bambino Gesù Children's Hospital, Rome, Italy

Disclosures: Sabrina Rossi: None; Renata Boldrini: None; Daniele Castiglia: None; Elisa Pisaneschi: None; Andrea Diociaiuti: None; Alessandra Stracuzzi: None; Giovanna Zambruno: None; Elisa Pisaneschi: None; Rita Alaggio: None; May El Hachem: None

Background: Inherited epidermolysis bullosa (EB) comprises a heterogeneous group of skin fragility disorders, due to mutations in at least 21 genes. Based on skin cleavage level, 4 major types are distinguished: EB simplex (EBS), junctional EB (JEB), dystrophic EB (DEB), and Kindler syndrome (KS). Laboratory testing is essential for EB diagnosis, particularly in newborn, when EB type/subtype with different prognosis are indistinguishable. We aimed to compare electron microscopy (EM) with immunofluorescence mapping (IFM) on frozen skin biopsies with a panel of antibodies for basement membrane zone adhesion proteins in a retrospective series with genetically confirmed diagnosis.

Design: The series consisted of 79 patients (M:F=1.3), including 41 infants younger than 1 month. Table 1 summarizes series characteristics with mutated genes. IFM was available in 78 cases and EM in 73.

Results: IFM allowed identification of EB type in 15/18 (83.3%) EBS, 20/20 (100%) JEB, 38/39 (97.4%) DEB and 1/1 KS, based mainly on cleavage level within EBS type and on cleavage level and/or altered protein for the JEB, DEB and KS types. EM led to correct type classification in 16/19 (84.2%) EBS, 18/18 (100%) JEB, 36/36 (100%) DEB, based on cleavage level for all types and/or abnormalities of tonofilaments, hemidesmosomes and anchoring fibrils, for EBS, JEB and DEB, respectively. As to EBS subtypes, only EM allowed identification of generalized severe EBS (6/6 cases), confirming tonofilament clumping as the hallmark of this subtype. However, IFM was diagnostic of other EBS subtypes showing absence of defective proteins, e.g. in 3/3 cases of KRT14 recessive subtype. Within JEB and DEB groups, IFM allowed subtype definition: absence of laminin332 for generalized severe JEB (14/14 cases), reduction of either laminin332 (2/2 cases) or BP180 (3/3 cases) for generalized intermediate JEB, reduced ß4 integrin for JEB with pyloric atresia (1/1 case) and absence of collagen VII for generalized severe recessive DEB (8/8 cases). IFM and EM were equally valuable in identifying bullous dermolysis of the newborn (6/6 cases), which cannot be distinguished on genetic ground, based on collagen VII globules (IFM) or stellate bodies (EM) in basal keratinocytes.

SERIES CHARACTERISTICS		
SEX		Pts N
	M	45
	F	34
Age groups		
	≤1 month	41
	>1 month ≤ 12 months	19
	>1 year ≤ 18 years	13
	>18 years	6
EB type/subtype and mutated gene		
EBS		**19**
EBS, localized/generalized intermediate	KRT14	3
	KRT5	3
EBS, generalized severe	KRT14	6
EBS, autosomal recessive K14	KRT14	3
EBS with muscular dystrophy	PLEC	1
EBS, autosomal recessive exophilin 5	EXPH5	1
EBS, autosomal dominant KLHL24	KLHL24	2
JEB		**20**
JEB, generalized severe	LAMA3	2
	LAMB3	8
	LAMC2	4
JEB, generalized intermediate	LAMA3	1
	LAMB3	1
	COL17A1/BP180	3
JEB with pyloric atresia	ITGB4	1
DEB		**39**
Dominant DEB, all subtypes	COL7A1	10
Recessive DEB, generalized severe		8
Recessive DEB, all other subtypes		21
KS	FERMT1	**1**

Conclusions: IFM allows an accurate and rapid diagnosis (within 48 hours) in virtually all generalized severe JEB and DEB. EM remains the method of choice for identification of generalized severe EBS. Combined IFM and EM provide major clues to prognostication and care in EB newborns.

502 Pigmentation Intensity in Primary Cutaneous Melanomas from TCGA Shows an Association with Clinical and Pathological TNM Staging: Histo-Genomic Correlations Through Transcriptomic Analysis

Simon Roy[1], Philippe Echelard[2], Anne Xuan-Lan Nguyen[3], Leonardo Lando[4], Vincent Quoc-Huy Trinh[5]
[1]University of Montréal, Montréal, QC, [2]Université de Sherbrooke, Sherbrooke, QC, [3]McGill University, Montreal, QC, [4]Federal University of Goias, Goiania, GO, Brazil, [5]Vanderbilt University Medical Center, Nashville, TN

Disclosures: Simon Roy: None; Philippe Echelard: None; Anne Xuan-Lan Nguyen: None; Leonardo Lando: None; Vincent Quoc-Huy Trinh: None

Background: Pigmentation in cutaneous melanomas (CM) has been studied and shown to be implicated in disease pathogenesis. Amelanotic melanoma is associated with a greater Breslow depth, ulceration and mitotic rate than pigmented melanoma. In addition, the

proportion of melanin content in melanoma may influence survival time and response to radiotherapy modalities. The correlation between pigment quantification and clinical, pathologic and molecular findings from The Cancer Genome Atlas (TCGA) dataset remains unelucidated.

Design: We obtained clinical, pathological, histological and molecular data for CM using cBioportal, TCGABiolinks 3.7, GDC Legacy Archive and GDC Transfer Tool v1.3.0. Digital diagnostic and frozen section slides were reviewed by two observers in Aperio Imagescope v12.2.2.2.5015 and pigmentation was graded by consensus as a percentage of pigmented melanocytes within a tumor area. Pigmentation intensity scores were then stratified into 3 groups (pigment poor: 0-5%, pigment intermediate: 6-50%, pigment rich: 51-100%). Genes associated with pigmentation in melanoma (Pubmed-cited reviews, 2010-2018) were selected. Differential gene expression was tested in EdgeR in R from RNAseq data, with a false discovery rate (FDR) <0.05. Differentially expressed genes (DEGs) were identified by comparing pigment rich versus the rest of the study cohort.

Results: 109 primary CM are available from TCGA. 2 cases were excluded as they did not have digitalized histologic slides. At histological review, we observed 56 "pigment poor" cases, 39 "pigment intermediate" and 12 "pigment rich"; univariate analysis showed an association between pigmentation groups and AJCC stage ($p<0.0001$) and TNM T stage (table 1, $p<0.0001$). Breslow depth, melanoma subtype, mitotic rate, and lymphocytic infiltration were not associated with pigmentation in our analysis of the data. Differential gene expression analysis identified 229 differentially expressed genes. The top 10 DEGs included: SCN3B, RPS26P47, AC109466, ZNF385C, CCDC178, IGLL3P, ASCL4, SCGB2B2, IQCE, GAD2.

Table 1. Univariate analysis of clinical, histologic and genomic datapoints between each cutaneous melanoma pigmentation group

Factor	**Pigment poor** (0-5%) n=56	**Pigment intermediate** (6-50%) n=39	**Pigment rich** (51-100%) n=12	Total (n=107)	P
Clinical Characteristics					
Age	64.4±15.1	61.3±11.1	69.6±13.7	63.9±13.7	0.208
Sex Female Male	20 (35.7%) 36 (64.3%)	19 (48.7%) 20 (51.3%)	5 (41.7%) 7 (58.3%)	44 (41.1%) 63 (58.9%)	0.448
Death during follow-up	17 (30.4%)	8 (20.5%)	7 (58.8%)	32 (29.9%)	**0.043**
Personal Cancer History	1 (1.8%)	0 (0.0%)	0 (0.0%)	1 (0.9%)	0.632
Adjuvant treatment	6 (10.7%)	3 (7.7%)	1 (8.3%)	10 (9.3%)	0.550
Stage AJCC I II III IV	0 (0.0%) 3 (5.6%) 4 (7.4%) 47 (87.0%)	0 (0.0%) 2 (5.1%) 3 (7.7%) 34 (87.8%)	1 (9.1%) 0 (0.0%) 6 (54.5%) 4 (36.4%)	1 (1.0%) 5 (4.8%) 13 (12.5%) 85 (81.7%)	**<0.0001**
T Stage TX T1 T2 T3 T4	2 (3.6%) 0 (0.0%) 3 (5.4%) 4 (7.1%) 47(83.9%)	0 (0.0%) 0 (0.0%) 2 (5.1%) 3 (7.7%) 34 (87.2%)	1 (8.3%) 1 (8.3%) 0 (0.0%) 6 (50.0%) 4 (33.3%)	3 (2.8%) 1 (0.9%) 5 (4.7%) 13 (12.1%) 85 (79.4%)	**<0.0001**
N Stage NX N0 N1 N2 N3	2 (3.6%) 10 (17.9%) 32 (57.1%) 5 (8.9%) 7(12.5%)	0 (0.0%) 5 (12.8%) 26 (46.4%) 5 (12.8%) 3 (5.4%)	0 (0.0%) 1 (8.3%) 7 (58.3%) 2 (16.7%) 2 (16.7%)	2 (1.9%) 16 (15.0%) 65 (60.7%) 12 (11.2%) 12 (11.2%)	0.813
M Stage MX M0 M1	3 (5.4%) 50 (89.3%) 3 (5.4%)	1 (2.6%) 38 (97.4%) 0 (0.0%)	0 (0.0%) 12 (100.0%) 0 (0.0%)	4 (3.7%) 96 (89.7%) 3 (2.8%)	0.414
Pathological Characteristics					
Anatomical Site Head and neck Trunk Extremities Other	4 (7.1%) 26 (46.4%) 24 (42.9%) 2 (3.6%)	4 (10.3%) 16 (41.0%) 17 (43.6%) 2 (5.1%)	2 (16.7%) 6 (50.0%) 3 (25.0%) 1 (8.3%)	10 (9.3%) 48 (44.9%) 44 (41.1%) 5 (4.7%)	0.856
Breslow	13.2±14.4	11.7±11.3	4.7±3.8	11.7±12.7	0.158

Melanoma subtype Melanoma NOS Desmoplastic Acral Lentigo maligna	51 (91.1%) 2 (3.6%) 2 (3.6%) 1 (1.8%)	38 (97.4%) 1 (2.6%) 0 (0.0%) 0 (0.0%)	12 (100.0%) 0 (0.0%) 0 (0.0%) 0 (0.0%)	101 (94.4%) 3 (2.8%) 2 (1.9%) 1 (0.9%)	0.811
Mitoses per mm^2	7.8±7.2	4.4±3.9	1.3±0.4	6.2±6.3	0.296
Ulceration (presence)	44 (88.0%)	27 (84.4%)	7 (77.8%)	78 (85.7%)	0.697
Microvascular loops	29 (52.7%)	20 (55.6%)	3 (27.3%)	52 (51.0%)	0.241
Lymphocyte score Immune poor (0-2) Immune intermediate (3-4) Immune rich (5-6)	26 (72.2%) 6 (16.7%) 4 (11.1%)	10 (43.5%) 7 (30.4%) 6 (26.1%)	5 (71.4%) 0 (0.0%) 2 (28.6%)	41 (62.1%) 13 (18.7%) 12 (18.2%)	0.133
Baseline molecular characteristics					
BRAF *Mutated* *Not mutated* *Unknown*	25 (44.6%) 31 (55.4%) 0 (0.0%)	17 (43.6%) 22 (56.4%) 0 (0.0%)	3 (25.0%) 8 (66.7%) 1 (8.3%)	45 (42.1%) 61 (57.0%) 1 (0.9%)	0.558
NRAS *Mutated* *Not mutated* *Unknown*	8 (14.3%) 48 (85.7%) 0 (0.0%)	3 (7.7%) 36 (92.3%) 0 (0.0%)	0 (0.0%) 11 (91.7%) 1 (8.3%)	11 (10.3%) 95 (88.8%) 1 (0.9%)	0.287
NF1 *Mutated* *Not mutated* *Unknown*	5 (8.9%) 51 (91.1%) 0 (0.0%)	2 (5.1%) 37 (94.9%) 0 (0.0%)	3 (25.0%) 8 (66.7%) 1 (8.3%)	10 (9.3%) 96 (89.7%) 1 (0.9%)	0.084
KIT *Mutated* *Not mutated* *Unknown*	3 (5.4%) 53 (94.6%) 0 (0.0%)	2 (5.1%) 37 (94.9%) 0 (0.0%)	1 (8.3%) 10 (83.3%) 1 (8.3%)	6 (5.6%) 100 (93.5%) 1 (0.9%)	0.873
CDKN2A *Mutated* *Not mutated* *Unknown*	3 (5.4%) 53 (94.6%) 0 (0.0%)	2 (5.1%) 37 (94.9%) 0 (0.0%)	0 (0.0%) 11(91.7%) 1 (8.3%)	5 (4.7%) 101 (94.4%) 1 (0.9%)	0.737
TERT amplification *Present* *Absent* *Unknown*	2 (3.6%) 54 (96.4%) 0 (%)	2 (5.1%) 37 (94.9%) 0 (%)	0 (0.0%) 11 (91.7%) 1 (8.3%)	4 (3.7%) 102 (95.3%) 1 (0.9%)	0.728
Number of mutations	483.1±1002.1	213.8±248.0	439.9±380.9	384.0±765.2	0.345
Fraction of genome altered	0.34±0.21	0.29±0.20	0.25±0.14	0.31±0.20	0.278

Figure 1 - 502

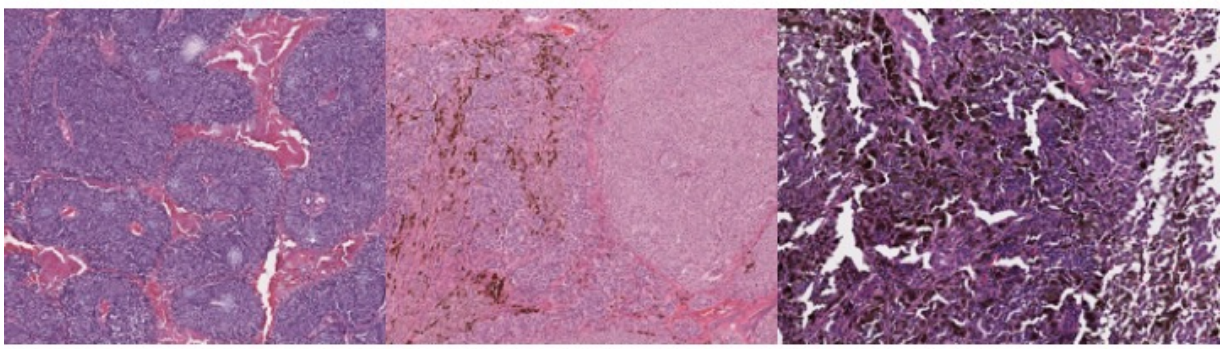

Figure 1. Different degrees of pigmentation in cutaneous melanoma (A/B/C). Pigment levels are qualified as poor (A), intermediate (B) and rich (C).

Figure 2 - 502

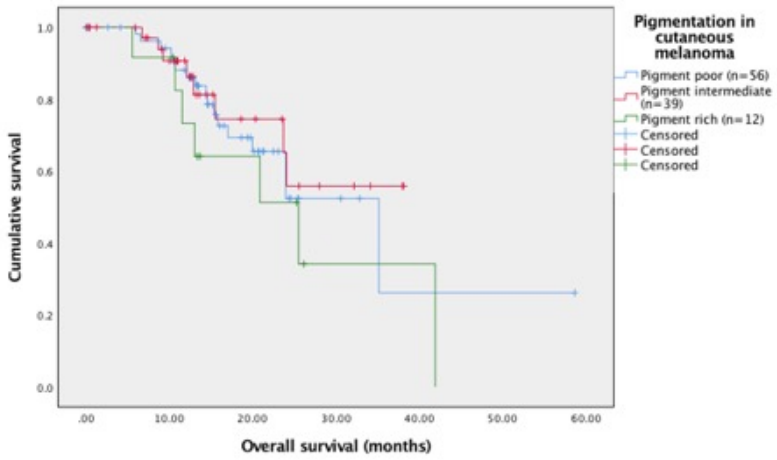

Figure 2. Overall-survival in cutaneous melanoma according to degree of pigmentation (log-rank P= 0.479).

Conclusions: Clinically, we detected that pigmentation was significantly associated with AJCC stage and TNM T stage. On the other hand, classic pathologic and mutational features were not significantly different amongst pigmentation groups. We identified differentially expressed genes amongst pigment-rich genes, and further validation studies are warranted.

503 Clinicopathologic Evaluation of Inpatient Dermatologic Consultations of Cutaneous Infections from a Large Tertiary Hospital

Behzad Salari[1], Ariana Ellis[2], Anthony Fernandez[3], Jennifer Ko[4], Steven Billings[5]
[1]Washington University in St. Louis, St. Louis, MO, [2]Cleveland Clinic, Boardman, OH, [3]Cleveland Clinic Foundation, Cleveland, OH, [4]Highland Hgts, OH, [5]Cleveland Clinic, Lerner College of Medicine, Cleveland, OH

Disclosures: Behzad Salari: None; Ariana Ellis: None; Anthony Fernandez: None; Jennifer Ko: None; Steven Billings: None

Background: Cutaneous infections from inpatient dermatology consultations are often biopsied. We reviewed all such biopsies to assess for patterns of cutaneous infections seen at a tertiary hospital.

Design: All biopsies from an inpatient dermatology consultation service over a 4-year period were reviewed. For inclusion, a documented infectious etiology from culture, molecular tests, or biopsy findings was required. Clinical information and culture/molecular results were obtained and pathology materials were reviewed.

Results: Of 115 patients with clinical impression including an infectious etiology, 75 patients with 79 biopsies met inclusion criteria. The median age was 57.1 years (range, 0.1–78.0 years; 43M; 32F). Forty-five percent were immunosuppressed and 33% had current malignancy. One-fourth were admitted due to cutaneous disease (Table 1). Of 79 biopsies, bacterial infections accounted for 35, fungal infections for 19, viral infections 12, and mixed infections 11. Additionally, there was a case each of scabies and Kaposi sarcoma. Of 35 bacterial infections, histopathologic diagnosis was rendered on 12. The remaining bacterial infections were diagnosed by culture. Most common isolates were *S. aureus* (9), methicillin resistant *S. aureus* (MRSA)(9), and *P. aeruginosa* (3). Of 19 fungal infections, all but one case of Rhizopus infection were recognized microscopically. Four angioinvasive fungi were identified (2 were confirmed to be Aspergillus and 1 Fusarium by culture). In one case cultures were negative. Remaining fungal infections included dermatophyte (6), Pityrosporum (4), and candidiasis (3). Of 12 viral infections, there were 10 herpesvirus infections recognized microscopically. Five were confirmed to be varicella zoster by DFA, and 1 herpes simplex virus by culture and DFA. Human papilloma virus was recognized in 2 patients. Eleven were mixed infections including candidiasis (6), *P. aeruginosa* (2), and MRSA (1).

Table 1- Characteristics and diagnosis of inpatient dermatopathology consultations						
	All patients	**Bacterial infection**	**Fungal infection**	**Viral infection**	**Mixed infections**	**Other**
Number of patients	75	34	19	11	9	2*
Number of biopsies	79	35	19	12	11	2
Age, years (median)	57.1	50.8	58.3	60.3	59.0	47.8
Gender, male	43 (57.3%)	22 (64.7%)	13 (68.4%)	4 (36.4%)	2 (22.2%)	2 (100%)
Ethnicity	54 (72.0%)	26 (76.5%)	13 (68.4%)	8 (72.7%)	7 (77.8%)	0
White	14 (18.7%)	7 (20.6%)	3 (15.8%)	2 (18.2%)	1 (11.1%)	1 (50%)
African-American	2 (2.7%)	0	1 (5.3%)	0	0	1 (50%)
Asian	2 (2.7%)	1 (2.9%)	1 (5.3%)	0	0	0
Hispanic	3 (4.0%)	0	1 (5.3%)	1 (9.1%)	1 (11.1%)	0
Other/unknown						
Reason for admission	18 (24.0%)	12 (35.3%)	1 (5.3%)	4 (36.4%)	0	1 (50%)
A. Primary dermatologic complaints						
B. Other complaints including dermatologic	4 (5.3%)	2 (5.9%)	0	0	1 (11.1%)	1 (50%)
C. Primary non-dermatologic complaints	53 (70.7%)	20 (58.8%)	18 (94.7%)	7 (63.6%)	8 (88.9%)	0
History of current immunosuppression	34 (45.3%)	15 (44.1%)	8 (42.1%)	6 (54.5%)	4 (44.4%)	1 (50%)
History of malignancy, active	25 (33.3%)	12 (35.3%)	5 (26.3%)	4 (36.4%)	3 (33.3%)	1 (50%)
Involved skin sites	20 (26.7%)	9 (26.5%)	7 (36.8%)	1 (9.1%)	3 (33.3%)	0
Single site	55 (73.3%)	25 (73.5%)	12 (63.2%)	10 (90.9%)	6 (66.7%)	2 (100%)
Multiple sites						
* One patient with scabies and one patient with Kaposi sarcoma.						

Conclusions: This study summarized the experience of cutaneous infections seen in dermatology inpatient consultations at a large tertiary hospital. Infections in this setting are more common in immunocompromised patients and those with malignancies. Bacterial infections were more likely to be a cause of admission, while fungal and viral infections most commonly developed as a secondary problem. Histopathologic examination resulted in an actionable diagnosis in 65% of cases with initial clinical impression including an infectious etiology.

504 Sebaceous Neoplasms: The Epidemiologic, Histopathologic and Immunohistochemical Features of 215 Near-Eastern Cases

Maelle Saliba[1], Muhammad Shaheen[1], Rana El Hajj[2], Fatmeh Abbas[1], Shaarif Bashir[3], Umer Nisar Sheikh[4], Asif Loya[3], Ibrahim Khalifeh[1]

[1]American University of Beirut Medical Center, Beirut, Lebanon, [2]American University of Beirut, Beirut, Lebanon, [3]Shaukat Khanum Memorial Cancer Hospital, Lahore, Punjab, Pakistan, [4]Shaukat Khanum Memorial Cancer Hospital, Lahore, Lahore, Pakistan

Disclosures: Maelle Saliba: None; Muhammad Shaheen: None; Rana El Hajj: None; Fatmeh Abbas: None; Shaarif Bashir: None; Umer Nisar Sheikh: None; Asif Loya: None; Ibrahim Khalifeh: None

Background: Sebaceous neoplasms (SNs) include a spectrum of lesions culminating with sebaceous carcinoma (SC), a rare but aggressive malignancy with heterogeneous clinicopathologic presentations. The epidemiologic, histopathologic and immunohistochemical features of SNs in the Near-East have yet to be reported.

Design: A total of 215 resected SNs (17 sebaceous adenomas, 15 sebaceomas and 183 SCs) from the Near-East were reviewed. Demographic and clinical information (size and anatomic location) were collected. Microscopic variables related to the tumoral features, background and host response were documented. Immunohistochemical analysis assessed the expression profile of CK5/6, P40, P63, P53, AR, EMA and p16.

Results: SNs displayed a wide age range (16-90 y) but predominantly affected patients in the 6th decade (M= 55.6 y SD 14.7), with no gender predilection. Lesions were ocular in 71.5% of cases [figure 1]. SCs were more frequently ocular (78.6%) while benign lesions were more likely to be extraocular (68.8%). SCs clinically presented as larger lesions (M=1.8 cm) as compared to sebaceomas (M=1.4 cm) and adenomas (M= 1.1 cm). Eyelid SCs were more likely to affect the mucosal surface than benign lesions (52 vs 20%). Microscopically, sebaceous differentiation was minimal in SCs (M=6%). Most SCs showed a nodular pattern (62.6%), infiltrative and comedocarcinoma patterns being less frequent (19.2% and 13.2%). An in-situ component was present in up to 75% of cases (66% flat, 15% nested and 3.3% pagetoid) and was identified in isolation in 3 cases. While most SCs showed severe cytologic atypia (67.0%), a minority displayed mild to moderate atypia (33.0%) similar to that in sebaceomas. Average mitotic activity per mm^2 ranged from 1.2 for adenomas, to 9.1 for sebaceomas and 30.5 for SCs. Perineural and lymphovascular invasion were each noted in 7.3% of SCs, while squamous differentiation was noted in up to 11.5% of SCs and 6.7% of sebaceomas. Immunohistochemical staining profiles are summarized in the annexed table.

Immunohistochemical Markers		Sebaceous Neoplasm	
		Benign	Malignant
CK56	Negative	0	1.1%
	Patchy	75.0%	76.4%
	Diffuse	**25.0%**	**22.5%**
P40	Negative	0	3.6%
	Patchy	0	1.2%
	Diffuse	**100.0%**	**95.3%**
P63	Negative	0	0.8%
	Patchy	0	3.1%
	Diffuse	**100.0%**	**96.2%**
P53	Not expressed	**3.3%**	**32.8%**
	Low expression	**86.7%**	**3.4%**
	High expression	**10.0%**	**63.8%**
AR	Negative	0	8.4%
	Patchy	6.5%	25.3%
	Diffuse	**93.5%**	**66.3%**
EMA	Negative	0	0
	Patchy	27.3%	19.3%
	Diffuse	**72.7%**	**80.7%**
P16	Negative	34.4%	10.8%
	Patchy	50.0%	19.9%
	Diffuse	**15.6%**	**69.3%**

Figure 1 - 504

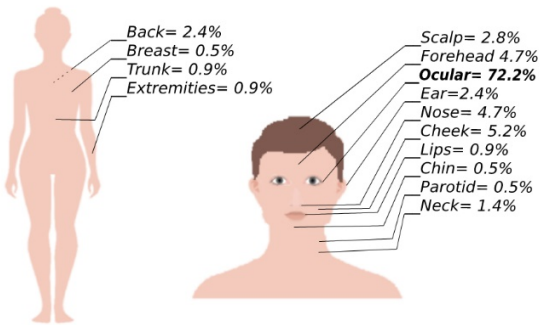

Anatomic distribution of Sebaceous Neoplasms

Conclusions: Like western SNs, Near-Eastern SNs exhibit a predilection to the head and neck. Differentiating between SCs, benign SNs and malignant diagnostic mimickers is challenged by considerable morphologic and immunohistochemical overlap. P40, a fairly specific squamous marker, almost invariably stains SNs, making the role of EMA ever more important in identifying SNs. While high p53 labeling index expression favors malignancy, strong AR expression favors benignity.

505 Diagnostic Utility of p16 and PRAME in Differentiating Nodal Nevi from Nodal Metastatic Melanoma

Sharlene See[1], Brian Finkelman[2], Anjana Yeldandi[3]
[1]Northwestern University, Chicago, IL, [2]Northwestern University Feinberg School of Medicine, Chicago, IL, [3]Northwestern Memorial Hospital, Chicago, IL

Disclosures: Sharlene See: None; Brian Finkelman: None; Anjana Yeldandi: None

Background: Lymph node status remains one of the most powerful predictors of melanoma recurrence and survival, making accurate distinction between nodal metastases and nodal nevi of paramount importance for practicing pathologists. p16, a tumor suppressor protein, has been shown to reliably distinguish nodal nevi from nodal melanoma, with positive staining in nevi and loss in melanoma. PRAME (Preferentially expressed Antigen in Melanoma) is believed to be predominantly positive in melanoma and negative in nevi. This study explores the diagnostic utility of p16 and PRAME in differentiating nodal nevi from nodal metastatic melanoma.

Design: We searched our pathology database for cases of nodal nevi and nodal metastatic melanoma. p16 and PRAME expression were assessed with immunolabeling quantified and scored by extent of nuclear positivity (1= 0-25%, 2= >25%-50%, 3= >50%-75% and 4= >75%). All cases with available material were scored and tabulated. Sensitivities and specificities were calculated, and discrimination assessed using the area under the receiver operating characteristic curve (AUC). Statistical significance for comparing AUCs was assessed using the DeLong method.

Results: Forty-six cases of nodal nevi and 55 cases of nodal metastatic melanoma were identified, with 44/46 nevi and 55/55 melanoma cases having lesional tissue present for p16, and 41/46 nevi and 53/55 melanoma cases having lesional tissue present for PRAME. Thirty-nine nodal nevi (88%) had >50% (score of 2-3) nuclear staining for p16. Meanwhile, none had >50% staining for PRAME. More than half (56%) of melanoma cases had <25% or complete loss (score 0) of nuclear staining for p16, while majority (95%) had >50% (score of 2-3) nuclear staining for PRAME. Using a cut-off value of 50%, (≤ 50% as negative and >50% as positive), PRAME had a sensitivity and specificity of 94% and 100%, respectively, in detecting metastatic melanoma, while p16 had a sensitivity and specificity of 89% and 65%, respectively, in detecting nodal nevi. PRAME showed significantly better discrimination (AUC = 0.97, 95% CI 0.94-1.00) than p16 (AUC = 0.77, 95% CI 0.69-0.85) for differentiating nodal nevi from nodal melanoma (p<0.001).

Figure 1 - 505

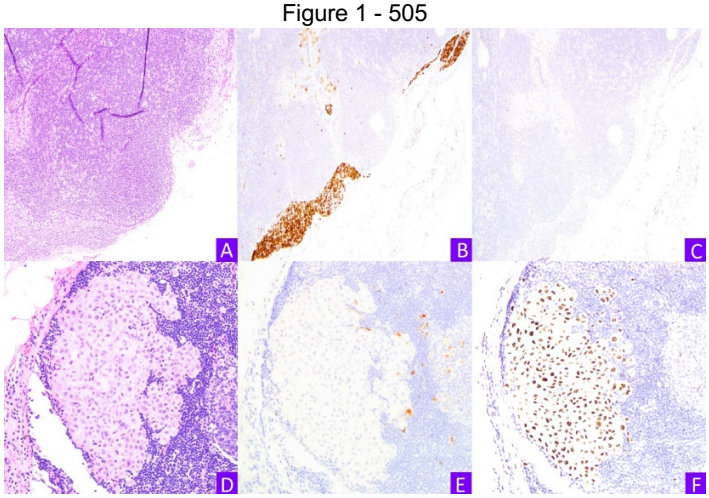

Conclusions: Our findings suggest that while both PRAME and p16 can be useful immunohistochemical stains in differentiating nodal nevi from nodal metastatic melanoma, PRAME is more accurate in discriminating between the two entities, with excellent sensitivity and specificity.

506 Understanding Clinical Responses to Immune Checkpoint Therapies Using a Novel Neoantigen-Rich Murine Melanoma Cell Model

Andreea Stancu[1], Lars Prestegarden[1], Hans Widlund[1]
[1]Brigham and Women's Hospital, Harvard Medical School, Boston, MA

Disclosures: Andreea Stancu: None; Lars Prestegarden: *Stock Ownership*, Cytovation; Hans Widlund: None

Background: Recent advances in the treatment management of malignant melanoma, including drugs that target the BRAF(V600E) melanoma oncogene and immune checkpoints inhibitors that unleash the immune system against the cancer, has dramatically improved the clinical course for many patients. However, only a fraction of patients achieves durable response from these treatments, and it has not

been yet well understood whom will benefit. Because there is a choice between therapies, informed decisions of whom to treat with what modality is key to improving outcomes and help develop combinatorial approaches. This is an outstanding quest which relies on improved in vivo models that faithfully recapitulate the clinical course. This work serves to characterize a highly immunogenic melanoma cell line that will support translational studies aimed at improved understanding of patient treatment responses.

Design: Recent advances in tumor genome sequencing have indicated that highly mutated tumors have a broad display of neoantigens that T cells readily detect and results with a therapeutic benefit from immune checkpoint therapies. For functional experiments there has been a lack of *in vivo* tumor models that genuinely recapitulates the meaningful responses seen in patients. The commonly used murine melanoma cells have a low level of immune infiltrates (Table 1).

Results: Through extending *in vitro* culture, our group has isolated a sub-clone from the SM1 primary mouse melanoma which we have termed SM1/X (SM1/eXtended culture) that readily engrafts as highly immune-infiltrated tumors in C57BL/6 mice. We have analyzed the response of established SM1/X tumors in C57BL/6 mice to combination immune checkpoint therapy, indicating profound treatment effects (Figure 1).

Cell line	Tumor type	Congenic mouse	Driver mutations	# non-synonymous mutations	Tumor Cd45+ cells
B16-BL6	Melanoma	C57BL/6	Unknown	398	5%
YUMM 1.7	Melanoma	C57BL/6	Braf(V600E);Pten^{null}; Cdkn2^{null}	371	17%
SM1/X	Melanoma	C57BL/6	BRAF(V600E)	1606	36%

Figure 1 - 506

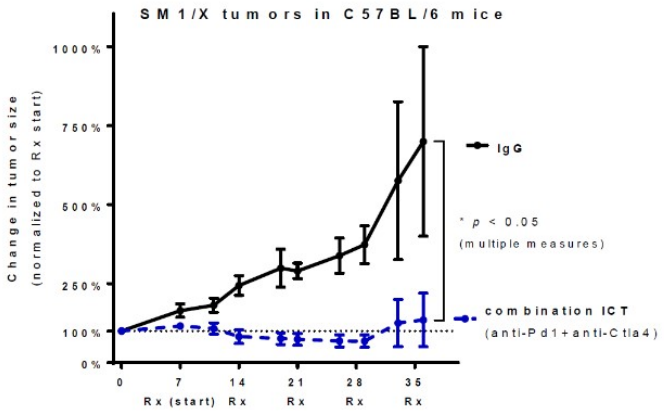

Figure 1 – Combination immune checkpoint therapy (anti-Pd1 [250µg] + anti-Ctla4[100µg]: weekly *i.p.*) against established subcutaneous SM1/X tumors [100mm^3@Rx start] leads to robust tumor control.

Conclusions: We identified a novel neoantigen-rich murine melanoma cell model that can help identify causal changes in the tumor immune components and provide a better understanding whom patients will benefit from immune checkpoint inhibitors treatment.

507 Immune-Related Pathologic Response (irPR) Scores in On-Treatment Biopsies from Anti-PD-1-Treated Patients Associates with Overall Survival and Immunotherapy-Driven Genomic Changes: A Validation Study

Julie Stein[1], Tricia Cottrell[2], Benjamin Green[3], Megan Wind-Rotolo[4], Evan Lipson[5], Janis Taube[1]
[1]Johns Hopkins University School of Medicine, Baltimore, MD, [2]Queen's University, Kingston, ON, [3]Johns Hopkins University, Seattle, WA, [4]Bristol-Myers Squibb, Lawrenceville, NJ, [5]Johns Hopkins University, Baltimore, MD

Disclosures: Julie Stein: None; Tricia Cottrell: None; Benjamin Green: None; Megan Wind-Rotolo: *Employee*, Bristol Myers-Squibb; *Employee*, Bristol Myers-Squibb; Evan Lipson: *Consultant*, Bristol-Myers Squibb; *Consultant*, Merck; *Consultant*, EMD

Serono; *Consultant*, Sanofi / Genzyme / Regeneron; *Grant or Research Support*, Bristol-Myers Squibb; Janis Taube: *Grant or Research Support*, Bristol Myers Squibb; *Advisory Board Member*, Bristol Myers Squibb; *Consultant*, Astra Zeneca; *Consultant*, Merck

Background: We previously demonstrated that immune-related pathologic response (irPR) scores significantly associated with overall survival (OS) in a discovery cohort of 51 patients (pts) with advanced melanoma receiving nivolumab on Arm 1 of CheckMate 038 (Stein et al. 2019, *Ann Oncol*). We now benchmark our scoring system against a genomic contraction assessment in these same pts. Moreover, we validate our previous findings using an independent cohort.

Design: We conducted pre- and on-treatment histologic (n=29 pairs, on-treatment taken median 3-4 wks) assessments from a validation cohort of pts with advanced melanoma receiving anti-PD-1 on Arms 3&4 of CheckMate 038 and pts treated as standard of care. irPR was scored on H&Es in a blinded fashion by two pathologists as previously described. Specifically, 0=no features of irPR (neovascularization, proliferative fibrosis, moderate-high tumor infiltrating lymphocytes, plasma cells, and lymphoid aggregates); 1=<3 co-localized features of irPR, or if more features are present, they are not co-localized; 2=$\geq$ 3 features of irPR are present but there is >10% residual viable tumor (RVT); and 3=$\geq$ 3 features of irPR are present and $\leq$10% RVT (major pathologic response on biopsy; MPR_{bx}). Additionally, genomic contraction/persistence for n=25 of the discovery cohort pts was available (Riaz et al, *Cell*, 2017), and this metric was tested against irPR scores.

Results: In the validation cohort, OS was significantly increased in pts with on-treatment irPR scores of 3 (MPR_{bx}), p=0.03, log-rank test, supporting the observations in the original discovery cohort. Additionally, there was a significant inverse correlation between on-treatment irPR score and net change in genomic assessment of tumor mutations (Pearson r, -0.75, p<0.0001).

Conclusions: irPR scores are associated with OS in an independent cohort of pts with advanced melanoma receiving anti-PD-1. Additionally, increased irPR scores are associated with immunotherapy-driven reduction in frequency of tumor somatic mutations, substantiating that irPR scoring reflects histologic features of immune-mediated tumor regression. Together, these findings lend support for further investigation of irPR scoring in prospective clinical studies as a potential biomarker of response to immunotherapy.

508 Porocarcinoma: A New Member of the NUTM1-rearranged Family

Todd Stevens[1], Carlos Prieto-Granada[1], Peter Pavlidakey[1], Diana Morlote[1], Jeffrey Swensen[2], Zoran Gatalica[2]
[1]The University of Alabama at Birmingham, Birmingham, AL, [2]Caris Life Sciences, Phoenix, AZ

Disclosures: Todd Stevens: None; Carlos Prieto-Granada: None; Peter Pavlidakey: None; Diana Morlote: None; Jeffrey Swensen: *Employee*, Caris Life Sciences; Zoran Gatalica: *Employee*, CARIS life sciences

Background: NUT carcinoma (NC), a lethal malignancy featuring fusions of the *NUTM1* gene (15q14) with various partners, most commonly *BRD4/3* and *NSD3,* typically arise in the lung, sinonasal tract, and mediastinum and feature primitive carcinoma with abrupt keratinization that can be diagnosed with a highly sensitive/specific NUT monoclonal antibody. Recognition of NC is important because many show a reprogrammed epigenome resulting in differentiation arrest that can potentially be reversed with bromodomain inhibitor therapy (BETi). Recently, the spectrum of *NUTM1*-rearranged neoplasia has been expanded to include soft tissue examples with sarcomatous morphology as well as primitive central nervous system tumors, etc. Poroid adnexal skin tumors are composed of a rather heterogenous group of lesions including hidracanthoma simplex, poromas, poroid hidradenomas and porocarcinomas. A recurrent molecular aberration aside from *HRAS* mutations was not known to occur in this group of lesions. However, a very recent report by Sekine et al described recurring *YAP1-NUTM1* fusions in both benign and malignant lesions in this poroid group.

Design: We subjected 10 cases of either classic porocarcinoma or adnexal carcinoma with porocarcinomatous features to NUT immunohistochemistry (IHC) using the C52B1 clone on a Leica Bond autostainer. 9 of these cases were subjected to gene fusion analysis by whole transcriptome sequencing (WTS) as well as mutational analysis by DNA next-generation sequencing (DNA NGS) (Caris Life Sciences).

Results: See Table 1 for results. 3 of the classic porocarcinomas showed diffuse nuclear labeling with NUT (Figure); 2 of these cases underwent WTS to reveal *YAP1-NUTM1* fusion; the third NUT-positive case has yet to be sequenced. WTS and NUT immunostaining of the remaining 7 cases failed to identify gene fusions or NUT expression, respectively.

Case	Diagnosis	Fusion	Pathogenic alterations by DNA NGS	NUT IHC	Age/Sex/Site
1	CP	*YAP1-NUTM1*	*CDKN2A* (p.E120*)	+	83/F/Foot
2	CP	*YAP1-NUTM1*	*MITF* (p.E318K)	+	59/F/Thigh
3	CP	NT	NT	+	51/M/Knee
4	CP	ND	QNS	-	81/M/Back
5	HGACPCF	ND	Amplifications of *CCND1* & *FGF3* *TP53* (p.Y236H) *BRCA2* (p.W1692fs) *AKT1* (p.E17K) *FGFR3* (p.G380R) *NSD1* (p.R2017W) *KMT2C* (p.Q3151*;p.R4478*) *KMT2D* (p.E865*)	-	82/F/Cheek
6	HGACPCF	ND	*p53* (p.R196*) *HRAS* (p.G13D) *TSC1* (p.E795*) *ASXL1* (p.R634*)	-	73/F/Cheek
7	HGACPCF	ND	*KMT2D* (p.Q3821*)	-	61/M/Lymph node metastasis
8	HGACPC and clear cell hidradenocarcinomatous features	ND	*NF1* (p.S1567*) *RB1* (p.Y813fs, p.Q217*) *TP53 (*p.R248W) *BRCA2* (p.R2099*) *KMT2C* (p.W4357*) *EP300* (c.4453-1G>A, p.S772*) *KDR* (p.R1032Q)	-	48/F/Axilla
9	Porocarcinoma in situ, transected	ND	*TP53* (p.H179N) *PTEN* (p.K267fs) *ASXL1* (p.G645fs) *KDM6A* (p.N634fs)	-	61/F/Foot
10	Porocarcinoma in situ, transected	ND	QNS	-	69/M/Foot

CP: Classic porocarcinoma; HGACPCF: high-grade adnexal carcinoma with porocarcinomatous features; ND: Not detected; NT: Not tested; QNS: DNA quantity not sufficient; F: Female; M: Male

Figure 1 - 508

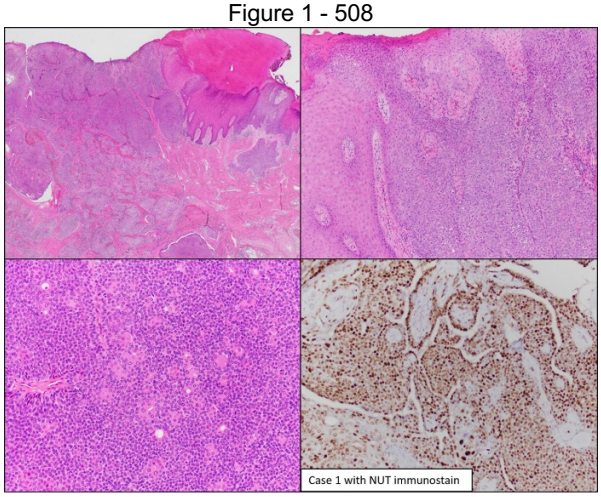

Conclusions: Porocarcinoma, in particular those with classic poroid morphology with cuticular cells forming morules, represent a new member of the growing *NUTM1*-rearranged neoplasia family. NUT immunohistochemistry and/or gene fusion analysis may prove useful in

distinguishing porocarcinoma from its mimics. Functional studies to determine if the *YAP1-NUTM1* fused tumors are susceptible to BETi are needed.

509 SATB2 is Frequently Expressed by Melanoma: A Diagnostic Pitfall

Jon Thomason[1], Ilham Farhat[1], Felipe Nör[2], Andrew Bellizzi[1], Sarag Boukhar[1]
[1]University of Iowa Hospitals and Clinics, Iowa City, IA, [2]University of Iowa College of Dentistry, Iowa City, IA

Disclosures: Jon Thomason: None; Ilham Farhat: None; Felipe Nör: None; Andrew Bellizzi: None; Sarag Boukhar: None

Background: The special AT-rich sequence binding-protein (SATB2) is a DNA-binding protein involved in chromatin remodeling and epigenetic regulation. SATB2 immunohistochemistry (IHC) is frequently used as a sensitive and specific marker for colorectal differentiation in carcinomas of unknown origin. Recent investigations have also identified frequent expression in osteosarcoma, Merkel cell carcinoma, and *BCOR*-rearranged sarcoma. In the past year we have seen two metastatic melanomas in which moderately strong SATB2-positivity caused significant diagnostic confusion. SATB2 expression in melanoma has not been systematically studied.

Design: SATB2, CDX2, and BRAF V600E (clone VE1) IHC was performed on tissue microarrays (TMAs) from 273 melanoma cases (ascertained between 2010 and 2017) from 248 patients (141 male, 107 female) with an average age of 68 (24 to 105).These included 137 primaries (90% skin, 5% sinonasal cavity, 5% other mucosal sites) and 136 metastases (32% lymph node, 18% brain/dura, 14% bone/soft tissue, 36% other). SATB2 and CDX2 IHC was assessed for intensity (0-3+) and extent (0-100%) of staining, and an H-score was calculated. BRAF V600E IHC was scored as positive or negative. Fisher's exact and Mann Whitney tests were used with $p<0.05$ considered significant.

Results: SATB2-positivity was identified in 44% of 273 cases with a mean/median and range of H-scores of 37/23 and 2-193, while CDX2 was uniformly negative. BRAF V600E-positivity was noted in 28% of tumors. SATB2-positivity was not significantly associated with any of the clinicopathologic variables (all $p>0.05$). Detailed data are presented in the Result Table. Among cutaneous primaries, SATB2 was expressed at similar frequencies across subtypes: 37% of 103 nodular, 59% of 56 superficial spreading, 58% of 12 lentigo maligna, 54% of 13 desmoplastic, 20% of 6 acral lentiginous, 40% of 5 spindle cell, 100% of 1 nevoid, and 40% of 77 not otherwise specified.

Association of SATB2-Positivity to Clinicopathologic Variables

	SATB2+ n (%)	p-value	H-score Mean, (Median)	p-value
Overall	119 (44)		37 (23) range: 2-193	
Men	60 (39)	0.086	36 (22)	0.97
Women	95 (50)		38 (27)	
Primary	57 (43)	0.9	40 (30)	0.13
Metastasis	62 (44)		34 (7)	
BRAF Positive	36 (47)	0.5	47 (30)	0.28
BRAF Negative	83 (42)		33 (23)	
Cutaneous	101 (43)	0.7	38 (23)	0.6
Non-cutaneous	18 (46)		34 (30)	

Conclusions: 1- SATB2 IHC is frequently (44%) positive in melanoma, typically of mild-to-moderate though occasionally of strong intensity, and, thus, should be used with caution in characterizing tumors of unknown origin.

2- Melanoma should always be considered in the differential diagnosis of a SATB2-positive undifferentiated malignancy, especially in a broad-spectrum epithelial marker-negative tumor.

510 Comprehensive Genomic Profiling (CGP) of Spindle Cell Melanoma Reveals Potential Therapeutic Implications and Significant Genomic Differences from Malignant Peripheral Nerve Sheath Tumor

Julie Tse[1], Erik Williams[1], Dean Pavlick[2], Julia Elvin[2], Jo-Anne Vergilio[2], Douglas Lin[2], Keith Killian[2], Shakti Ramkissoon[3], Eric Severson[3], Amanda Hemmerich[3], Claire Edgerly[3], Daniel Duncan[3], Richard Huang[4], Naomi Lynn Ferguson[3], Natalie Danziger[5], Siraj Ali[6], Jon Chung[2], Russell Madison[2], Alexa Schrock[2], Venkataprasanth Reddy[2], Jeffrey Ross[7]
[1]Boston, MA, [2]Foundation Medicine, Inc., Cambridge, MA, [3]Foundation Medicine, Inc., Morrisville, NC, [4]Foundation Medicine, Inc., Cary, NC, [5]Foundation Medicine, Inc., Somerville, MA, [6]Cambridge, MA, [7]Upstate Medical University, Syracuse, NY

Disclosures: Julie Tse: *Employee*, Foundation Medicine, Inc.; *Consultant*, Pathology Watch, LLC.; Erik Williams: *Stock Ownership*, F. Hoffman La Roche, Ltd.; *Employee*, Foundation Medicine, Inc.; Dean Pavlick: None; Julia Elvin: *Employee*, Foundation

Medicine; *Employee*, Hoffman La Roche; Jo-Anne Vergilio: *Employee*, Foundation Medicine, Inc; *Employee*, Foundation Medicine, Inc; Douglas Lin: *Employee*, Foundation Medicine; Keith Killian: *Employee*, FMI; Shakti Ramkissoon: *Employee*, Foundation Medicine/Roche; Eric Severson: *Employee*, Foundation Medicine; Amanda Hemmerich: *Employee*, Foundation Medicine, Inc; Claire Edgerly: *Employee*, Foundation Medicine, Inc.; Daniel Duncan: *Employee*, Foundation Medicine; Richard Huang: *Employee*, Roche/Foundation Medicine; Naomi Lynn Ferguson: *Employee*, Foundation Medicine; Natalie Danziger: *Employee*, Foundation Medicine Incorporated; Siraj Ali: *Employee*, Foundation Medicine; *Advisory Board Member*, INcysus Therapeutics; *Consultant*, Takeda; Jon Chung: *Employee*, Foundation Medicine; *Stock Ownership*, Roche; Russell Madison: *Employee*, Foundation Medicine Inc.; *Stock Ownership*, Roche; Alexa Schrock: *Employee*, Foundation Medicine; *Stock Ownership*, Roche; Venkataprasanth Reddy: *Employee*, Foundation Medicine; Jeffrey Ross: *Employee*, Foundation Medicine

Background: Spindle cell melanoma (SCM) has unique clinical and pathologic features compared to other variants of cutaneous melanoma (MM). SCM, including desmoplastic melanoma, comprises is a rare variant of MM, but is unusual with absence of immunostaining for most melanocytic markers and a higher propensity for local recurrence. SCM is often pathologically and clinically indistinguishable from malignant peripheral nerve sheath tumor (MPNST), a sarcoma arising from perineural connective tissue. We used comparative CGP of SCM and MPNST to evaluate for distinguishing molecular differences. We also investigated genomic alterations (GA) in SCM to identify potential therapeutic implications.

Design: Our database contained 77 SCM and 337 MPNST which had underwent hybrid capture-based CGP using a panel of 300+ genes. Tumor mutational burden (TMB, mutations per megabase) was calculated from 1.1Mbp of sequenced DNA and microsatellite stability (MSI) was determined on the basis of 114 homopolymeric loci. The results were analyzed for all classes of GA. Patient demographic data were collected.

Results: SCM patients had a mean age of 68 years. The most common GA occurred in the *TERT* promoter (*TERTp*) (74%). Other GA were in *NF1* (66%), *TP53* (62%), *CDK2NA* (54%), *GRM3* (15%), and *CDKN2B* (15%). Median TMB was 27.7 and 62% cases had a high TMB >20. Frequency of *BRAF* GA was reduced compared to classic MM, but significantly greater than MPNST (p<0.05%).

Compared to SCM, MPNST patients were significantly younger with a mean age of 42 (p <0.05). The most commonly altered genes were *CDKN2A* (60%), *NF1* (55%), *CDKN2B* (41%), *TP53* (26%), and *SUZ12* (19%); *TERT*p GA were not detected (0%). Median TMB of 3.2 was significantly lower (p<0.05) and only 7.7% cases had TMB >20. MSI-high was not detected (Table 1).

Table 1. Summary of comparative CGP in spindle cell melanoma vs. malignant peripheral nerve sheath tumor

	SCM	**MPNST**	***P* value**
Number of cases	77	337	
Mean age in years	68	42	***p < 0.05***
Male to female ratio	2:1	2:1	***p < 0.05***
Comparison of selected known or likely pathogenic GA *TERTp* *NF1* *TP53* *CDKN2A* *CDKN2B* loss *NRAS* *BRAF* *NF2*	74% 66% 62% 54% 15% 14% 13% 11%	0% 55% 26% 60% 41% 2% 4% 7%	***p < 0.05*** *p = 0.13* ***p < 0.05*** *p = 0.44* ***p < 0.05*** ***p < 0.05*** ***p < 0.05*** *p = 0.24*
Other commonly known or likely pathogenic GA	*GRM3* 15% *CBL* 14% *HGF* 15% *ATM* 11% *ERBB4* 11%	*SUZ12* 19% *PTEN* 9% *EED* 8% *MDM2* 8%	
Mean TMB (mut/Mb)	56.8	8.2	***p < 0.05***
Median TMB (mut/Mb) (range)	27.7 (0.9 – 314.1)	3.2 (0.8 – 253.5)	***p < 0.05***
TMB >20 mut/Mb	62.3%	7.7%	***p < 0.05***
MSI-High	0%	0%	

Conclusions: SCM is an aggressive malignancy difficult to distinguish from MPNST, but accurate identification is critical to clinical management. Comparative CGP revealed two significant genomic differences: 1) high frequency of *TERTp* mutations in SCM with absence in MPNST and 2) high TMB in SCM. Along with histopathologic, clinical, and radiological data, our results suggest CGP is valuable to the accurate identification of SCM. In addition, relatively increased frequency of high TMB in SCM compared to overall MM (62% vs. 34%) and GA in *NF1* (66% vs. 19%) may predict more favorable response to immunotherapies and reduced sensitivity to *MEK* inhibition in patients with this variant of MM.

511 Real-Time Molecular Detection of Basal Cell Carcinoma with Rapid Evaporative Ionization Mass Spectrometry

Kaitlin Vanderbeck[1], Natasja Janssen[2], Martin Kaufmann[2], Alice Santilli[2], Kevin Ren[3], David Berman[2], Gabor Fichtinger[2], Parvin Mousavi[2], John Rudan[1], Douglas McKay[1], Ami Wang[4]
[1]Queen's University/Kingston Health Sciences Centre, Kingston, ON, [2]Queen's University, Kingston, ON, [3]Queen's University/ Kingston Health Sciences Centre, Kingston, ON, [4]Kingston, ON

Disclosures: Kaitlin Vanderbeck: None; Natasja Janssen: None; Martin Kaufmann: None; Alice Santilli: None; Kevin Ren: None; David Berman: None; Gabor Fichtinger: None; Parvin Mousavi: None; John Rudan: None; Douglas McKay: None; Ami Wang: None

Background: Basal Cell Carcinoma (BCC) is the most common type of skin cancer with histologic subtypes associated with locally aggressive behavior and high risk of recurrence. Typically, BCCs are managed by complete surgical excision followed by histologic confirmation of diagnosis and margin status. Incomplete tumor removal and surgical revision may be disfiguring and cause significant stress for patients. Further, with the rising incidence of BCCs, appropriate treatment represents an increasing burden on the healthcare system. Rapid Evaporative Ionization Mass Spectrometry (REIMS) has recently emerged as a revolutionary real-time tissue identification technique based on the analysis of cell particles within the smoke released during electrosurgical tissue dissection. In this pilot study, we aim to evaluate the feasibility and accuracy of REIMS for intra-operative molecular tissue characterization during BCC resection.

Design: Fresh specimens were obtained from patients in an out-patient setting. REIMS spectra were obtained by burning BCC and benign skin (Figure 1). The specimen and burnt areas were analyzed by REIMS and examined by a dermatopathologist for histopathologic validation. Mass spectra from 43 specimens acquired from 36 confirmed BCC cases were subjected to principal component analysis (PCA) and linear discriminant analysis (LDA) to create a tissue characterization model using Abstract Model Builder (Waters Corp.).

Results: PCA analysis based on a range of ions revealed a distinct signature for the two tissue types (Figure 2). Of note, several spectra contained a mixture of tissue types when analyzing small specimens. With these mixed spectra excluded, a PCA/LDA-based tissue characterization model demonstrated that BCC and benign skin were correctly classified in 88 and 80% of cases respectively, based on cross-validation.

Figure 1 - 511

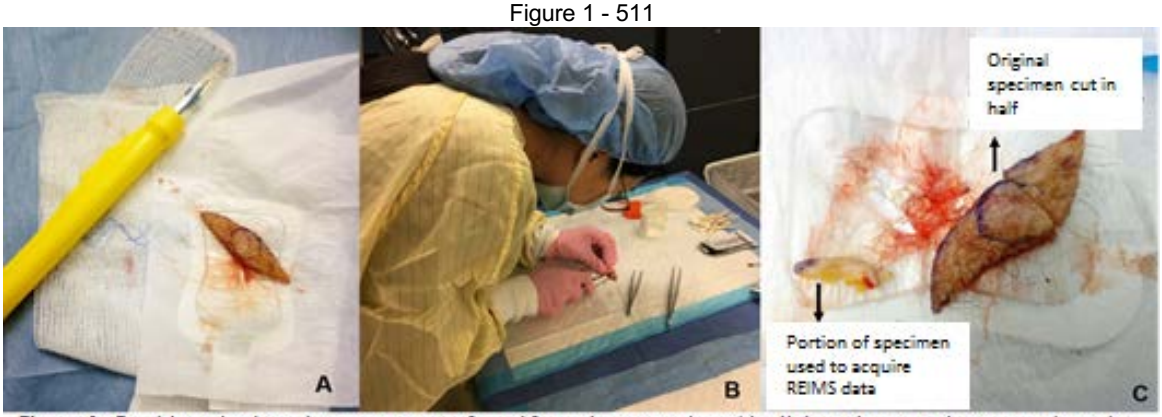

Figure 1: Freshly excised specimens were transferred from the out-patient skin clinic to the operating room where the mobile mass spectrometer was positioned (A). The dermatopathologist cut a thin slice of tissue (B), areas containing BCC and surrounding benign skin and adipose tissue were identified and burned (C).

Figure 2 - 511

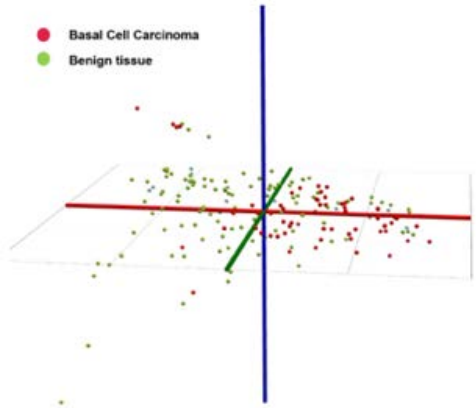

Figure 2: Spectra were obtained from BCC and normal benign tissue. Each data point represents one acquired mass spectra.

Conclusions: While our results demonstrate the potential utility of REIMS in real-time tissue characterization during BCC resection, diagnostic accuracy must be further validated before REIMS-based margin assessment is introduced into clinical practice. We anticipate that both specific pathologic validation of the spectra used for model-building and the analysis of larger samples where cross-contamination of spectra is less likely will improve diagnostic accuracy of our BCC recognition model. Intraoperative BCC recognition may lead to improved intra-operative evaluation of resection margins and better clinical outcomes for patients.

512 Histopathological Risk Factors in Melanoma: A Retrospective Cohort Study in Argentinian Population

Victoria Volonteri[1], Adriana Rinflerch[1], Melina Pol[2], Cecilia Roude[1], Vanina Pagotto[1], Gaston Galimberti[1], Luis Mazzuoccolo[2], Hernan Garcia-Rivello[3]

[1]Hospital Italiano de Buenos Aires, Capital Federal, Ciudad Autónoma de Buenos Aires, Argentina, [2]Hospital Italiano de Buenos Aires, Buenos Aires, Argentina, [3]Hospital Italiano Bs As, IMTIB, IUHI DA Patologia, Buenos Aires, Argentina

Disclosures: Victoria Volonteri: None; Adriana Rinflerch: None; Melina Pol: None; Cecilia Roude: None; Vanina Pagotto: None; Gaston Galimberti: None; Luis Mazzuoccolo: None; Hernan Garcia-Rivello: None

Background: Melanoma is a malignant neoplasia of melanocytes with a 5-year survival rate of only 15-20% once the tumor has metastasized to distant tissue. Over the last decades the incidence of Melanoma has been increasing. The prognosis of melanoma depends on the stage in which it was diagnosed, which mainly takes into account histological characteristics in addition to other factors. In our country there are no official statistics regarding melanoma.

Design: A retrospective cohort study was carried out, including population with microscopically confirmed invasive cutaneous melanoma in our hospital between July 2006 and June 2016. We included patients with primary diagnosis of invasive cutaneous melanoma and excluded those with just in situ melanoma, no follow-up information or a primary report of metastasis of melanoma. Cases were categorized by age at diagnosis, gender, anatomic site, histologic subtype, Breslow depth, presence of ulceration, sentinel lymph node status and presence of distant metastasis. Patient follow-up and survival were also evaluated.

Results: 504 cases of invasive cutaneous melanoma were identified in the database. Of these patients, 52.8% were men (n = 266), and 47.2% were women (n = 238). When divided by age 72.02% corresponded to the ≥51 years old population. In males, 53.76% of the tumors were localized on the trunk. In females, 47.06% were localized on upper and lower extremities, followed by 33.61% on the trunk (Table 1). When sorting by Breslow's depth, those with >4 mm thickness usually presented ulceration at diagnosis, a higher mitotic rate and sentinel lymph node positivity. (Graphic 1). The superficial spreading histological subtype was the most common histology in ≤30 year old patients (75%) and nodular in group age ≥51 (36.36%). Regarding the cumulative incidence of metastasis and survival rates, 196 patient were included, leaving those without a 5 year follow-up out. Considering Breslow category, there were differences in cumulative incidence of metastasis. Patients with Breslow >2mm had a cumulative incidence at 5 year of 46% while for patients with Breslow <2 was 8% (Graphic 2). The overall survival rate was 79% at 5 years. Factor associated to survival were age, sex and Breslow.

Table 1:

	AGE GROUP (AT DIAGNOSIS)		
	≤30	31-50	≥51
	3.18 (n=16)	24.8 (n=125)	72.02 (n=363)
GENDER			
Male	25 (4)	49.6 (62)	55.1 (200)
Female	75 (12)	50.4 (63)	44.9 (163)
SUBTYPE			
Superficial spreading	75 (12)	64.8 (81)	50.96 (185)
Nodular	12.5 (2)	24.8 (31)	36.36 (132)
Malignant lentigo	0 (0)	0 (0)	6.06 (22)
Acral lentiginous	0 (0)	0.8 (1)	1.65 (6)
Other	12.5 (2)	9.6 (12)	4.96 (18)
SLN			
Positive	16.67 (1)	18.84 (13)	24.48 (47)
Negative	83.33 (5)	81.16 (56)	71.51 (118)
METASTASIS			
Yes	0 (0)	13.6 (17)	18.73 (68)
No	100 (16)	86.4 (108)	81.27 (295)
BRESLOW			
0.01-1.00	62.5 (10)	56.8 (71)	42.15 (153)
1.01 - 2	25 (4)	24 (30)	23.7 (86)
2.01 - 3	12.5 (2)	8.8 (11)	9.09 (33)
3.01 - 4	0 (0)	5.6 (7)	8.81 (32)
>4.1	0 (0)	4.8 (6)	16.25 (59)

Figure 1 - 512

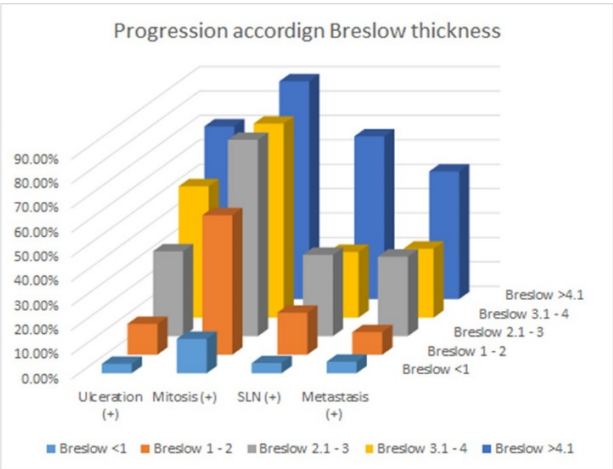

Figure 2 - 512

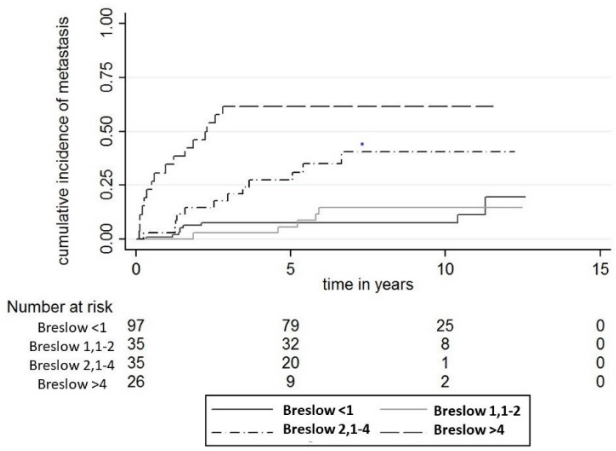

Conclusions: This retrospective study allowed us to describe the epidemiologic pattern of melanoma survival and prognostic factors of importance in our Hospital divided by age group. We found our data was similar to previously published bibliograph.

513 Clinical, Histopathologic, and Molecular Profile of RAF1-Fusion Positive Melanoma

Erik Williams[1], Nikunj Shah[2], Vincent Miller[2], Dean Pavlick[2], Jo-Anne Vergilio[2], Meagan Montesion[2], Radwa Sharaf[2], Keith Killian[2], Natalie Danziger[3], Julia Elvin[2], Douglas Lin[2], Siraj Ali[4], Julie Tse[1], Mark Mochel[5]
[1]Boston, MA, [2]Foundation Medicine, Inc., Cambridge, MA, [3]Foundation Medicine, Inc., Somerville, MA, [4]Cambridge, MA, [5]Virginia Commonwealth University School of Medicine, Richmond, VA

Disclosures: Erik Williams: *Stock Ownership*, F. HoffmanLa Roche, Ltd.; *Employee*, Foundation Medicine, Inc.; Nikunj Shah: None; Vincent Miller: *Employee*, Foundation Medicine / Roche; *Stock Ownership*, Foundation Medicine / Roche; *Advisory Board Member*, Revolution Medicines; *Stock Ownership*, Revolution Medicines; Dean Pavlick: *Employee*, Foundation Medicine; *Stock Ownership*, F. Hoffmann-La Roche AG; Jo-Anne Vergilio: *Employee*, Foundation Medicine, Inc; *Employee*, Foundation Medicine, Inc; Meagan Montesion: *Employee*, Foundation Medicine; *Stock Ownership*, Roche; Radwa Sharaf: *Employee*, Foundation Medicine; Keith Killian: *Employee*, FMI; Natalie Danziger: *Employee*, Foundation Medicine Incorporated; Julia Elvin: *Employee*, Foundation Medicine, Inc; *Employee*, Hoffman La Roche; Douglas Lin: *Employee*, Foundation Medicine; Siraj Ali: *Employee*, Foundation Medicine; *Advisory Board Member*, Incysus Therapeutics; *Consultant*, Takeda; Julie Tse: *Employee*, Foundation Medicine, Inc.; *Consultant*, Pathology Watch, LLC.; Mark Mochel: None

Background: Activating mutations in the MAPK pathway, particularly in *BRAF* and *NRAS*, occur frequently in melanoma. Activating *RAF1* structural variants have also been reported in a subset of melanoma cases, and rare case reports have identified a marked response of *RAF1*-fusion-positive cases to MEK inhibitor therapy.

Design: Our case archive of clinical samples that had undergone comprehensive genomic profiling using a hybrid capture based DNA sequencing platform was searched for melanoma with known or likely activating structural variants in *RAF1.* Tumor mutational burden (TMB, mutations/Mb) was determined on 0.8-1.1 Mbp of sequenced DNA and microsatellite instability (MSI) was determined on 114 loci. Pathology reports and histopathology were reviewed. Patient clinical data was collected.

Results: From a series of 7900 melanomas, 42 cases (0.5%) featured gene fusions that created known or likely activating structural variants in *RAF1*. 5' rearrangement partners were predominantly intrachromosomal (n=18), and recurrent partners included *MAP4* (n=4), *CTNNA1* (n=3), *LRCH3* (n=2), *GOLGA4* (n=2), *CTDSPL* (n=2), and *PRKAR2A* (n=2). *RAF1* breakpoints occurred in intron 7 (n=34), intron 9 (n=4), intron 5 (n=2), and intron 6 (n=2). Median age was 62 years and 57% were male. Cases consisted of 9 primary tumors and 33 metastases (14 regional lymph nodes and 19 distant sites). 41 cases were skin primary, while one case was mucosal (anal) primary. The majority (n=41) demonstrated epithelioid-type histology; a single desmoplastic melanoma was identified. 98% (n=41) were wild-type for *BRAF*, *NRAS*, and *NF1* genomic alterations ("triple wild-type") vs. 26% of the melanoma cohort without *RAF1* fusion. The most frequently mutated genes besides *RAF1* were *TERTp* (62%), *CDKN2A* (62%), *TP53* (12%), and *PTEN* (10%). Median TMB was 9.8 (range 0-57.4, 48% >10, 17% >20), significantly lower than the primary skin and anus melanoma cohort without *RAF1* fusion (median TMB=13.8, 54% >10, 37% >20; p=0.04, unpaired t test). All cases tested were MSI stable.

Conclusions: *RAF1* fusion represents a significant subset of triple-wild-type melanoma (2% of triple-wild-type melanoma, overall). Recurrent fusion partners and *RAF1* breakpoints were present, and histologic findings were uniform. Frequent accompanying mutations

in *TERTp* and *CDKN2A* were identified, typical for skin primary melanoma, but TMB was significantly lower. Our findings provide compelling rationale for comprehensive genomic profiling of melanoma to more fully inform therapeutic options.

514 Increased mRNA Level of Neurogenic Locus Notch Homolog Protein 4 Associates with Chemoresistance and Conveys Poor Prognosis in Melanoma

Lijun Xue[1], Justin Kerstetter[1]
[1]*Loma Linda University Medical Center, Loma Linda, CA*

Disclosures: Lijun Xue: None; Justin Kerstetter: None

Background: Notch signaling, one of the most activated pathways in cancer cells, contributes the cancer metastasis. Neurogenic locus notch homolog protein 4 (NOTCH4) encodes a transmembrane protein with epidermal growth factor homology. The role of NOTCH4 in melanoma is not known.

Design: The human melanoma gene expression datasets with survival information, including TCGA(n-539), GSE65904(n=214), MTAB4725(n=204), and GSE54467(n=79), were obtained from TCGA and GEO databases. The hazard ratio (HR) was estimated by using Cox proportional model. The meta-analysis, pooled analysis, and stratification analysis were conducted to reduce biases and confounders. In stratification analysis, the HRs of chemotherapy for melanoma in subgroups of gene-high (HR-h) and gene-low (HR-l) were calculated for each gene in TCGA dataset. The TNM stage of melanoma was taken considered to adjust the HRs. The ratio of HR-h/HR-l was considered as resistance index (RI).

Results: Those genes having higher RI (larger or equal to 3) were considered as chemoresistance genes. There are 15 chemoresistance genes selected in this analysis. The prognostic values of these genes were also examed by using meta-analysis and pooled analysis. Among these 15 genes, the neurogenic locus notch homolog protein 4 (NOTCH4) not only impacted the efficacy of chemotherapy, but also significantly affected patient's survival in melanoma. The HRs of chemotherapy (yes vs. no) were 0.548 (95% CI 0.33-0.90) and 1.59 (95% CI 1.01-2.51) in subgroups of NOTCH4_low and NOTCH4_high, respectively. The RI of NOTH4 gene was 3.11. This result suggested that chemotherapy could significantly reduce the relative risk of death in NOTCH4_low melanoma patients, but it could significantly increase the risk of death in NOTCH4_high subgroup. Further meta-analysis with four gene expression datasets indicated that the HR of NOTCH4 (high-vs low) on melanoma was 1.15 (95% 1.01-1.32, p=0.033). The gene set enrichment analysis and protein-protein interaction analysis revealed that expression of NOTCH4 could significantly enrich the molecular functions of transcription regulator activity, RNA polymerase II general transcription initiation factor activity.

Figure 1 - 514

Figure 1

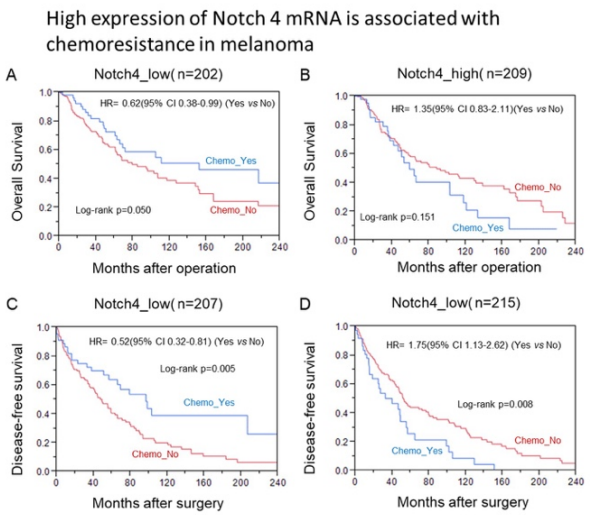

Figure 2 - 514

Figure 2

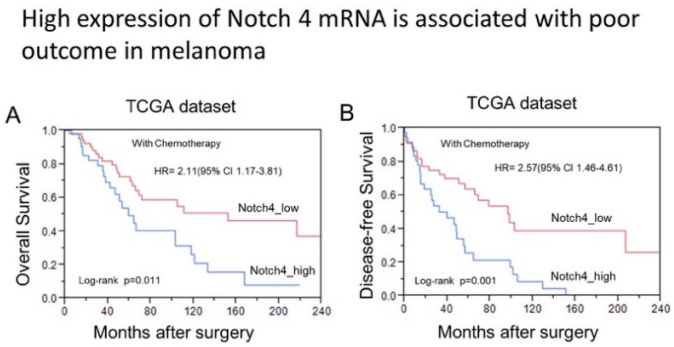

Conclusions: High expression of NOTCH4 mRNA enhanced the chemoresistance through modulating transcription activity in melanoma. It could be served as the prognostic and therapeutic biomarker for melanoma. Inhibitor targeting NOTCH4 might improve chemotherapy efficacy and prolong the survival time for melanoma patients.

515 Epigenetic Marker Expression is of Limited Diagnostic Utility in Spitzoid Melanocytic Neoplasms

Stephanie Yagi[1], Bonnie Balzer[1], David Frishberg[2], Wonwoo Shon[1]
[1]Cedars-Sinai Medical Center, Los Angeles, CA, [2]Cedars-Sinai Medical Center, West Hollywood, CA

Disclosures: Stephanie Yagi: None; Bonnie Balzer: None; David Frishberg: None; Wonwoo Shon: None

Background: Spitzoid melanocytic neoplasms, including Spitz nevi, atypical Spitz tumors, and Spitzoid melanoma, often present many challenges in dermatopathology practice. Reduced level of epigenetic marker 5-Hydroxymethylcytosine (5-hmC) has been reported to be a common event in melanoma, and immunohistochemistry for 5-hmC has been shown to be useful in evaluating problematic melanocytic lesions. However, we recently encountered a loss of 5-hmC expression in several examples of unequivocal Spitz nevus.

Design: Formalin-fixed, paraffin-embedded whole tissue sections from 12 Spitzoid melanocytic lesions (10 conventional Spitz nevi, 1 desmoplastic intradermal Spitz nevus, and 1 BAP1-deficient nevus) were retrieved from our surgical pathology archive. Representative hematoxylin and eosin-stained slides were re-reviewed for each case to confirm the diagnosis. In all cases, nuclear 5-hmC (brown chromogen) and cytoplasmic Melan-A Red (red chromogen) double immunohistochemical staining was performed. Nuclear 5-mC (red chromogen) was also evaluated in 11 cases of Spitz nevus.

Results: Loss of 5-hmC expression was seen in all cases of conventional Spitz nevus (complete loss: 4 cases; partial loss: 6 cases). Both the desmoplastic intradermal Spitz and BAP1-deficient nevus showed a diffuse and strong nuclear expression of 5-hmC. All evaluated cases revealed obvious retention of 5-mC nuclear staining.

Conclusions: In contrast to prior studies, significant loss of 5-hmC expression is not restricted to melanomas and borderline melanocytic lesions but can also be found in benign Spitz nevi. Thus, caution is warranted when using this epigenetic marker for evaluation of Spitzoid melanocytic neoplasms. Because the loss of 5-hmC was not accompanied by a comparable decrease in 5-mC level, it is conceivable that the loss of 5-hmC in conventional Spitz nevi reflects a defect in the Ten-eleven Translocation enzyme-mediated conversion.

516 BAP1-Inactivated Melanocytic Tumors Demonstrate Prominent Centrosome Amplification and Associated Loss of Primary Cilia

Julia Ye[1], Kathleen Sheahon[1], Philip LeBoit[1], Timothy McCalmont[1], Ursula Lang[2]
[1]University of California San Francisco, San Francisco, CA, [2]San Francisco, CA

Disclosures: Julia Ye: None; Kathleen Sheahon: None; Philip LeBoit: None; Timothy McCalmont: None; Ursula Lang: None

Background: BRCA1-associated protein 1 (BAP1) is a tumor suppressor whose loss has been associated with a number of malignancies, including uveal melanoma, mesothelioma, melanoma, and renal cell carcinoma, which together comprise the BAP1 tumor predisposition syndrome. The primary cilium is a nearly ubiquitous cell surface organelle with roles in signal transduction and links to the cell cycle. Prior work has demonstrated primary cilia loss in BAP1-inactivated melanocytic tumors, a characteristic that differentiates melanoma, which fail to ciliate, from melanocytic nevi, which retain primary cilia. Studies in breast cancer and renal cell carcinoma cell lines have shown that BAP1 is involved in centrosome and mitotic spindle formation, while BAP1 loss is associated with mitotic abnormalities (Zarrizi et al., 2014; Peng et al., 2015). As the formation of the primary cilia begins on the mother centriole, we investigated the connection between the presence of primary cilia and centrosome status in BAP1-inactivated melanocytic tumors.

Design: We collected 14 cases of melanocytic tumors with BAP1 inactivation demonstrated by immunohistochemistry. We performed immunofluorescence staining for SOX-10 to highlight melanocytes, gamma-Tubulin to identify centrioles, and acetylated alpha-Tubulin to detect the ciliary axoneme. Using fluorescence microscopy, we calculated the ciliation index (C.I., percentage of melanocytes with a primary cilium). Additionally, we counted the number of melanocytes containing more than 2 centrioles (centrosome amplification).

Results: BAP1-inactivated melanocytic tumors display decreased cilia formation (C.I. range 0-31%; average 9%, SD 9.5%), consistent with prior data. These tumors also demonstrate extensive dysregulation in centrosome formation, with an average of 12% (SD 7%) of melanocytes containing more than 2 centrioles.

Conclusions: These data suggest that centrosome amplification could be a mechanism by which primary cilia are lost in BAP1-inactivated melanocytic tumors. Further work will examine whether abnormalities in primary cilia and centrosomes are present in other BAP1-inactviated tumors, such as mesothelioma and renal cell carcinoma. The results of these studies could help elucidate how centrosome and cilia formation are connected to the role of BAP1 in genomic stability, cell cycle progression, mitotic spindle formation, and chromosomal stability.

517 Proliferating Pilar Tumors: Could Immunohistochemistry be Helpful to Differ Benign and Malignant Forms?

Pelin Yildiz[1], Ovgu Aydin Ulgen[2], Cansu Yol[3], Cuyan Demirkesen[4]
[1]Bezmialem Vakif University, Medical Faculty, Istanbul, Fatih, Turkey, [2]Istanbul University-Cerrahpasa, Cerrahpasa Medical Faculty, Istanbul, Turkey, [3]Istanbul University-Cerrahpasa, Cerrahpasa Medical Faculty, Istanbul, Fatih, Turkey, [4]Acibadem University School of Medicine, Istanbul, Kadikoy, Turkey

Disclosures: Pelin Yildiz: None; Ovgu Aydin Ulgen: None; Cansu Yol: None; Cuyan Demirkesen: None

Background: Proliferating Pilar Tumors (PPTs) follicular outer root sheath derived tumors, having trichilemmal type of keratinization with epithelial proliferation. Most of them have a benign course. According to the review of Folpe et al. the malignant form has a combination of this features: rapid growth, diameter>5 cm, infiltrative growth pattern, significant cytologic atypia with mitotic activity and the presence of atypical mitotic figures, There is a debate to differentiate benign and malignant forms. This may be the result of adversity in the usage of these criteria and incompatible clinical behavior of the tumor with histological features. In literature, some immunohistochemical (IHC) stains were suggested to help for the differentiation of benign and malignant forms. In our study, Ki67, p27 and p53 stains were applied to discuss the relationship between these markers staining quantification intensity and tumoral behavioral pattern as a support to solve this dilemma.

Design: The study includes 11 benign, 9 malignant PPTs, between January 2013-2019. After reviewing slides, Ki67, p27 and p53 immunostains were applied. The staining intensity(strong, moderate, weak and negative), positive cell numbers and marker indexes(%) were scored using an image analysis software application-Virasoft.

Results: Overall, there was no association between Ki67 and p53 staining density and histopathological features. When strong and moderate p27 positive cell numbers were counted, a statistically significant difference was found between benign and malignant tumors(p=0.030). The percentage of strong and moderate stained cells was 37.9 ± 22.5% in the benign and 14.5 ± 18% in the malignant group.

Conclusions: In literature p53, Ki67 and p27 have been tried solely or combined with other markers to determine whether any panel of stains can help to distinguish benign/malignant PPTs. Our study includes the largest group of patients to whom this 3 stain combination has been applied so far. We found that there is no significant relationship between Ki67 and p53 indexes and tumoral subclassification. Loss of

p27, have been related to aggressive behavior in some tumors. A statistically significant difference was found between our benign and malignant PPTs. In literature, few malignant PPTs were reported and still poses diagnostic challenge. Immunohistochemistry may play an important role in supporting diagnosis in future. Hopefully, our study would be a step for further studies to form an IHC panel for routine usage.

518 Gene Expression Profile of the Skin in the Keratin 15-Map2k6 Transgenic Mice by Microarray Analysis

Kate Yu[1], Yingqi Xu[2], Xihua Hu[2]
[1]Robert Wood Johnson Barnabas Health/Saint Barnabas Medical Center, Livingston, NJ, [2]China Medical University, Shenyang, Liaoning, China

Disclosures: Kate Yu: None; Yingqi Xu: None; Xihua Hu: None

Background: Congenital generalized hypertrichosis terminalis (CGHT) is one of the least well understood of genetic hair disorders. We have previously demonstrated an association with copy number mutations on 17q24.2-q24.3. The minimal disease genomic region of the copy-number variations (CNVs) contains ABCA5, ABCA6, ABCA10, and MAP2K6. A previous large-scale survey of CNVs in the Han Chinese population has found that 4 of the 300 individuals carried a 203-kb CNVs encompassing the 3 ABCA genes. MAP2K6 is a key component in cellular signal transduction pathway that affect growth factor-induced proliferation and gene expression. Thus we inferred that MAP2K6 was the leading candidate gene from the overlapping region in our patients.

Design: We generated transgenic (TG) mice over-expressing Map2k6 under control of Keratin 15 promoter (K15-Map2k6), which drives expression of a transgene specifically in the reservoir of stem cells in the hair follicle (HF) bulge. The expression profile of K15-Map2k6 skin was investigated using microarray analysis.

Results: K15-Map2k6 mice are characterized by epidermal thickening and hyperplasia of HFs, compared with the age-matched wild-type (WT) controls. From 45,037 mouse probes, differential expression in 510 genes (127 upregulated and 383 downregulated, $p<0.05$, fold change ≥2 or ≤0.5) in skin from TG mice were discovered and compared with skin from WT mice. The top canonical pathways identified due to significant changes in gene expression between conditions were as follows: Cell communication, MAPK signaling, and cytokine-cytokine receptor interaction, known for their role in inducing epidermis hyperplasia and hair growth. Among the dysregulated genes, numerous genes encode structural proteins such as keratins (5 genes) and keratin associated proteins (2 genes), markers of epidermal hyperplasia (3 genes), and hair morphogenesis and growth (9 genes), ascertained by conducting real-time PCR on skin RNA produced at postnatal day 12 during first hair growth cycle.

Table 1 Validation of the differential expression of the selected genes in the K15-Map2k6 transgenic skin

Class	Gene name	Transgenic/wild type Fold change	
		Microarray	Real time PCR
MAPK signaling associated factor	Map2k6	2.970	2.895
	Mef2c	2.306	2.233
	Stat1	1.941	1.886
	Mapkap2	1.875	1.812
	TNFAIP3	0.235	0.206
	MAPK12	2.301	2.245
Keratin	Krt6b	14.810	14.739
	Krt6a	4.129	4.055
	Krt16	3.077	3.141
	Krt27	2.376	2.305
	Krtap16	6.252	6.315
	Krtap15	3.999	4.063
Epidermal differentiation	Krt10	0.635	0.562
Hair morphogenesis and growth	MMP19	2.350	2.289
	MMP12	2.080	2.125
	Tchh	3.610	3.545

Figure 1 - 518

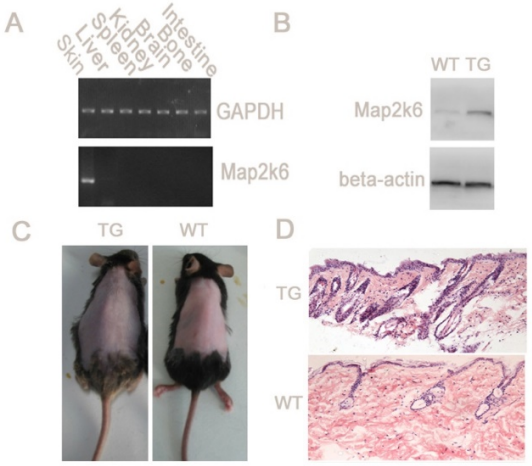

Figure 1. Generation of transgenic mice expression of Map2k6 and analysis of hair follicle proliferation and differentiation. A. RT-PCR analysis of total RNA from skin, liver, spleen, kidney, brain, bone, and intestine, using the SV40 specific primer, shows that expression of the transgene is skin-specific in transgenic lines B. Western blot analysis of Map2k6 expression from adult back skin (postnatal day 20) of a K15-Map2k6 transgenic (TG) and wild-type (WT) mice. C. Shaved back skin of TG and WT mice at postnatal day 18. D. HE-stained back skin sections from TG and WT mice at postnatal day 18 indicate hyperplasia of hair follicles.

Figure 2 - 518

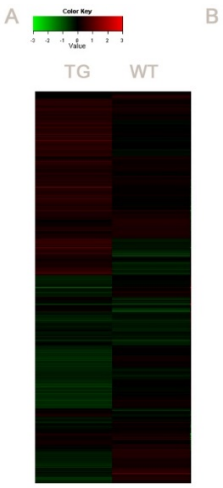

B

KEGG Pathway	Gene Counts	*p*-value
Cell Communication	10	2.52397E-12
Focal adhesion	9	2.91761E-09
Cytokine-cytokine receptor interaction	9	2.54256E-08
MAPK signaling pathway	9	4.06309E-08
Calcium signaling pathway	8	7.11104E-08
Tight junction	7	8.6001E-08
PPAR signaling pathway	5	1.78992E-06
Regulation of actin cytoskeleton	5	0.000258263
Starch and sucrose metabolism	4	2.88472E-06
Glycolysis / Gluconeogenesis	4	1.43554E-05
GnRH signaling pathway	4	0.000128546
Leukocyte transendothelial migration	4	0.000257313
Purine metabolism	4	0.000774478
Metabolism of xenobiotics by cytochrome P450	3	0.000903927
Fc epsilon RI signaling pathway	3	0.001231515
Carbon fixation	3	3.50581E-05
Arginine and proline metabolism	3	0.000101659
Wnt signaling pathway	3	0.007767894
Jak-STAT signaling pathway	3	0.008193083

Figure 2. Gene expression profile in K15-Map2k6 and wild-type mice skins using microarray. A. Hierarchical clustering represents differential expression of the genes between K15-Map2k6 (TG) and wild-type (WT) mice skins. B. Kyoto Encyclopedia of Genes and Genomes (KEGG) pathway associated with Map2k6 overexpression.

Conclusions: K15-Map2k6 mice resemble some characteristics of the human hypertrichosis phenotypes. It define a novel mechanism that integrates Map2k6 and MAPK pathway to coordinate the delicate balance between proliferation and differentiation during HF development through the activation of MAPK signaling pathway involving transcriptional factors Mef2c, Stat1 and TNFAIP3, further leading to transcriptional activation of downstream target keratin proteins and Tchh, while inhibiting the epidermal differentiation.

519 Sox9 Regulates Hair Growth and is Associated with Congenital Generalized Hypertrichosis Terminalis

Kate Yu[1], Xianan Guo[2], Xihua Hu[2]
[1]Robert Wood Johnson Barnabas Health/Saint Barnabas Medical Center, Livingston, NJ, [2]China Medical University, Shenyang, Liaoning, China

Disclosures: Kate Yu: None; Xianan Guo: None; Xihua Hu: None

Background: Congenital generalized hypertrichosis terminalis (CGHT) is characterized with excessive growth of pigmented terminal hairs and often accompanied with gingival hyperplasia. We have previously identified a genetic locus for CGHT and found four overlapping 17q24.2-q24.3 copy-number variations (CNVs), including three nonrecurrent microdeletions in three Chinese families and one de novo inverted microduplication in a sporadic case. Recently, it has been shown that CNVs can have a position effect on expression of the key developmental regulator genes flanking the CNVs. Sox9, a gene 1-2 Mb downstream of these variants, was described as an essential regulator in hair differentiation, and mouse skin inactivated for the *Sox9* lacked external hair. Several tissue-specific long distance regulatory elements of Sox9 have been identified within the CNV region. We inferred that specific changes in the surrounding chromatin might lead to enhanced tissue-specific expression of Sox9 and excessive hair growth.

Design: We generated transgenic (TG) mice over-expressing Sox9 under control of Keratin 15 promoter (K15-Sox9), which drives expression of a transgene specifically in the reservoir of stem cells in the hair follicle (HF) bulge. The expression profile of K15-Sox9 skin was investigated using microarray analysis.

Results: K15-Sox9 mice show lengthening of the anagen phase of first hair growth cycle, elongation of the guard and awl hair shafts, and irregular HF diameters in the skin of K15-Sox9 transgenic (TG) mice. Gene expression microarray comparing K15-Sox9 and wild-type (WT) skin found that 222 genes were differentially expressed (110 upregulated and 112 downregulated, $p<0.05$, fold change ≥ 2 or ≤ 0.5). Gene Ontology (GO) annotation and Kyoto Encyclopedia of Genes and Genomes (KEGG) pathway analyses showed that the differentially expressed genes enriched in important hair follicle development pathways, including MAPK signaling, Wnt signaling, Toll-like receptor signaling, and cell adhesion. In addition, 10 differentially expressed genes were validated using quantitative real-time PCR on skin RNA produced at postnatal day 15.

Table 1 Validation of the differential expression of the selected genes in the K15-Sox9 transgenic skin

Class	Gene name	Transgenic/wild type Fold change	
		Microarray	Real time PCR
Sox9	Sox9	3.012	2.940
MAPK signaling associated factor	Mef2c	2.156	2.078
	Mapk3	1.983	1.916
	TNFAIP3	0.479	0.403
Wnt/β-catenin signaling associated factor	Ctnnβ1	2.199	2.131
	Ctnnβip1	1.943	1.889
	Wnt10b	2.121	2.078
Epidermal proliferation and differentiation	Krt6b	2.708	2.651
Hair growth	Tchh	2.013	1.954
	Fgf13	2.181	2.122

Figure 1 - 519

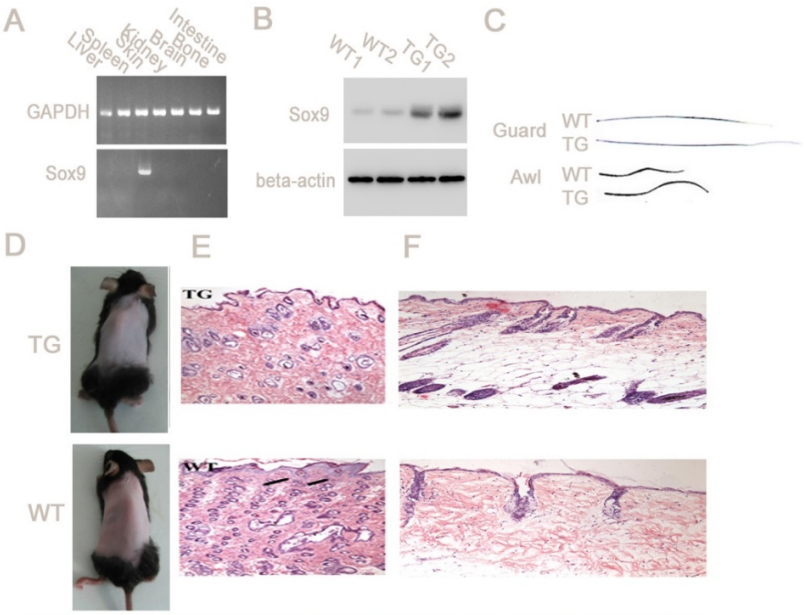

Figure 1. Generation of transgenic mice expression of Sox9 and analysis of hair length and cycling. A. RT-PCR analysis of total RNA from liver, spleen, skin, kidney, brain, bone, and intestine, using the SV40 specific primer, shows that expression of the transgene is skin-specific in transgenic lines. B. Western blot analysis of Sox9 expression from adult back skin at postnatal day 12 (#1) and 18 (#2) of a transgenic (TG) and wild-type (WT) mice. C. Guard and awl hair shafts of TG mice are elongated compared with that of WT. D. Shaved back skin of K15-Sox9 and WT mice at postnatal day 18. E. HE-stained back skin transverse sections from TG and WT mice at day 7. Follicles are irregularly shaped and spaced, clustered in TG mice, and in the irregular angling relative to skin surface. Follicles appear rudimentary (denoted by arrows) in WT mice. F. HE-stained back skin longitudinal sections from TG and WT mice at day 18 show anagen hair follicles (HFs) in TG mice and telogen HFs in WT mice.

Figure 2 - 519

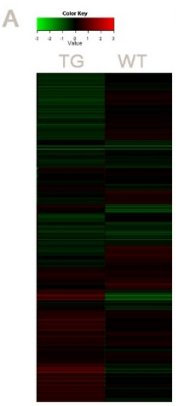

B

KEGG Pathway	Gene Counts	*p*-value
MAPK signaling pathway	7	5.83849E-09
Antigen processing and presentation	6	5.48442E-10
Cell adhesion molecules (CAMs)	5	4.2073E-07
Melanogenesis	5	4.28927E-08
Cytokine-cytokine receptor interaction	5	3.92353E-06
Wnt signaling pathway	4	1.09953E-06
Jak-STAT signaling pathway	4	4.81328E-07
Gap junction	4	2.08345E-06
Leukocyte transendothelial migration	4	4.46163E-06
Tight junction	4	8.6707E-06
Purine metabolism	4	1.41514E-05
Toll-like receptor signaling pathway	4	4.81328E-07
Natural killer cell mediated cytotoxicity	3	0.000251765
Axon guidance	3	0.000257541
Calcium signaling pathway	2	0.015278195

Figure 2. Gene expression profile in K15-Sox9 and wild-type mice skins using microarray. A. Hierarchical clustering represents differential expression of the genes between K15-Sox9 (TG) and wild-type (WT) mice skins. B. Kyoto Encyclopedia of Genes and Genomes (KEGG) pathway associated with Sox9 overexpression.

Conclusions: Collectively, our findings support an enhanced expression of SOX9 is associated with CGHT and suggest a novel mechanism that integrates Sox9 and MAPK and Wnt/β-catenin pathway in epidermal signal leading to hair overgrowth. Ongoing expression profiling experiments will give more clues to the molecular basis for the same phenotypes.

520 Gene Expression of the Tumor Micro Environment in Acral Lentiginous Melanoma

Michael Zaleski[1], George Jour[2], Denai Milton[1], Adi Diab[1], Wen-Jen Hwu[1], Victor Prieto[1], Carlos Torres-Cabala[1], Phyu Aung[1]
[1]The University of Texas MD Anderson Cancer Center, Houston, TX, [2]NYU Langone Health, New York, NY

Disclosures: Michael Zaleski: None; George Jour: None; Victor Prieto: None; Carlos Torres-Cabala: None; Phyu Aung: None

Background: Immunotherapies (IT) targeting the tumor micro environment (TME) have shown revolutionary results as a treatment (TX) for advanced melanoma. Yet, dramatic responses to IT in melanoma patients is seen in only a small subset of cases highlighting the

complexity of the TME. Several subtypes of melanoma exist and knowledge of the TME in rare subtypes is scarce. Primary acral lentiginous melanoma (PALM) arises from the acral skin, is aggressive, rare, and genetically distinct from primary cutaneous melanoma (PCM). The TME composition in ALM has not been well established. Herein, we aim to investigate the composition of the TME in PALM and seek to identify potential signatures that might lead to the development of new therapeutic targets and predictive biomarkers.

Design: Our cohort includes 35 tumors (18-PALM, 9-PCM, 8-NALM). Tumoral RNA was investigated via gene expression analysis, carried out with a customized 770-gene expression panel combining markers for 24 different immune cell types and 30 common cancer antigens, including key checkpoint blockade genes analyzed with the N-counter system. Differential gene expression (DGE) pathway analysis were performed using R package ($p<0.01$; FDR<0.01) through comparisons with PCM and non-lentiginous melanoma arising at acral sites (NALM). Molecular findings were correlated with clinicopathologic features, treatment status, and disease specific and overall survival.

Results: PALM and PCM TMEs showed a predominance of cytotoxic TCD8+ compared to NALM ($p<0.001$;$p<0.01$, respectively). An additional Mast cell signature was noted in PCM ($p<.01$). NALM TME showed a scarce TCD8+ signature.

Most PALM showed relative abundance of CD8 over exhausted CD8 and Tregs ($p<0.01$) (Figure1) that significantly associated with stage I/II presentation and epithelioid cytology ($p<0.05$). PALMs with exhausted CD8 signatures significantly associated with ulceration and PNI ($p=0.01$). DGE identified significant upregulation of ICAM3, TYK2 and CD164 in PALM cases ($P<0.01$) which correlated with enrichment in the PI3K/Akt/mTOR, NF-kB, TNF, ERK, adhesion, and chemokine pathways ($p <0.01$) (Table1/Figure2).

Gene	Log2 fold change	P-value	Function
ICAM3-mRNA	7.97	1.97e-08	Adhesion, Regulation
YTHDF2-mRNA	7.76	3.89e-08	Associated with carcinogenesis
IFNAR1-mRNA	6.74	6.71e-08	Pathogen Defense
IRF4-mRNA	-4.83	8.59e-08	B-Cell Functions, Regulation, T-Cell Functions
CD164-mRNA	4.96	4.99e-07	Proliferation, adhesion, and differentiation
IKBKG-mRNA	-3.55	5.95e-07	Associated with carcinogenesis within NF-kB pathway
ZNF205-mRNA	-3.06	7.96e-07	Cell Functions
TYK2-mRNA	5	8.19e-06	Cytokines, Pathogen Defense, Regulation

Figure 1 - 520

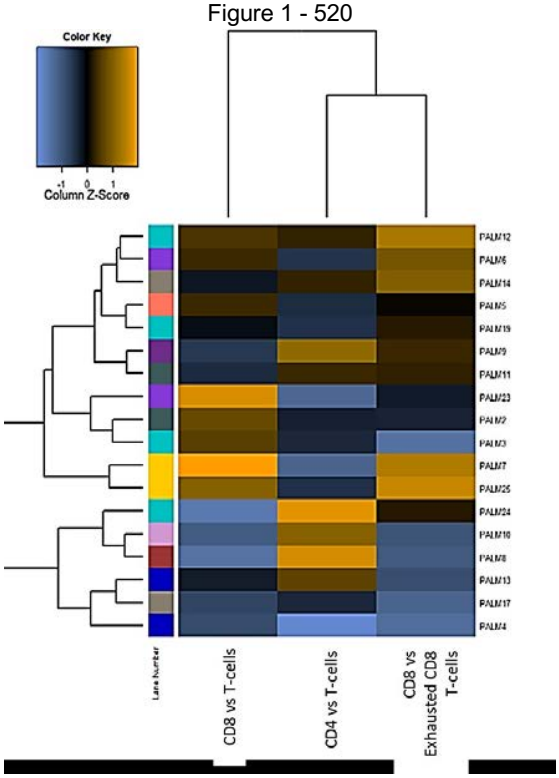

Figure 2 - 520

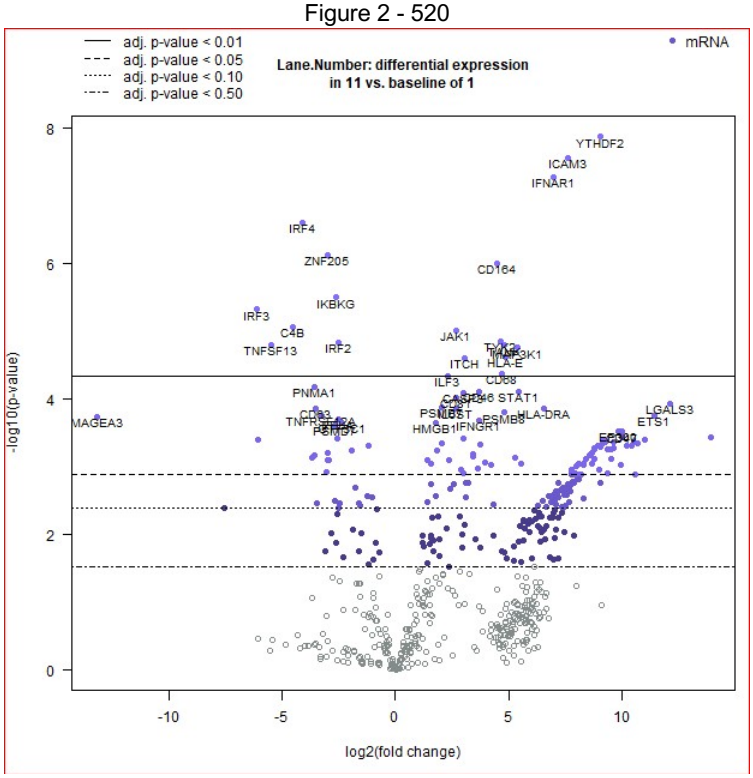

Conclusions: PALM TME is distinct from NALM TME, showing a preponderance of TCD8+ cells over T-regs, suggesting a possible predictor for better response to IT. Upregulation of *TYK2* represents a potential for combinational regimen with selective TYK2 inhibitors in cases where IT monotherapy fails. Validation of the findings through mechanistic studies is warranted.

521 Multiple Spitz Nevi: A Unique Entity with Diverse Pathological Features

Yan Zhou[1], Kyu Young Song[1], Alessio Giubellino[1]
[1]*University of Minnesota, Minneapolis, MN*

Disclosures: Yan Zhou: None; Kyu Young Song: None; Alessio Giubellino: None

Background: Development of multiple Spitz nevi, namely the occurrence of two or more Spitz nevi in a single patient, is a rare phenomenon. Previous studies proposed that multiple Spitz nevi can develop either in grouped, disseminated or random fashion. Rare malignant transformation or disease progression has been reported in patients with multiple Spitz nevi. Some of these patients do not belong inside known categories of Spitz nevi.

Design: In order to characterize this rare entity and factors affecting prognosis, we searched our institution database, yielding a total of 218 cases of Spitz and Spitzoid neoplasms in the last fifteen years. Among these, we identified a total of thirty-seven lesions from six patients with multiple Spitz and Spitzoid nevi at our institution. The clinicopathologic features and prognosis were studied and compared with prior literature.

Results: At the time of diagnoses of Spitzoid lesions, patient ages ranged from 8 to 38 years. All patients developed these lesions within 1-3 years and current follow-up frame ranges from 0.5-12 years. The total number of Spitz neoplasms ranged from two to eight lesions in a single patient. Fourteen of twenty four lesions were located in the upper and lower extremities; ten lesions were located in trunk as well as head and neck regions. Only two patients presented with Spitz lesions exclusively in the extremities. One patient had germline BAP1 mutation and developed Spitzoid melanoma arising from a BAPoma, which has spitzoid features. One patient with germline HRAS mutation did not develop malignant transformation. Besides the patients with known mutation-related Spitz nevi, all other lesions do not share morphological similarities to Spitz neoplasms with known molecular characterizations (BAPoma, Spitz neoplasms with HRAS-mutation or with various kinase fusions such as ALK, NTRK). This phenomenon suggests that they may represent uncovered subtypes of Spitz neoplasms. All patients, except one, have history of other melanocytic lesions. Of note, three of six patients have multiple other types of atypical or dysplastic nevi, requiring close follow-up.

Conclusions: Malignant transformation is rare, but may occur in patient with multiple Spitz and Spitzoid nevi; molecular analysis provides crucial prognostic information. Multiple Spitz neoplasms is a unique entity for further study of yet undiscovered underlying pathogenetic gene alterations.

522 A Deep Learning-Based Approach for Localization and Diagnosis of Non-Melanoma Skin Cancers from Whole Slide Digital Pathology Images

Yufei Zhou[1], Andrew Janowczyk[1], Cheng Lu[1], Rainer Grobholz[2], Ian Katz[3], Anant Madabhushi[1]
[1]*Case Western Reserve University, Cleveland, OH,* [2]*Aarau, AG, Switzerland,* [3]*Southern Sun Pathology, Thornleigh, NSW, Australia*

Disclosures: Yufei Zhou: None; Andrew Janowczyk: None; Cheng Lu: None; Rainer Grobholz: None; Ian Katz: None; Anant Madabhushi: *Consultant*, Inspirata Inc.; *Stock Ownership*, Inspirata Inc

Background: Non-melanoma Skin Cancer (NMSC) is the most common type of cancer among all Caucasians and has a growing incidence rate. It mainly comprises basal cell carcinoma (BCC, 75% of incidents) and squamous cell carcinoma (SCC, majority of the rest), with each type composed of several forms (e.g., invasive and in-situ). In this study, we present a computational approach employing deep learning neural networks for accurate localization and diagnosis of BCC and SCC lesions on whole slide images (WSIs) of tissue pathology.

Design: A cohort of 87 patients was curated for this study, in turn comprising 114 digitized H&E stained whole slide images (WSI) at 20x magnification. The cohort comprises 10 benign cases, 56 BCC cases, 10 SCC-In Situ cases, and 11 SCC-Invasive cases. 551 region of interests (ROIs) identified by pathologists were extracted from the WSIs. Patients were randomly split into training and testing sets, at a ratio of 1:1. 12068 non-overlapping patches (6229 in the training set and 5839 in the testing set) of size 512x512 pixels were extracted from all ROIs in the cohort and used to train and test the DL models. The patient-level prediction was further inferred by the voting of patch-level prediction. Our cascaded DL pipeline involved 1) localizing potential cancer regions at 5x magnification, 2) differentiating BCC from SCC at 20x, and 3) differentiating InSitu/Invasive SCC at 20x. We employed a DenseNet (Huang et al., 2016) DL architecture and visualized the resulting predictions with Gradient-weighted Class Activation Mapping (Grad-CAM) (Selvaraju et al., 2018).

Results: Table-1 shows that the DL models yield a high area under the receiver operating characteristic curve (AUC). The model for the cancer localization achieves 0.99 AUC even when employing lower magnification (5x) images.

Binary Classification	Magnification	Training Patches	Testing Patches	Patient-level AUC
Benign vs. Cancerous	5x	6229	5839	**0.99**
BCC vs. SCC	20x	4252 (67% BCC+ 32% SCC)	4238 (72% BCC+ 28% SCC)	0.95
SCC-In Situ vs. SCC-Invasive	20x	3572 (49% SCC-In Situ + 51% SCC-Invasive)	1177 (78% SCC-In Situ + 22% SCC-Invasive)	**0.96**

Figure 1 - 522

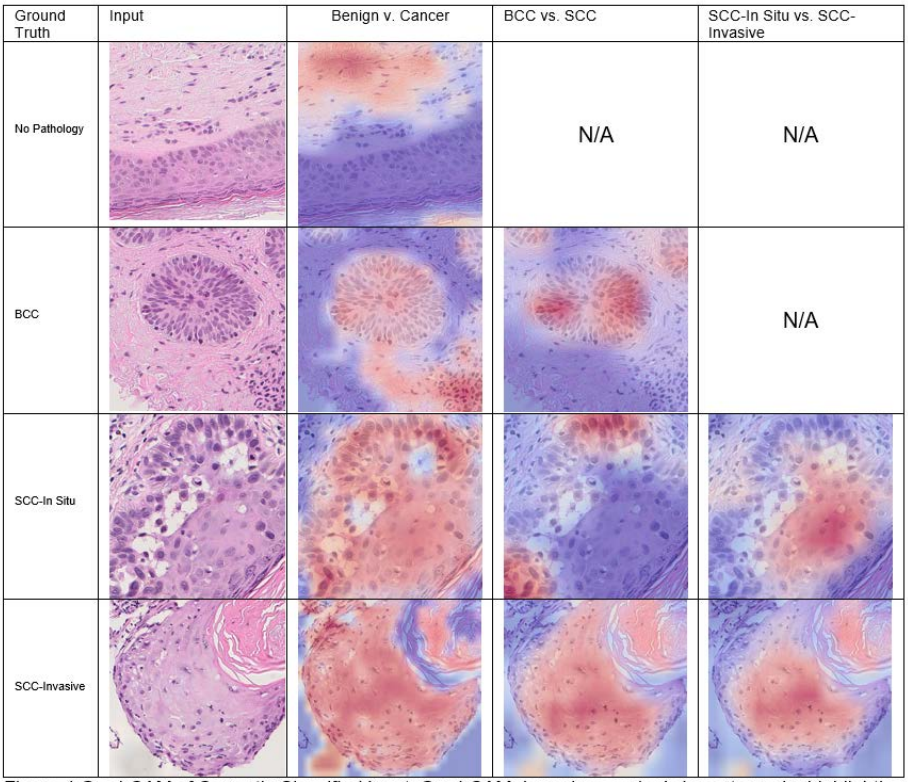

Figure-1 Grad-CAM of Correctly Classified Input. Grad-CAM demarks a region's importance by highlighting areas driving the classification in warmer colors (i.e., red). For instance, in the 2nd row, the Grad-CAM suggests that the cancer localization model focuses on the nest of basal cells to identify the BCC sub-type. In the 3rd row, the DL model appears to focus on the epidermal region to determine the invasive status of the SCC. In the 4th row (SCC-invasive), adjacent keratinization regions appear to also be contributing to the identification of the SCC differentiation as well as this SCC sub-type.

Conclusions: The experiments suggest that our cascaded DL model is capable of both localizing and differentiating NMSC. Further independent validation of these preliminary findings is warranted.